FORCES BETWEEN BILAYERS

By

Johannes Marra

A Thesis submitted for the degree of

Doctor of Philosophy

at the Australian National University

Canberra, December 1985

PREFACE

This dissertation is an account of research carried out at the Department of Applied Mathematics, Research School of Physical Sciences, Australian National University, between September 1982 and December 1985.

Except where otherwise stated, the work is my own. The material in Chapter 4 is the result of research carried out in collaboration with Dr J.N. Israelachvili.

None of the work reported here has been submitted to any other institution of learning for any degree.

J. Marra

PUBLICATIONS

1. J. Marra, H.A. van der Schee, G.J. Fleer, and J. Lyklema. "Polyelectrolyte Adsorption from Saline Solutions", in *Adsorption from Solution*, Ottewill, R.H., Rochester, C.H., and Smith, A.L. (eds.) (Academic Press, London, 1983), 245.

2. J. Marra. "Controlled Deposition of Lipid Monolayers and Bilayers onto Mica and Direct Force Measurements between Galactolipid Bilayers in Aqueous Solutions", *J. Colloid Interf. Sci.* **107** (1985) 446.

3. J. Marra. "Direct Measurements of Attractive Van der Waals and Adhesion Forces between Uncharged Lipid Bilayers in Aqueous Solutions", *J. Colloid Interf. Sci.* (1986) in press.

4. J. Marra and J.N. Israelachvili. "Direct Measurements of Forces between Phosphatidylcholine and Phosphatidylethanolamine Bilayers in Aqueous Electrolyte Solutions", *Biochemistry* **24** (1985) 4608.

5. J.N. Israelachvili and J. Marra. "Direct Methods for Measuring Conformational Water Forces (Hydration Forces) between Membrane and Other Surfaces", *Methods in Enzymology* (1986) in press.

6. J. Marra. "Direct Measurement of the Interaction between Phosphatidylglycerol Bilayers in Aqueous Electrolyte Solutions", *Biophys. J.* (1986) (in press).

7. J. Marra. "Effects of Counterion Specificity on the Interaction between Quaternary Ammonium Surfactants in Monolayers and Bilayers", *J. Phys. Chem.* (submitted).

ACKNOWLEDGEMENTS

I would like to thank the members of the Department of Applied Mathematics, Research School of Physical Sciences, Australian National University, for kindly receiving me and improving my physical insight and scientific knowledge.

Let me first of all acknowledge my supervisors Drs J.N. Israelachvili and R.G. Horn who initiated me into membrane biophysics and the direct force measurement technique. Without their guidance and advice, this work would not have been possible. Our senior technical officer, Mr A.R. Reading, deserves praise for his professional and always friendly technical assistance in the laboratory.

During the past three years, I have greatly benefitted from many stimulating discussions, not only on matters scientific, with Professor Ninham and Drs R.M. Pashley, S. Marcelja, and H.K. Christenson. Dr Pashley generously provided me with the computer program for computing the theoretical double-layer forces.

From outside the department, I thank Professor S.G.A. McLaughlin and Dr D. Sornette for their inspiring discussions and suggestions, the latter also for playing many enjoyable tennis matches with me. Many thanks go to Norma Chin for her professional typing of this thesis.

Finally, I gratefully acknowledge financial support from the Australian National University.

ABSTRACT

Direct measurements are reported of the full interbilayer force laws (force vs. distance) between bilayers of zwitterionic phosphatidylcholines (PC) and phosphatidylethanolamines (PE), uncharged galactolipids, anionic phosphatidylglycerols (PG), and cationic dioctadecyldimethylammonium surfactants (DOA) in aqueous electrolyte solutions. Bilayers were in each case deposited on molecularly smooth mica surfaces and the interbilayer forces then measured at a distance resolution of 1-2 Å. Three types of forces were identified: attractive van der Waals forces, repulsive electrostatic double-layer forces, and (at short range) repulsive steric-hydration forces.

Accurate measurements have been made of the van der Waals forces between uncharged bilayers. In high salt, the van der Waals force between galactolipid bilayers is screened to about half its strength in pure water, which agrees with the theoretical prediction. On the other hand, the van der Waals force between uncharged PE or PC bilayers is already quite weak in pure water. It is proposed that the high concentration of ionic groups between the bilayer surfaces may already screen the van der Waals force in pure water.

Double-layer forces between bilayers arise when the bilayers carry a net surface charge. This occurs when the amphiphile headgroups are ionized or, in case they are zwitterionic, when ion binding takes place. From the measured double-layer forces as a function of the bilayer separation and electrolyte concentration, the binding of various cations to PE, PC and PG, and the binding of various anions to DOA surfactants is investigated. Excellent agreement of the measured double-layer forces with theory is obtained. Slight deviations only occur at surface separations less than 25 Å, which might be related to discrete charge effects and/or ion-ion correlation effects.

A short-range steric-hydration repulsion was observed only between uncharged galactolipid bilayers and zwitterionic phospholipid bilayers. The short-range repulsion,

which balances the van der Waals force at separations of 10-30 Å, is apparently due to a combination of hydration and steric repulsion, the latter arising from thermal motions of headgroups and thickness fluctuations of fluid bilayers. No repulsive hydration forces were measured between the ionic PG and DOA bilayers.

It is shown that for two bilayers in "contact" at their equilibrium separation, their adhesion energies vary on addition of salt due to changes in the repulsive double-layer and hydration forces rather than to a change in the attractive van der Waals force.

Also, it is concluded that bilayer fusion is not simply related to the interbilayer force-law, but must be related to a structural instability of the membrane (see also Horn (1984)).

An idea about the relative intrabilayer interactions and the equilibrium headgroup area of the amphiphiles in bilayers is obtained by comparing the monolayer compression isotherms for different electrolyte solutions. It emerged that a correlation between interbilayer and intrabilayer interactions can only be drawn to a limited extend, which is mainly due to the complexity of the short-range forces and counterion specificities involved in the intrabilayer interactions.

Table of Contents

PREFACE ii

PUBLICATIONS iii

ACKNOWLEDGEMENTS iv

ABSTRACT v

CHAPTER 1. THE INTERACTIONS BETWEEN AMPHIPHILIC SURFACES: GENERAL OVERVIEW 1

1.1 INTRODUCTION 1
1.2 DOUBLE-LAYER FORCES 4
1.3 THE ELECTRICAL DOUBLE-LAYER FREE ENERGY OF A CHARGED AMPHIPHILIC MONOLAYER AT THE AIR/WATER INTERFACE 10
1.4 VAN DER WAALS FORCES AND HYDROPHOBIC FORCES 11
1.5 HYDRATION FORCES 14
1.6 AIMS AND OUTLINE OF THIS WORK 15

CHAPTER 2. MATERIALS AND EXPERIMENTAL METHODS 18

2.1 MATERIALS 18
2.2 SURFACE TENSION MEASUREMENT TECHNIQUE 19
2.3 LANGMUIR-BLODGETT DEPOSITION TECHNIQUE 21
2.4 THE DIRECT FORCE MEASUREMENT TECHNIQUE 22

CHAPTER 3. FORCES BETWEEN GALACTOLIPID BILAYERS 28

3.1 INTRODUCTION 28
3.2 RESULTS 28
3.2.1 Monolayer Compression Isotherms and Langmuir-Blodgett Deposition 28
3.2.2 Thickness of the Deposited Bilayers and Operational Definition of the Bilayer-Water Interface 29
3.2.3 Van der Waals Forces and Hydration Forces between Galactolipid Bilayers 31
3.3 DISCUSSION 35

CHAPTER 4. FORCES BETWEEN BILAYERS OF THE ZWITTERIONIC PHOSPHOLIPIDS PC AND PE IN AQUEOUS SOLUTIONS 39

4.1 INTRODUCTION 39
4.2 RESULTS 40
4.2.1 Monolayer Compression Isotherms of PC and PE 40
4.2.2 Deposition of PE and PC Bilayers onto Mica 42
4.2.3 The Bilayer-Water Interface and the Bilayer Thickness 45
4.2.4 Forces in Pure Water 47
4.2.5 Forces in Monovalent Electrolyte Solutions 51

4.2.6 Forces in Divalent Electrolyte Solutions 54
4.2.7 Fusion 61
4.3 DISCUSSION 63

CHAPTER 5. FORCES BETWEEN MOLECULES IN MONOLAYERS AND BETWEEN BILAYERS OF PHOSPHATIDYLGLYCEROL 72

5.1 INTRODUCTION 72
5.2 RESULTS 74
5.2.1 Monolayer Compression Isotherms of DMPG and DSPG 74
5.2.2 Langmuir-Blodgett Deposition of PG on Mica 74
5.2.3 Forces between DSPG Bilayers 75
5.2.4 Forces between DMPG Bilayers 81
5.2.5 The Contraction of a DMPG Monolayer at the Air-Water Interface following Addition of $CaCl_2$ 84
5.3 DISCUSSION 85

CHAPTER 6. EFFECTS OF COUNTERION SPECIFICITY ON THE INTERACTIONS BETWEEN QUATERNARY AMMONIUM SURFACTANTS IN MONOLAYERS AND BILAYERS 89

6.1 INTRODUCTION 89
6.2 RESULTS 92
6.2.1 Monolayer Compression Isotherms 92
6.2.2 The Deposited Headgroup Area 93
6.2.3 Forces between DOA Bilayers 94
6.3 DISCUSSION 99

CHAPTER 7. SUMMARY OF THE RESULTS AND POTENTIAL FOR FUTURE STUDIES 102

7.1 SUMMARY AND CONCLUSIONS 102
7.2 POTENTIAL FOR FUTURE STUDIES 106

BIBLIOGRAPHY 110

CHAPTER 1

THE INTERACTIONS BETWEEN AMPHIPHILIC SURFACES: GENERAL OVERVIEW

1.1 INTRODUCTION

In the past decade, considerable progress has been achieved in the determination of surface forces, in particular their range and magnitude (Israelachvili, 1985a). At the current level of understanding, an arbitrary distinction is usually made between long-range forces and short-range forces. Long-range forces comprise the electrostatic double-layer force and the electrodynamic van der Waals force. Their properties form the basis of the DLVO theory (Verwey and Overbeek, 1948) which is regarded as a cornerstone of colloid science. A much lesser understood long-range force which only recently has been measured between hydrocarbon surfaces in water (Israelachvili and Pashley, 1982) is the strongly attractive hydrophobic force.

Additional short-range forces arise from the differences in the organization and structuring of solvent molecules near the surfaces as compared to solvent molecules in the bulk of the solution, and are generally referred to as solvation forces. Of particular interest is the tight association and/or polarization of water molecules near hydrophilic surfaces like phospholipid bilayers (Lis et al., 1982a) and the adsorption of hydrated ions to mineral surfaces (e.g. clay) (Van Olphen, 1977; Pashley, 1981). These phenomena give rise to a strongly repulsive and/or oscillatory short-range force called the hydration force. Whereas continuum theory is quite able to explain the general properties of long-range forces, the molecular nature of solvent molecules must be considered to explain short-range forces.

A knowledge of the forces between amphiphilic surfaces such as lipid bilayers and

surfactant monolayers across water is necessary for understanding the properties of many colloidal and biological systems. The interaction between micelles, vesicles and surfactant coated colloidal particles determines whether they remain dispersed or whether they aggregate and/or precipitate out of solution. Effective detergent action and the formation and stability of soap films, foams, and liquid-crystalline surfactant phases are ultimately dependent on these interactions as well. In the spontaneous formation process of surfactant aggregates like vesicles and micelles, the shape and the size of the assemblies in concentrated solutions bears a relationship to the interaction between them (Brady et al., 1985). More generally: the explanation of the phase behaviour of surfactant/water and surfactant/water/oil systems (e.g. microemulsions) is only possible from a consideration of the interactions existing in these systems.

In the biological area: membrane-membrane and vesicle-membrane interactions underlie all phenomena involving intermembrane coupling such as adhesion, membrane stacking, and fusion. They are relevant to the understanding of biological phenomena like endocytosis, exocytosis, fertilization, and cell recognition in immunological processes. In the field of neurobiology, the transmission of impulses across a synapse seems to be related to the aggregation and fusion of synaptic vesicles along the presynaptic membrane (Gray, 1973). In the area of photosynthesis, it is believed that the stacking of thylakoid membranes is involved in the photophosphorylation process (Punnett, 1970; Chow et al., 1981).

Many biological membranes contain 50% or more protein by weight, and given that these proteins often protrude beyond the lipid headgroups, it is clear that when two membranes approach each other, it are the proteins that 'see each other first' and so are likely to dominate intermembrane interactions. The observations that the aggregation and fusion of membranes is often protein specific (Baker et al., 1980; Hong et al., 1982) and that the fusion of model membranes can be triggered by micromolar amounts of Ca^{2+} only in the presence of Ca-specific proteins further enhance this view. On the other hand, fusion also occurs between pure phospholipid bilayers (Papahadjopoulos, 1978; Ohki, 1982; Cohen et al., 1982; Ahkong et al., 1975), and many lipids (e.g.

lysolecithin, phosphatidylethanolamine, etc.) are effective fusogens. The role of lipids may therefore not be a purely passive one, and it is almost certain that the total interaction between any two real membranes is a cooperative process involving the concerted action of both the lipids and proteins.

Apart from intermembrane interaction, also intramembrane interactions deserve attention. One can distinguish between lateral interactions in the hydrocarbon interior of the bilayer and lateral interactions in the polar headgroup region of the bilayer. The hydrophobic bilayer interior is a relatively homogeneous region of hydrocarbon chains interacting through fairly well-understood van der Waals attractive and steric repulsive forces (Seelig and Seelig, 1974; Marcelja, 1974; Schindler and Seelig, 1975; Gruen, 1980). By contrast, the hydrophilic polar headgroup region containing hydrated and/or ionized charged groups in contact with the aqueous medium is far less understood. Here the interactions are very different, and include steric interactions, dipolar and electrostatic forces involving specifically bound and free counterions, strongly associated water and hydrogen bonds. All these factors contribute to the physical state of the bilayer surface.

Lateral interactions between molecules determine the effective shape of the molecules (Israelachvili et al., 1976; Mitchell and Ninham, 1981; Ninham et al., 1983) and their self-assembly into aggregate structures. A detailed knowledge of the effective shape of the molecules allows us to predict size and geometry of the aggregates. In mixtures of amphiphiles, the often observed phase separation of the molecular species is a consequence of differences in the lateral interactions between the species (Findlay and Barton, 1978). In a number of cases, the fusion between phospholipid vesicles has been explained as the result of a difference in lateral interactions between the lipid headgroups on the inner membrane leaflet and between the lipid headgroups on the outer membrane leaflet of the vesicle, leading to a structural instability of the membrane (Cohen et al., 1980; Liao et al., 1979). Long-range interactions determine whether two vesicles in thermal motion can approach each other close enough to come into adhesive contact, possibly followed by fusion which mixes the contents of the two vesicles. Thus the complete fusion process may be a complex one, involving both inter- and

intra-bilayer interactions. Because both types of interaction are largely determined by the chemical nature and properties of the bilayer surface, it can be anticipated that correlations exist between these two (Israelachvili and Sornette, 1985). Together, these forces give bilayers and membranes their highly versatile and complex properties.

1.2 DOUBLE-LAYER FORCES

Many amphiphilic molecules carry an electrical charge due to ionization of or ion binding to the polar headgroup. When the amphiphiles assemble into aggregates like bilayers, the inter-bilayer interaction is to a large extent determined by the electrostatic forces between the bilayers. In this section, the relevant formulae will be given that describe these forces. The present approach follows the procedure given by Chan, Pashley and White (1980).

In an electrolyte solution, an electrically charged surface gives rise to a diffuse space charge of opposite sign near the surface. It extends some distance into the solution and essentially screens the surface charge. The properties of this so-called diffuse double-layer charge are described by the Gouy-Chapman theory (Verwey and Overbeek, 1948).

Now, when two charged planar surfaces approach each other, at some distance the diffuse double-layers of the surfaces will overlap, giving rise to an electrostatic repulsion between the surfaces. The repulsion is caused by the perturbation of the isolated diffuse double-layers of the surfaces through the presence of the other surface, which increases the free energy and can be treated as an osmotic pressure between the two surfaces. This osmotic pressure is related to the the difference in ion concentration in the region between the surfaces compared with the bulk concentration. When the distribution of ions in this region is known, it becomes possible to calculate the surface repulsion. This can be done by applying the Gouy-Chapman model of the diffuse double-layer, which uses the Poisson equation to describe the potential gradient between the surfaces:

$$\frac{d^2\psi(x)}{dx^2} = -\frac{4\pi\rho(x)}{\epsilon}. \tag{1}$$

ρ(x) is the local net space charge density of ions (of both sign) in a medium of dielectric

constant ϵ (ϵ = 80 for aqueous media). ψ(x) is the mean local electrostatic potential. In the special case of two equally charged surfaces, it is obvious that the potential profile and ion distribution between the surfces must be symmetric about the midplane x = m between the surfaces. Then, Eq. (1) easily allows us to calculate the charge density σ on the surface, since the total accumulated space charge in the x direction per unit area from x = 0 to x = m must balance the surface charge per unit area, i.e.

$$\sigma = -\int_{x=0}^{x=m} \rho(x)dx = \left[\frac{\epsilon}{4\pi}\frac{d\psi}{dx}\right]_{x=0}^{x=m} = -\frac{\epsilon}{4\pi}\left(\frac{d\psi}{dx}\right)_{x=0}. \tag{2}$$

Using the Boltzmann distribution for each ionic species n_i with a bulk concentration $n_i(\infty)$ and a valency z_i, we have for $n_i(x)$:

$$n_i(x) = n_i(\infty)\ exp(-z_i e\psi(x)/kT). \tag{3}$$

Together with the charge density equation

$$\rho(x) = \sum_i e z_i n_i(x), \tag{4}$$

we can integrate Eq. (1) to obtain the potential profile and the ion distribution between the surfaces. Of course, the results must be symmetric about the midplane between the two (equally charged) surfaces.

Now, the interaction pressure between the charged surfaces is equal to the osmotic pressure Π at the midplane between the surfaces according to

$$\Pi = kT\sum_i (n_i(m) - n_i(\infty)), \tag{5}$$

where $n_i(m)$ is the concentration of ion 'i' at the midplane x = m where a potential ψ(m) exists. Using Eq. (3) at x = m, we obtain that

$$\Pi = kT\sum_i n_i(\infty)\left[exp(-z_i e\psi(m)/kT) - 1\right]. \tag{6}$$

Thus, the problem reduces to that of finding ψ(m).

Let us now consider a single z:z electrolyte species. The scaled Poisson-Boltzmann equation (Eq. (1) combined with Eqs. (3) and (4)) for the potential distribution between two planar charged surfaces is given by

$$\frac{d^2Y}{dX^2} = sinhY \tag{7}$$

where Y is the scaled potential $ze\psi(x)/kT$ and X is the scaled distance κx measured from the midplane between the surfaces with

$$\kappa^2 = \frac{8\pi n(\infty)z^2e^2}{\epsilon kT}; \tag{8}$$

(κ^{-1} is the Debye screening length). A first integration of Eq. (7) yields

$$\frac{dY}{dX} = Q \cdot Sgn(Y_m). \tag{9}$$

With Q defined as

$$Q = [2(coshY - coshY_m)]^{1/2}. \tag{10}$$

Y_m is the scaled midplane potential. Now,

$$\frac{dQ}{dY} = \frac{sinhY}{Q}$$

$$= \frac{Sgn(Y_m)}{Q}\left[\left(\frac{Q^2}{2} + coshY_m\right)^2 - 1\right]^{1/2}. \tag{11}$$

Eq. (9) combined with Eq. (11) gives

$$\frac{dX}{dQ} = \left[\left(\frac{Q^2}{2} + coshY_m\right)^2 - 1\right]^{-1/2}. \tag{12}$$

At the midplane, both $Q = 0$ and $X = 0$. If we know the value of $Q = Q_s$ at the surfaces, then for a given starting value of Y_m, we can integrate Eq. (12) from $Q = 0$ to $Q = Q_s$ numerically. From the given Q_s, the scaled distance $X = X_s$ is obtained and hence the surface separation $D = 2X_s/\kappa$ for the given starting value of Y_m. At that surface separation, the double-layer repulsion is given by

$$\Pi(D) = 2n(\infty)kT(coshY_m - 1). \tag{13}$$

Thus, a set of values (D, Y_m) can be generated. The interaction energy per unit surface area, E(D), is numerically computed from

$$E(D) = \int_D^\infty \Pi(D)dD. \tag{14}$$

In the present study, interactions between charged amphiphilic surfaces have often been measured in solutions containing a mixture of 1:1 and 2:1 electrolyte, i.e. NaCl and $CaCl_2$. Suppose we have a total Cl^- concentration $[Cl^-] = n$, then $[Ca^{2+}] = \frac{1}{2} n (1 - \alpha)$ and $[Na^+] = \alpha n$, if α denotes the fraction of the Cl^- concentration which comes from the presence of NaCl electrolyte. From Eq. (6) we now derive that at the midplane

$$\Pi = nkT[(exp\langle Y_m\rangle + \alpha exp\langle -Y_m\rangle + \frac{1}{2}(1 - \alpha)exp\langle -2Y_m\rangle) - \frac{1}{2}(3 + \alpha)]$$
$$= nkTp \tag{15}$$

where p is a "dimensionless pressure".

Taking $X = \kappa x$ with $\kappa^2 = 4\pi e^2 n(3 - \alpha)/(kT\epsilon)$, we obtain from Eqs. (1) and (3) that again

$$\frac{dY}{dX} = Q \cdot Sgn(Y_m) \tag{16}$$

with Q now defined as

$$Q = \left(\frac{2}{3-\alpha}\right)^{1/2} \left[\left(e^Y + \alpha e^{-Y} + \frac{1}{2}(1-\alpha)e^{-2Y}\right) - (p + \frac{1}{2}(3 + \alpha)\right]^{1/2}. \tag{17}$$

Note that

$$\frac{dQ}{dY} = \frac{e^Y - e^{-Y} - (1 - \alpha)e^{-2Y}}{(3 - \alpha)Q}. \tag{18}$$

From Eq. (16) and (18) we finally derive

$$\frac{dX}{dQ} = \frac{Sgn(Y)(3 - \alpha)}{(e^Y - \alpha e^{-Y} - (1 - \alpha)e^{-2Y})}. \tag{19}$$

In Eq. (19), Eq. (17) must be used to get e^Y in terms of Q. Once this is done, the values $X_s = \kappa.D/2$ can again be generated as a function of the given Q_s at the surfaces for a given starting value of Y_m.

It remains to be indicated how the value Q_s at the surface is determined. This depends on the type of boundary conditions:

(i) Constant surface potential ψ_s. In this case Q_s is calculated directly from Eqs. (10) or (17) taking $Y = Y_s$ which is independent of the surface separation.

(ii) Constant surface charge σ. From Eq. (2) we see that this condition leads to a constant value of $(dY/dX)_{X=X_s}$, i.e.

$$\left(\frac{dY}{dX}\right)_{X=X_s} = \frac{4\pi e}{\epsilon kT\kappa} \cdot \sigma \tag{20}$$

and Q_s follows from Eq. (9) or Eq. (16).

(iii) Surface charge regulation. The previous two boundary conditions are extreme cases and often do not describe the boundary conditions of real surfaces adequately. In recent years, it has become apparent that ions may well adsorb to or desorb from charged surfaces as they interact (Pashley, 1981). This situation is somewhere in between the two extremes of constant charge and constant potential.

In the following chapters, we will deal with two types of charged amphiphilic surfaces: zwitterionic surfaces which acquire a net charge through the binding of cations, and ionic surfaces whose charge is reduced through the binding of counterions. Both cases will be discussed here to derive the boundary conditions.

a. Zwitterionic Surfaces

Here, each amphiphile headgroup is intrinsically uncharged. When specific binding of say Ca^{2+} takes place on the headgroups, this binding can as a first approximation be described through the intrinsic binding constant K_{Ca}, using a mass action law relating the ion concentration in the bulk $[Ca^{2+}]_\infty$ to the number density of bound ions $[SCa^{2+}]_0$ on the bilayer surface. The intrinsic binding constant K_{Ca} for the reaction

$$[S_u]_0 + [Ca^{2+}]_0 \rightleftharpoons [SCa^{2+}]_0 \tag{21}$$

where $[S_u]_0$ is the surface density of unbound neutral amphiphiles, is given by

$$K_{Ca} = \frac{[SCa^{2+}]_0}{[S_u]_0[Ca^{2+}]_0} = \frac{[SCa^{2+}]exp(2Y_s)}{[S_u]_0[Ca^{2+}]_\infty}. \tag{22}$$

Here, Eq. (3) has been used to relate $[Ca^{2+}]_0$ to $[Ca^{2+}]_\infty$. For the charge density we have

$$\sigma = 2e[SCa^{2+}]_0 \tag{23}$$

and for the total amphiphile density $[S]_0$ we have

$$[S]_0 = [S_u]_0 + [SCa^{2+}]_0. \tag{24}$$

Combining Eqs. (22)-(24), we derive

$$\frac{\sigma}{2e} exp(2Y_s) = K_{Ca}[Ca^{2+}]_\infty \left([S]_0 - \frac{\sigma}{2e}\right) \tag{25}$$

which is the required boundary condition (for any surface separation). Thus, with a given value for Y_m, any value of Q_s at the surface generates a surface separation D which is consistent with an existing surface potential and surface charge according to Eq. (25). Of course, this procedure is only possible when K_{Ca}, $[Ca^{2+}]_\infty$ and $[S]_0$ are known quantities.

b. Ionic Surfaces

Here, the charge on the bilayers originates from the ionized headgroups of the amphiphiles. An example is phosphatidylglycerol which carries one negatively charged phosphate group at pH $\simeq$ 7. The bilayer charge can be reduced through specific binding of say Na^+ and Ca^{2+} ions. We then can define intrinsic binding constants K_{Na} and K_{Ca} for the reactions

$$[Na^+]_0 + [S^-]_0 \rightleftharpoons [SNa]_0$$

$$[Ca^{2+}]_0 + [S^-]_0 \rightleftharpoons [SCa^+]_0 \tag{26}$$

analogous to Eq. (22). Here, $[S^-]_0$ is the surface density of charged unbound headgroups. The equation for the surface charge σ becomes

$$\sigma = e([SCa^+]_0 - [S^-]_0), \tag{27}$$

and for the total amphiphile density we now have

$$[S]_0 = [S^-]_0 + [SNa]_0 + [SCa^+]_0. \tag{28}$$

With these conditions, the required boundary condition can easily be derived to be

$$\frac{K_{Ca}[Ca^{2+}]_\infty - exp(2Y_s)}{K_{Na}[Na^+]_\infty + 2exp(Y_s)} = \frac{\sigma.exp(Y_s)}{(e[S]_0 - \sigma)}. \tag{29}$$

Of course, a similar equation is valid when the binding of H^+ and Ca^{2+} ions is considered or when the binding of say Cl^- or SO_4^{2-} ions to a cationic bilayer composed of quaternary ammonium surfactants is investigated.

In the following chapters, we will analyse the experimentally measured forces

between charged bilayers as a function of their separation. What essentially will be done is that the measured double-layer interactions are analysed with the given formulae in this section, which allow us to fit a binding constant with which it becomes possible to obtain at each surface separation a surface potential and surface charge consistent with Eq. (25) or Eq. (29).

At this stage, it is worthwhile to point out the various implicit assumptions made in this section. The Gouy-Chapman theory treats the ions as point charges, assumes a smeared out surface charge, and takes the dielectric constant ϵ to be independent of the electric field and ion concentration. Also, in writing down Eq. (26), it has been assumed that Ca^{2+} does not bridge two adjacent amphiphiles but binds on single headgroups only. We will be able to see from the fit of the experimental results to the theory outlined whether these assumptions are reasonable or not.

Finally, the recent theoretical work of Guldbrand et al. (1984) and Kjellander and Marcelja (1985a) indicates that we should expect deviations from the standard Poisson-Boltzmann treatment of the double-layer force, in particular for divalent counterions at small surface separations and high charge densities. They attribute these deviations to correlations between the counterions in the double-layer and correlated fluctuations between the ions adsorbed on both surfaces, leading to an extra attractive interaction (similar to the van der Waals dispersion force type) which has a strength at least comparable to the conventional van der Waals attraction. However, the theory has not been worked out completely and an unresolved issue is the deconvolution of the ion binding phenomenon and the ion-ion correlation effect which both lead to a reduction in the double-layer force. We will return to this issue in the Chapters 4, 5 and 6.

1.3 THE ELECTRICAL DOUBLE-LAYER FREE ENERGY OF A CHARGED AMPHIPHILIC MONOLAYER AT THE AIR/WATER INTERFACE

When a monolayer is spread on water in a Langmuir trough, the monolayer compression isotherm can be measured which gives the surface pressure Π as a function of the headgroup area of the amphiphiles. In general, the expansion of the monolayer will depend on the electrolyte species and concentrations present in the subphase.

Because the compression isotherm provides an insight into the lateral interactions existing between adjacent amphiphiles, it is of interest to calculate how much of the measured surface pressure is due to diffuse double-layer contributions only.

The theory for a single charged surface gives the diffuse double-layer contribution Π^{el} to the surface pressure Π of a charged monolayer as

$$\Pi^{el} = \int_0^{\psi_s} \sigma . d\psi_s, \tag{30}$$

where ψ_s is the potential of the outer Helmholtz plane, i.e. the plane from where the diffuse double-layer charge originates. In the presence of a Stern layer, the value for ψ_s will be different from the actual surface potential.

The general expression for σ in terms of ψ_s is (at 25 °C)

$$\sigma = \frac{Sgn(\psi_s)e}{273}\left(\sum_j n_i\left[exp\left(-\frac{ez_i\psi_s}{kT}\right) - 1\right]\right)^{1/2}, \tag{31}$$

where n_i should be expressed in moles/litre, gives σ in units C/Å^2. In the general case of a mixture of 1:1 and 2:1 electrolyte, Eq. (30) has to be integrated numerically, using Eq. (31). When only a 1:1 electrolyte is present or when the 2:1 electrolyte concentration is much smaller than the 1:1 electrolyte concentration, Eq. (30) is integrated readily to

$$\Pi^{el} = \frac{4kT(\sqrt{n})}{273}\left[cosh\left(\frac{e\psi_s}{2kT}\right) - 1\right], \tag{32}$$

a result first obtained by Payens (1955). Here Π^{el} has dimensions J/Å^2. In Eq. (32) we can substitute the value of ψ_s which is obtained from the analysis of the measured double-layer forces between bilayers of the same amphiphiles. It should be noted, that here the Π^{el} only accounts for contributions from the diffuse double-layer. When a Stern layer is present, the total "electrostatic surface pressure" will be larger (see Chapter 6).

1.4 VAN DER WAALS FORCES AND HYDROPHOBIC FORCES

Attractive interactions play an important role in the stabilization of amphiphilic aggregates, in particular biological assemblies. Biological assemblies are built up from a mixture of lipids, proteins and polysaccharides, which interact with each other in a

complicated way. How these molecules can form stable assemblies like membranes, cells, cell organelles, etc., is one issue. The other issue deals with the interactions between the separate assemblies, which stabilize or destabilize them as building blocks of biological tissues.

The first issue is to a large extent accounted for by the hydrophobic interaction. The hydrophobic interaction (Franks, 1973) is a strong long-range attractive interaction between hydrocarbon molecules in water and has been shown to be stronger (Israelachvili and Pashley, 1982) and therefore more important than the van der Waals attraction alone. It is responsible for the low solubility of hydrocarbon in water and is probably involved in the conformation of proteins (Kauzmann, 1959). Although a clear theoretical description of the hydrophobic interaction is still lacking, it is believed to be caused by the strong, entropically unfavourable orientation of water molecules near hydrocarbon molecules.

The second issue is accounted for by an interplay of van der Waals forces, electrostatic forces, and hydration and steric forces. The hydrophilic headgroups of the amphiphiles face the water phase, and determine to a large extent the interaggregate interactions. The hydrophobic interior is shielded by these headgroups from the water phase so that no long-range hydrophobic attraction is expected and only attraction through the van der Waals interaction will remain. Therefore it should be the van der Waals attraction which is either partly or totally responsible for adhesion (Parsegian, 1973), and membrane stacking (Sculley et al., 1980). Because van der Waals interactions are the result of the attraction between the interiors of the aggregates across water, the interaction is (apart from the influence of the aggregate geometry) largely non-specific. A modification of the non-specificity of the van der Waals interaction may be expected to come from the interfacial region, and an example of that will be presented in this thesis.

The non-retarded van der Waals interaction energy E(D) per unit area between two half-spaces separated from each other by a distance D can be given by the Hamaker equation

$$E(D) = -\frac{A}{12\pi D^2} \tag{33}$$

where A is the non-retarded Hamaker constant.

According to Lifshitz theory (Parsegian and Ninham, 1970; Mahanty and Ninham, 1976) the non-retarded Hamaker constant can be written as

$$A = A(T) + A(disp). \tag{34}$$

A(T) represents the temperature-dependent part, and A(disp) the dispersion part of the total Hamaker constant. In the presence of electrolyte, the temperature-dependent term will be screened (Davies and Ninham, 1972; Mitchell and Richmond, 1973), the temperature-dependent term now reflecting correlations between the fluctuations in the Onsager-Samaris profiles of the ionic species set up by image effects. For $\kappa D \ll 1$ (pure water), with κ^{-1} the Debye screening length (Eq. (8)), the form of A(T) for two hydrocarbon slabs interacting across water is given by the limiting expression

$$A(T) = \frac{3}{4}\, kT\left(\frac{\epsilon_w - \epsilon_{hc}}{\epsilon_w + \epsilon_{hc}}\right)^2, \tag{35}$$

where ϵ_w and ϵ_{hc} represent the dielectric constants of water and hydrocarbon at zero frequency, respectively. A(T) can easily be calculated to have a value of about 3×10^{-21} J. Using refractive index data for water and hydrocarbon (Parsegian and Ninham, 1970), Lifshitz theory also predicts a similar value for A(disp), so the theoretical value for the net hydrocarbon/water Hamaker constant A is about 6×10^{-21} J.

In the presence of electrolyte, the expression for A(T) becomes quite complicated. However, for $\kappa D > 2$ the expression becomes simplified (Mahanty and Ninham, 1976) and (to about 10% accuracy) is given by

$$A(T) = A(T,\kappa = 0)\cdot 2\kappa D e^{-2\kappa D}\cdot\left\{1 + O\left(\frac{1}{\sqrt{\kappa D}}\right) + \ldots\right\}. \tag{36}$$

In other words, theory predicts that the temperature-dependent attractive van der Waals force should be screened and essentially disappear by $\kappa D > 2$ on addition of electrolyte. The dispersion part remains unaffected by electrolyte.

Eq. (33) is only valid for short surface separations, say less than 40 Å. Beyond that distance, retardation sets in which makes the interaction less than what is predicted by Eq. (33). Under those circumstances, the full Lifshitz theory must be used to describe the van der Waals interaction properly.

1.5 HYDRATION FORCES

Taking into account only attractive van der Waals and repulsive double-layer forces (DLVO theory; Verwey and Overbeek, 1948), we expect that in the absence of any strong double-layer repulsion - as would arise for nonionic and zwitterionic headgroups or in high salt for charged amphiphiles - all surfaces would come into strong irreversible adhesive contact with no water remaining between them. That this does not occur is due to the existence of an additional strongly repulsive short-range($<$ 3 nm) force, commonly referred to as a solvation force or (in water) a hydration force which has now been found to occur in several systems. In particular, this force occurs between nonionic surfactant bilayers with polyoxyethylene headgroups (I.G. Lyle and G.J.T. Tiddy, unpublished work), between zwitterionic lipid bilayers (see Chapter 4), and between galactolipid bilayers (see Chapter 3). Their highly hydrated headgroups ensure that their bilayers and vesicles will not adhere strongly, let alone fuse, even under conditions where there is no repulsive double-layer force.

Repulsive hydration forces between two surfaces arise whenever there are strongly hydrated surface groups. As the two surfaces approach each other, the water between them must be removed to the bulk solution. For the hydrated surface groups, this is energetically unfavourable, and appears as a repulsive force between them (Parsegian et al., 1979).

Hydration forces can be intrinsic to a surface, or they can be regulated. Thus, between uncharged zwitterionic bilayers, they are mainly intrinsic since the hydrophilic headgroups are covalently attached to the surfaces. Regulated hydration forces (or "secondary hydration forces") occur between surfaces containing charged or ionic groups where the cations or anions bound to these surfaces can be regulated (ion exchanged) by changing the solution conditions; and since different ions have different hydrations, the hydration forces themselves are thereby also regulated (Pashley, 1981).

The range of the hydration forces so far measured between amphiphilic surfaces is 2-3.5 nm, below which the force rises steeply, dominating over the van der Waals and double-layer forces.

Concerning theoretical interpretations of hydration forces, the literature is confusing and the matter wide open. Continuum mean-field theories of solvation forces in general and hydration forces in particular predict an exponential force-law (Marcelja and Radic, 1976; Gruen and Marcelja, 1983; Jonsson and Wennerstrom, 1983). Helfrich (1978) and Sornette and Ostrowsky (1984) have however noted that thermal curvature fluctuations of fluid bilayers will give rise to a repulsive 'steric' or undulation force that is also exponentially repulsive, whose strength depends on the fluidity (e.g. the curvature modulus) of the interacting bilayers. Meanwhile, Jonsson and Wennerstrom (1983) have proffered yet another interpretation of these forces based on the electrostatic interaction between the lecithin headgroup dipoles (zwitterions) on one surface with their images reflected by the opposing surface. Again, an exponential repulsion is predicted depending now on the positional correlations between headgroups in each bilayer.

Finally, Kjellander and Marcelja (1985b) have investigated the influence of the dipolar nature of zwitterionic surfaces on the water structure near the surfaces. According to their theory, the electric field between the oppositely charged groups on the bilayer surface strongly orientates the water molecules in the vicinity of the surface. When these bilayers are brought together, the water structure becomes disturbed which is energetically unfavourable, resulting in a repulsion.

We may mention that Monte-Carlo and molecular dynamics studies of solvation forces where the discrete molecular nature of the solvent is taken into account, predict an oscillatory force-law with distance. We return to reassess these differing theoretical views in later chapters.

1.6 AIMS AND OUTLINE OF THIS WORK

The aim of this work is to acquire an insight into the interactions existing between phospholipid bilayers and surfactant bilayers. The earliest work in this area has been done by Lyklema and Mysels (1965) and Clunie et al. (1967), which involved soap films

where the pressure across the aqueous layer was measured as a function of the water layer thickness. In later work, measurements have been carried out of the osmotic or hydrostatic "swelling" pressures between stacked multi-bilayers of phospholipids, the bilayer spacings being monitored by X-ray diffraction (Le Neveu et al., 1976, 1977; Parsegian et al., 1979). All these methods have in common that they only can measure repulsive forces. In the present work, use is made of the direct force measurement technique developed by Israelachvili, which has previously been used extensively to study the forces between molecularly smooth mica surfaces. With this technique, also the forces between two CTAB bilayers adsorbed from solution on mica have been measured (Pashley and Israelachvili, 1981). In the present study, these mica surfaces are coated with a bilayer of amphiphiles using the Langmuir-Blodgett deposition technique. With this technique, the supporting mica surfaces do not interfere with the bilayer interactions, while the surface smoothness is retained. The present experiments extend the work by Horn (1984) on the measurements of repulsive, attractive and adhesive forces between amphiphilic surfaces and should be of interest to biologists, colloid chemists and physicists.

In summary, Chapter 2 discusses the experimental procedures. Chapter 3 deals with the interactions between uncharged galactolipid bilayers which are of particular interest for measuring the van der Waals force and its screening through electrolyte. Chapter 4 describes the measured interactions between zwitterionic bilayers. Here, special attention is given to the van der Waals interaction, the steric-hydration force, and the binding of divalent cations which gives the bilayers a finite surface charge. The results give an insight into the origin of the short-range steric-hydration force and the molecular nature of the zwitterionic surfaces. Chapter 5 presents results on the forces between charged phosphatidylglycerol bilayers. They permit a detailed investigation of the DLVO theory, since at high pH the surface charge is known a priori. Some evidence is obtained concerning the existence of ion-ion correlation effects. Finally, Chapter 6 describes the forces between bilayers of double-chained quaternary ammonium salt surfactants. They are of interest for the study of the effects of counterion specificity on

the spontaneous formation process of vesicles. Both Chapters 5 and 6 discuss the correlations between interbilayer interactions and intrabilayer interactions. The latter interactions are studied by recording the monolayer compression isotherms on different electrolyte solutions. An evaluation of the obtained results and suggestions for potential future studies in this field are given in Chapter 7.

CHAPTER 2

MATERIALS AND EXPERIMENTAL METHODS

2.1 MATERIALS

High purity synthetic L-α-dilauroylphosphatidylcholine (DLPC), L-α-dimyristoylphosphatidylcholine (DMPC), L-α-dipalmitoylphosphatidylcholine (DPPC), L-α-distearoylphosphatidylcholine (DSPC), L-α-dipalmitoylphosphatidylethanolamine (DPPE), L-α-dimyristoylphosphatidylglycerol (DMPG), and L-α-distearoyl- phosphatidylglycerol (DSPG) were purchased in lyophylized powder form from Avanti Polar Lipids Inc. (Birmingham, Alabama). Plant monogalactosyldiglyceride lipids (MGDG) and plant digalactosyldiglyceride lipids (DGDG) were purchased in chloroform-methanol solution from Lipid Products (Nutfield Nurseries, Surrey, U.K.). The galactosyl diglycerides were reported to be mostly 18:3 and of purity 99%$^+$. All lipids were used without further purification. Dioctodecyldimethylammomium bromide surfactants (DOA) were Eastman (Rochester, New York) and purified by recrystallization from acetone. Fig. 1 gives the headgroup structure of all these amphiphiles.

Hexane-ethanol mixtures or chloroform were found to be suitable spreading solvents for all amphiphiles. All organic liquids were distilled twice before use. Water was purified in the following consecutive steps: distillation, treatment overnight with activated charcoal, filtration through a 0.05-μm-pore size nucleopore filter, and a final distillation from an all-pyrex still.

Amphiphiles were spread on an all-Teflon Langmuir trough standing in a dust-free laminar flow cabinet. A 9:1 hexane-ethanol spreading solvent was used to spread the phosphatidylcholines and the quaternary ammonium bromide surfactants. DPPE was spread from a 4:1 hexane-ethanol mixture. Complete dissolution of DPPE in this spreading solvent was only possible by heating the solution up to 40 $^\circ$C. Galactolipids

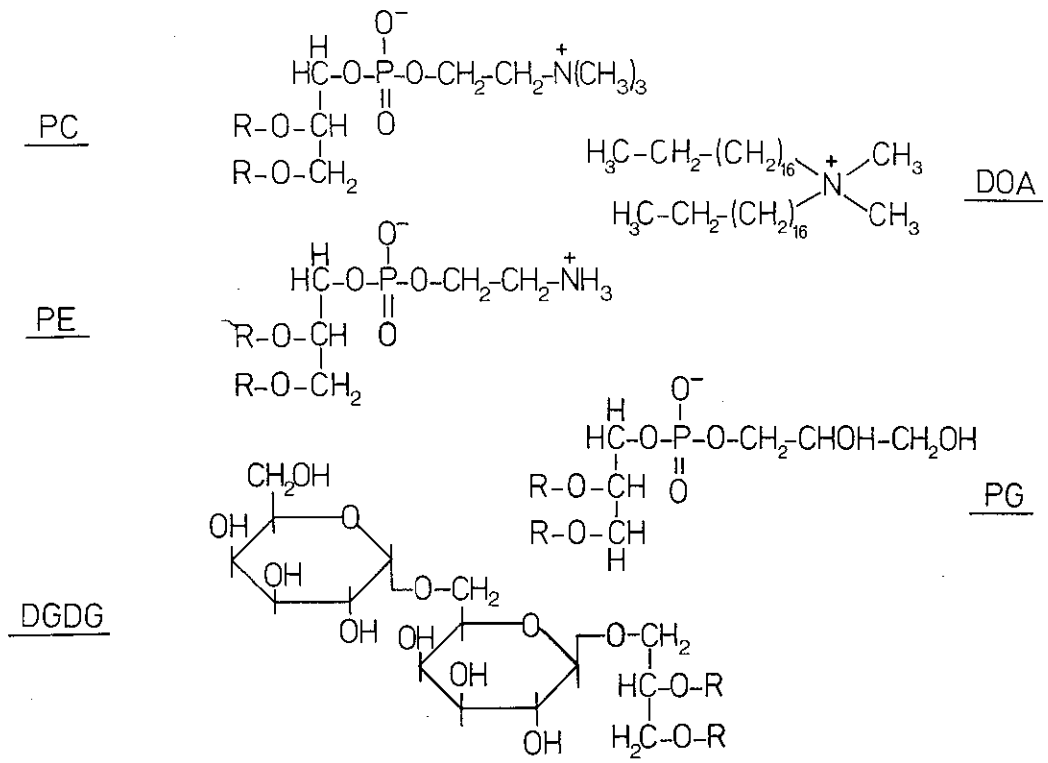

Fig. 1: Headgroup structure of phosphatidylcholine (PC), phosphatidylethanolamine (PE), digalactosyldiglyceride (DGDG), phosphatidylglycerol (PG), and dioctadecyldimethylammonium surfactant (DOA). MGDG has only one sugar molecule in its headgroup.

were dried by evaporation under a stream of N_2 and redissolved in the spreading solvent hexane (for MGDG) or a 9:1 mixture of hexane-ethanol (for DGDG). Phosphatidylglycerols were dissolved and spread from chloroform.

After spreading the amphiphiles on water, the spreading solvent was allowed to evaporate for 5 min. before surface pressure versus headgroup area (Π-A) isotherms were measured or before the monolayer was compressed to the surface pressure at which Langmuir-Blodgett deposition of the lipids was done.

2.2 SURFACE TENSION MEASUREMENT TECHNIQUE

The surface tension of the monolayer was measured with the "maximum force on a vertical rod" method as described by Padday et al. (1975). The method is based on the fact that if a cylindrical rod is pulled up through a liquid surface, it lifts up some liquid before finally detaching (see Fig. 2). As the rod is raised, its apparent weight as measured by a balance rises to a maximum value and then falls prior to detaching. The

surface tension is obtained directly from this maximum weight (after an adjustment for the weight of the rod). The rod was hung by a fine thread from under a bottom-loading balance of sensitivity 1 mg. This balance rests on a platform that can be raised or lowered smoothly at (variable) speeds down to about 1.0 mm/min and in this way pulls the rod up through the liquid surface at a regulated speed.

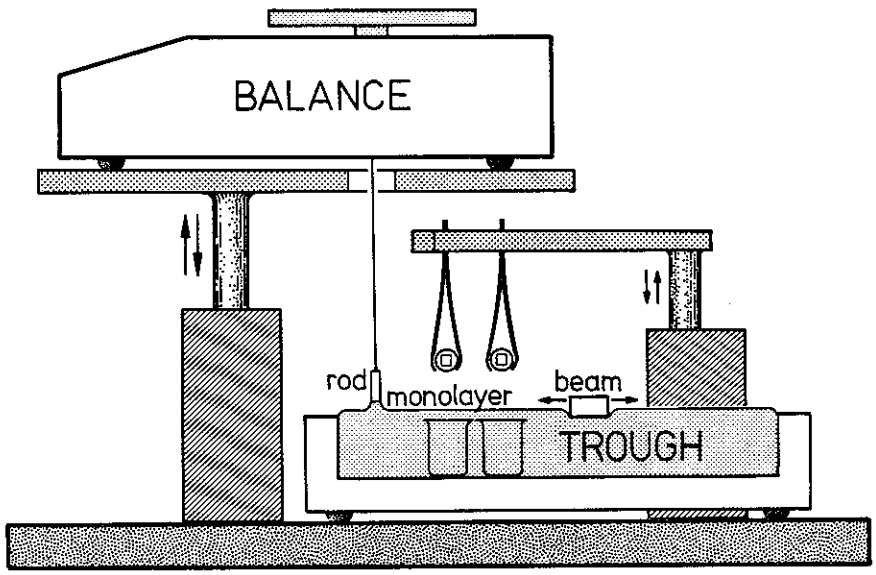

Fig. 2: Schematic drawing of the Langmuir trough. The surface tension is measured with a vertical cylindrical rod, attached to a bottom-loading balance. Langmuir-Blodgett deposition of monolayers or bilayers of lipids is done on two small mica surfaces, glued on glass discs which are clamped in two tweezers. The tweezers are attached to a horizontal steel arm which can be raised or lowered at a speed of 0.2 mm/s. For the calibration depositions, the arm supports a large mica sheet (not shown).

The method does not require any knowledge of the contact angle of the liquid attached to the rod. Use was made of a stainless steel rod of diameter 0.5 cm with sharp circular edges. After consulting the tables given by Padday et al. (1975) it was found that the surface pressure of a monolayer at the air-water interface at 21 °C depends on the maximum weight of water W underneath the rod according to $\Pi = -0.544 \cdot W + 92.556$, where Π is in dyne/cm and W is expressed in mg. With this method, surface pressures can be measured which are accurate to 0.5 dyne/cm.

2.3 LANGMUIR-BLODGETT DEPOSITION TECHNIQUE

Calibration depositions of Langmuir-Blodgett lipid films onto molecularly smooth mica sheets of length 10 cm and width 2 cm were carried out giving a total mica surface area of 40 cm^2. Each sheet was attached with two small alligator clips to a horizontal steel arm (see Fig. 2) which could be raised or lowered at a speed of 0.2 mm/s.

After sweeping the water surface in the trough several times to remove any surface-active contaminants, the mica was immersed in the water keeping its sides vertical with respect to the water surface. When the mica was fully immersed in the water, a monolayer was spread on the water surface. After allowing the spreading solvent to evaporate, the monolayer was compressed until some desired surface pressure was reached at which deposition was carried out. To deposit the lipids, the mica was raised vertically through the air-water interface keeping the surface pressure constant by slowly moving the barrier over the surface. When the mica was fully removed from the water, it was dried for 20 min. in the air of a laminar flow cabinet. Measurement of the contact angle of a water droplet on a DPPE monolayer-covered mica surface showed an advancing contact angle of 106 °. From this it follows that the surface has become hydrophobic. Clearly, the polar headgroups are directed towards the mica, while the lipid hydrocarbon tails are facing the water phase. Comparing the total mica surface area with the surface area in the trough swept by the barrier during deposition (in order to keep the deposition pressure constant) gives the average headgroup area per amphiphile on the mica. The headgroup area per amphiphile in the trough at a certain surface pressure is obtained from the Π-A isotherm.

A second layer of amphiphiles can now be deposited by lowering the monolayer-covered surface into the Langmuir trough at constant surface pressure until it is fully immersed. The headgroup area in the second layer is again found by measuring the surface area swept by the barrier during deposition.

Deposition of the first and second layers was attempted at such surface pressures (not necessarily equivalent to each other) that the amount of lipid deposited was not too sensitive to the applied surface pressure, at the same time giving a headgroup area in the

second layer which corresponds with reported equilibrium headgroup areas in lipid bilayers or vesicles.

When the forces between two deposited bilayers were to be measured, deposition was done onto two small molecularly smooth mica sheets previously glued on two cylindrically curved glass discs (see next section). The glass discs with the mica sheets were clamped in two tweezers attached with clips to the movable horizontal steel arm (see Fig. 2) and deposition was done in the same way as with the large mica sheets. It was assumed that the headgroup area of the deposited amphiphiles was equal to the values obtained from the calibration deposition experiments using the larger mica sheets.

Once the bilayers are deposited, the glass discs can not be retracted from the water as this causes the second layer to desorb. For this reason, the glass discs were put in 5-ml glass beakers standing under water in the Langmuir trough as shown in Fig. 2. The force measurement apparatus was filled with water the previous day and the water was presaturated with amphiphiles from a crystal to prevent desorption of the bilayers from the mica during the subsequent experiment. In this way, thermodynamic equilibrium was established between amphiphiles in solution and amphiphiles in the bilayers. After removing the front plate from the apparatus the glass discs are transferred under water from the trough to the force measurement apparatus where they are mounted under water. Finally, the front plate is bolted to the front of the apparatus which closes it off so that direct force measurements can now be carried out.

2.4 THE DIRECT FORCE MEASUREMENT TECHNIQUE

The force measurement device developed by Israelachvili measures the force between two mica surfaces in a crossed cylinder configuration as a function of the surface separation. A detailed account of the technique has been given before (Israelachvili and Adams, 1978) and in this section, only a brief summary will be presented.

The basic apparatus is shown in Fig. 3. It has a removable front plate with a number of inlets used for filling and draining the apparatus. The mica surfaces are mounted on two silica-glass discs with cylindrically polished surfaces facing each other with the cylinder axes perpendicular to one another. The mica sheets are first carefully

cleaved from large thick mica sheets, so that they have a uniform thickness of a few μm and a surface area of about 0.5 cm^2. Once cleaved, they are immediately placed on another freshly cleaved but thicker larger sheet (the backing sheet) where they are held down firmly by strong adhesive forces. Thus, one side of the mica sheets is protected from contamination. The exposed side of the mica sheets is then silvered by vacuum evaporation with a 480 Å thick highly reflecting layer of pure silver. Then, two silvered mica sheets of equal thickness are picked up from the backing sheet and glued down on the silica discs using a Shell epoxy resin 1004 thermosetting glue (silvered sides down). After the Langmuir-Blodgett deposition of amphiphiles on the mica is carried out, one disc is mounted on a rigid support, the other is positioned, facing the first one, on the end of a spring with a known spring constant (see Fig. 3).

The distance between the two surfaces is measured by use of an optical technique using "multiple beam interference fringes" (or fringes of equal chromatic order, FECO (Israelachvili, 1973)). The mica sheets with their outer surfaces silvered, together with the intervening medium form a symmetrical three layer interferometer. If the two surfaces are in contact and white light is passed normally through, then the emerging light consists of discrete wavelengths λ_n^0 (n = 1,2,3,...) which can be separated and measured as sharp fringes in an ordinary grating spectrometer relative to the wavelength of the mercury green and yellow lines. If the two mica surfaces are then separated by a distance D, these fringes shift to longer wavelengths λ_n^D given by

$$tan\left(\frac{2\pi\mu D}{\lambda_n^D}\right) = \frac{2\bar{\mu}sin[\pi(1\text{-}\lambda_n^0/\lambda_n^D)/(1\text{-}\lambda_n^0/\lambda_{n\text{-}l}^0)]}{(1+\bar{\mu}^2)cos[\pi(1\text{-}\lambda_n^0/\lambda_n^D)/(1\text{-}\lambda_n^0/\lambda_{n\text{-}1}^0)]\pm(\bar{\mu}^2\text{-}1)} \tag{37}$$

where + refers to odd order fringes (n odd) and - refers to even order fringes (n even). $\bar{\mu} = \mu_{mica}/\mu$, where μ_{mica} is the refractive index of mica at λ_n^D, and μ the refractive index of the medium between the two mica surfaces at λ_n^D. The fringe order is calculated using the formula

$$n = \lambda_{n\text{-}1}^0/F_n(\lambda_{n\text{-}1}^0 - \lambda_n^0)$$

$$F_n = 1.024 + \frac{1}{n}. \tag{38}$$

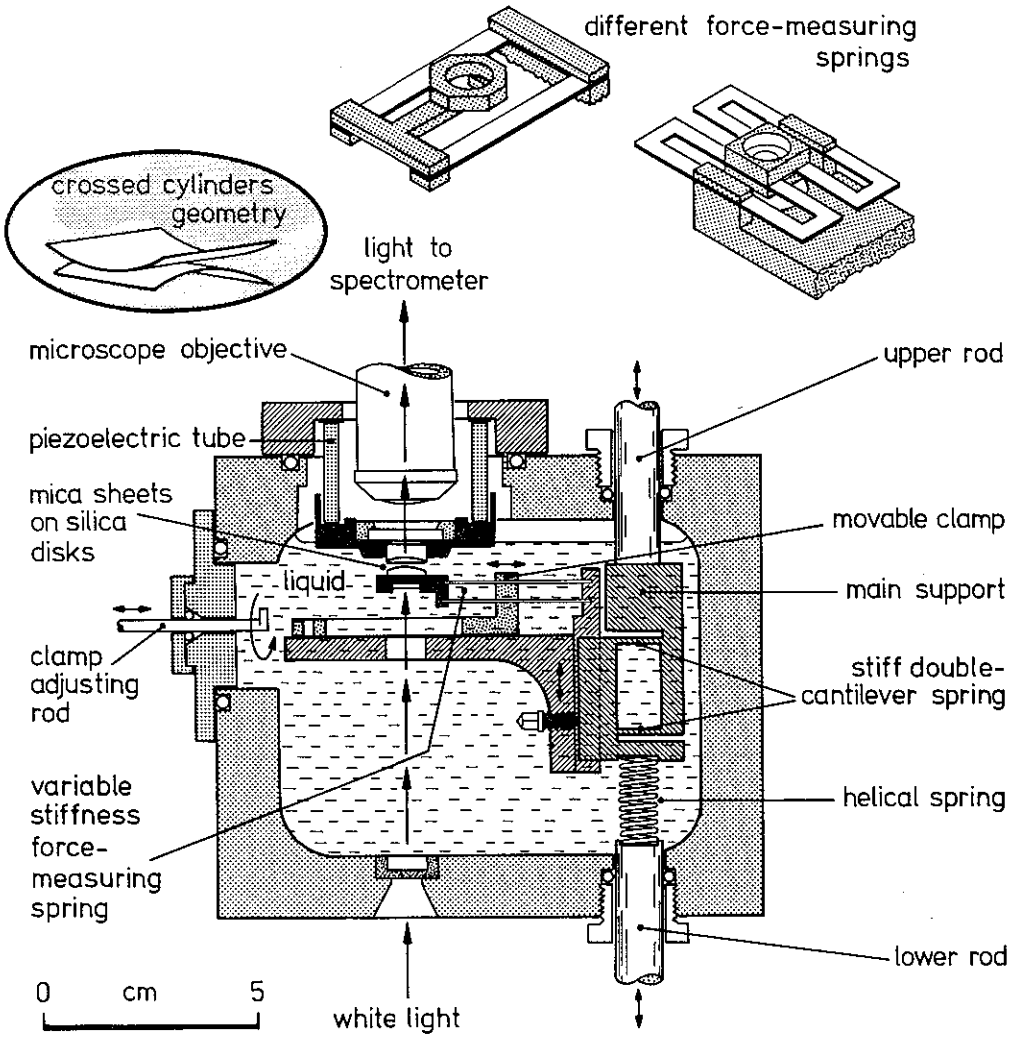

Fig. 3: Schematic drawing of the force measurement apparatus. The force is measured between two molecularly smooth curved surfaces in liquid with a surface separation resolution of ~ 1 Å^2 using white light and multiple beam interferometry. The mica surfaces are glued onto two optically polished silica-glass discs. The lower disc is mounted on a double-cantilever force-measuring spring whose stiffness can be varied by a factor of 1000 by shifting the position of the dove-tail clamps using the positioning rod. This spring can be replaced by any of the other non-variable springs shown above. The spring shown at the right has the advantage of being non-tilting and non-shearing which is important when large surface forces are present.

By use of Eq. (37), both the distance D and the medium refractive index μ can be determined independently by measuring the shifts in wavelengths of an odd and an even fringe. The accuracy is often as good as 1 Å for D.

Because mica is birefringent, the fringes generally appear as doublets, the

separation of which depends on the relative crystallographic orientation of the two mica sheets. Wavelength measurements are performed on one of these components only and the refractive index for this component is calculated from the separation of the doublet and a knowledge of the mean refractive index of the mica, which in nature exists as brown mica or green mica. The mean refractive index of brown and green mica is reported (Israelachvili and Adams, 1978) as

$$\mu_{Brown} = 1.5820 + \frac{4.76 \times 10^5}{(\lambda_n^D)^2/\mathring{A}};$$
$$\mu_{Green} = 1.5930 + \frac{4.76 \times 10^5}{(\lambda_n^D)^2/\mathring{A}}. \tag{39}$$

If the mica sheets were exactly parallel, the fringes would appear as vertical lines in the spectrometer. Because of the crossed cylinder geometry, which to leading order is equivalent to a sphere on a flat, the shape of the fringes is parabolic. The entrance slit of a spectrometer samples a cross-section of the surfaces defined by the positioning of a two prism system used to direct the light beam into the spectrometer. By using a system of three prisms, a cross-section of the surfaces at right angles to the first can be studied. This allows the measurement of the radii of curvature in two perpendicular directions from the shapes of the parabolic fringes during an experiment. The mean radius of curvature is calculated by taking the geometric average $(R_1R_2)^{1/2}$ of the two radii (typically 1-2 cm). Thus, the fringe profile seen in the spectrometer essentially reflects the shape of a slice through the curved surfaces and gives information on the local radius of curvature as well as on surface deformations occurring under the influence of strong forces. The lateral resolution is of the order of a few microns and is limited by the magnification of the optical system (about 25× in these experiments). Because the refractive index of the medium between the surfaces can be measured, it also provides a method for the determination of the quantity of material deposited or adsorbed on the surfaces when its refractive index is known beforehand. Finally, from the shapes of the two initially curved surfaces any adhesive deformation and fusion of bilayers can be directly monitored with time during the course of an experiment.

The distance between the two surfaces is controlled by use of a three stage mechanism of increasing sensitivity. The coarse control uses a stepper motor attached to the upper rod in Fig. 3 which allows a positioning to within 1 μm; the medium control consists of a synchronous motor connected to the lower rod and allows positioning to about 10 Å. A piezoelectric crystal (which expands or contracts vertically by $\sim$ 5 Å per volt applied axially across the cylindrical wall of the rigid support) is used for the final positioning to about 1 Å.

Given the facility for moving the surfaces toward or away from each other and, independently, of measuring their separation each with a sensitivity or resolution of about 1 Å, the force measurements themselves now become straightforward. The force is measured by expanding or contracting the piezoelectric crystal by a known amount and then measuring optically how much the two surfaces have actually moved. Any difference in the two values when multiplied by the stiffness of the measuring spring gives the force difference between the initial and final positions. In this way, both repulsive and attractive forces can be measured with a sensitivity of about 10 mdyne, and a full force-law can be obtained over any distance.

In the present study, an important experimental advance is the introduction of a variable spring (see Fig. 3). This was particularly useful in the measurement of van der Waals forces between uncharged amphiphile bilayers (see Chapters 3 and 4). When two surfaces approach each other and the gradient of the surface force equals the spring constant, an instability occurs and the surfaces suddenly jump into contact (see Fig. 4). By varying the spring constant we obtain the gradient of the attractive force as a function of the surface separation at which they jump into contact. Also, the surfaces will jump apart from each other at a surface separation where the gradient of the interaction force equals the spring constant. From Fig. 4 which gives the typical interaction force between two uncharged bilayer surfaces, it is seen that this occurs almost exactly at the minimum located at $D = D_0$ in the force versus distance curve.

The force measurements between the cylindrically curved bilayers are quantitatively analyzed using the Derjaguin approximation (Derjaguin, 1934). When two

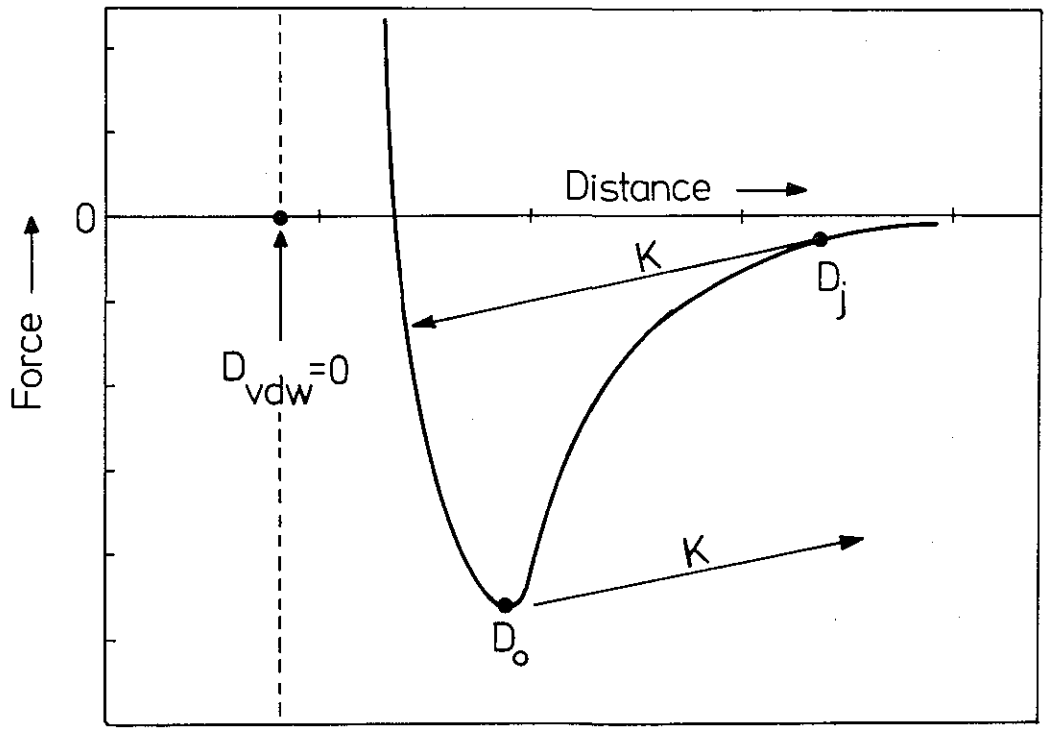

Fig. 4: Schematic picture of the interaction force between two uncharged lipid bilayers as a function of the distance D between them. The anhydrous bilayer/water interface is located at D = 0, and the effective van der Waals plane is at $D_{VDW} = 0$ (see also Chapter 3). When the bilayers are brought together, they jump into contact from $D = D_j$ as indicated by the arrow where the gradient of the interaction force equals the spring constant K. Upon separation of the bilayers, they jump apart from $D = D_0$.

crossed cylindrically curved surfaces of radii R at a separation D exert a force F(D) on each other, then according to the Derjaguin approximation, the equivalent interaction energy E(D) between two flat surfaces per unit area is related to F(D) by

$$E(D) = \frac{F(D)}{2\pi R} \tag{40}$$

provided that $R \gg D$. In the present experiments, the bilayers have a radius of curvature of about 1.5 cm. Interactions between bilayers were only measurable at surface separations less than 2000 Å, so that the Derjaguin approximation should be valid.

CHAPTER 3

FORCES BETWEEN GALACTOLIPID BILAYERS

3.1 INTRODUCTION

Galactosyl diglyceride lipids are the most abundant lipids in plant cell thylakoid membranes. The recent neutron diffraction work by R.V. McDaniel (unpublished) has elucidated the bilayer structure of DGDG. He reports the polar headgroups of DGDG to be orientated approximately parallel to the plane of the bilayer and also identified the existence of a hydration force using the osmotic stress technique described by Le Neveu et al. (1976, 1977) and Parsegian et al. (1979).

In the present study, the emphasis will be on the measurement of the attractive and adhesion forces between galactolipid bilayers, which are inaccessible with the osmotic stress technique. The short-range hydration forces and the monolayer compression isotherms of MGDG and DGDG were studied as well. The simultaneous measurements of the monolayer compression isotherms and the interbilayer forces are important to understand the packing properties of galactolipids in highly curved bilayer membranes like the inner thylakoid margins in plant cells (Murphy, 1982).

3.2 RESULTS

3.2.1 Monolayer Compression Isotherms and Langmuir-Blodgett Deposition

Fig. 5 gives the measured monolayer compression isotherms of the galactolipids. Both monolayers are seen to be of the liquid-expanded type which must be a consequence of unsaturation of the hydrocarbon chains. That the DGDG monolayer is slightly more expanded than the one of MGDG is probably the result of the difference in the sizes of their headgroups.

Fig. 6 gives the deposition of the galactolipids at various surface pressures on a first layer of DPPE which was deposited at a deposition pressure of 33 dyne/cm giving

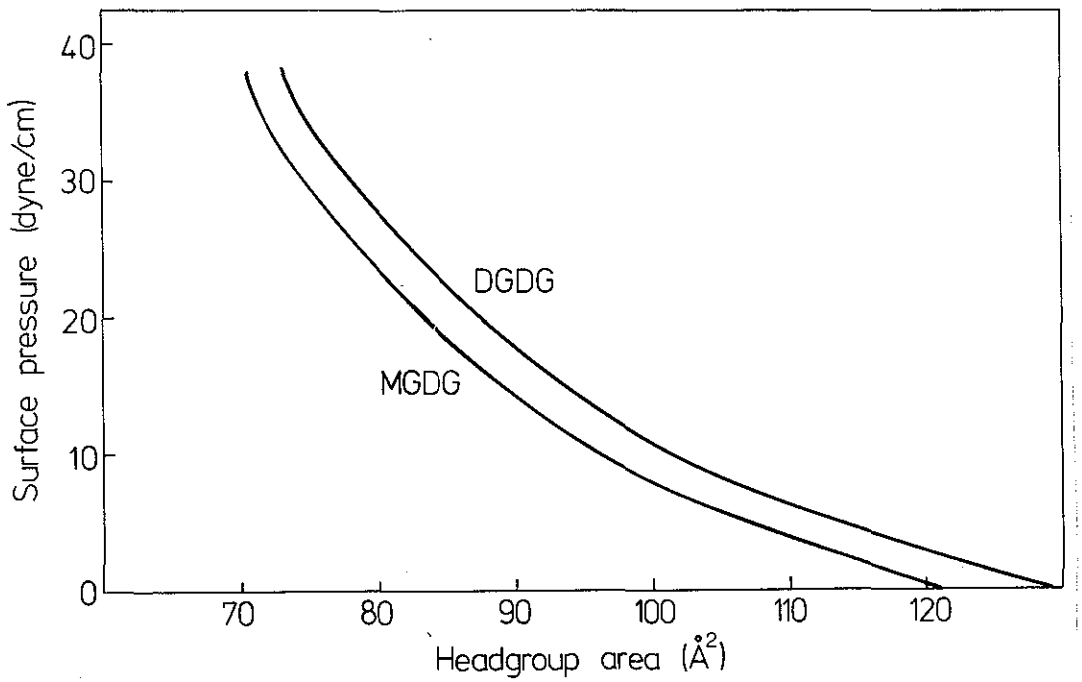

Fig. 5: Monolayer compression isotherms of monogalacotyldiglyceride (MGDG) and digalactosyldiglyceride (DGDG) at 21 °C.

rise to a deposited headgroup area of 42 $Å^2$. This first layer of DPPE appeared to be particularly suitable for the deposition of a second layer of lipids especially when they exist in the fluid phase (see Chapter 4). We see in Fig. 6 that beyond a surface pressure of 26 dyne/cm, the headgroup area of the deposited galactolipids becomes the same as the headgroup area of the galactolipids at the air/water interface. Although the equilibrium headgroup area of these lipids in a bilayer is uncertain, it was assumed that this area is about 72 $Å^2$ for MGDG and 75 $Å^2$ for DGDG. To obtain these headgroup areas, the deposition of the galactolipids was done at 32 and 35 dyne/cm, respectively.

3.2.2 Thickness of the Deposited Bilayers and Operational Definition of the Bilayer-Water Interface

Before describing results of force measurements between bilayer surfaces at the angstrom level, it is appropriate first to establish where these surfaces are. This point is particularly important for bilayers because unlike solid surfaces, they are fluid and dynamically mobile-characterized by thermal undulations and fluctuations of the bilayers as a whole, the hydrocarbon-water interface and the protruding headgroups.

The configuration of the bilayers deposited on the two apposing mica surfaces is

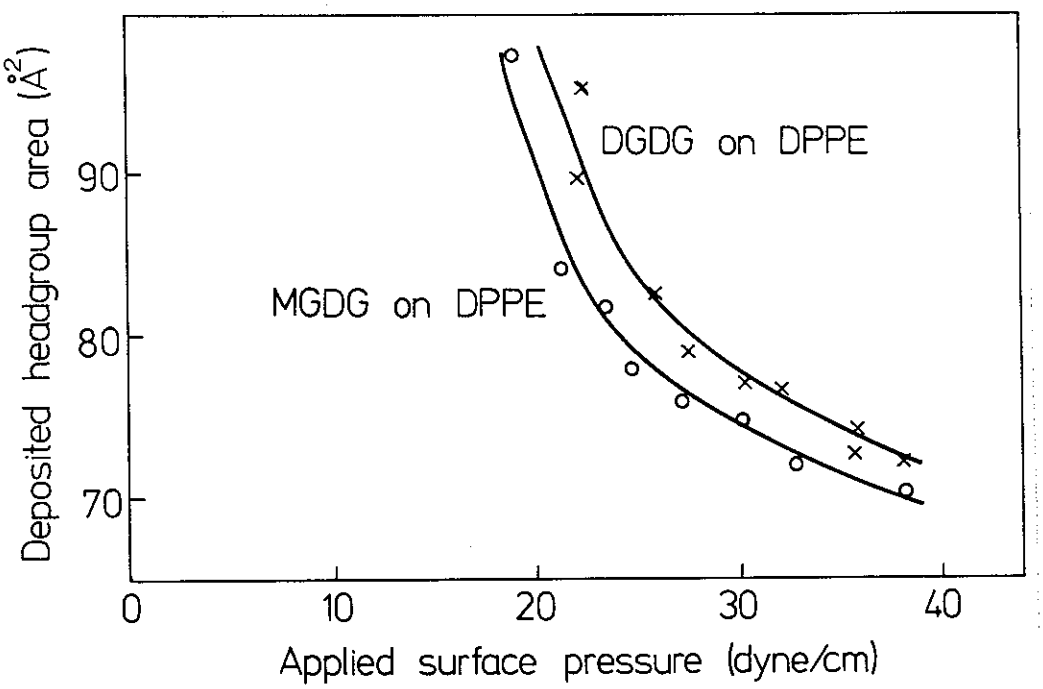

Fig. 6: Deposition of the galactolipids MGDG and DGDG as second layers on a first layer of DPPE, where the DPPE is deposited at a headgroup area of 42 $Å^2$.

shown schematically in Fig. 7 where the interbilayer separation is defined by D. D = 0 corresponds to hypothetical contact with no water left between the two bilayers. Of course, in practice headgroup penetration into the aqueous space and the hydration force needed to fully dehydrate them may be so large that D = 0 is never attained, but this does not alter the convenience of this operational definition of D, which is the same as that adopted by Le Neveu, Rand, Parsegian, Lis, and co-workers for describing interbilayer forces in zwitterionic multibilayer systems using an osmotic stress technique.

Using a liquid hydrocarbon density of 0.80 (the value for octadecane) we calculate for the volume of the hydrocarbon chains of two 18:3 galactolipid molecules in the fluid phase a value of 2200 $Å^3$. This is added to the volume of two propanediol-molecules-241 $Å^3$ (glycerol backbone) and the volume of two galactose molecules (46.5 $Å^3$ per HCOH group)-558 $Å^3$. With a headgroup area of 72 $Å^2$ for MGDG, this results in an anhydrous MGDG bilayer thickness T = 42 Å. For a DGDG bilayer with a headgroup area of 75 $Å^2$, an anhydrous bilayer thickness T = 47 Å is calculated in the same way.

As is seen in Fig. 7, the distance D follows from the definition $D = T_1 - T$. The

calibration of $T_1 = 0$ was conveniently accomplished at the end of an experiment by slowly draining the apparatus of water which removes the second monolayer, exposing only the hydrophobic first layer, and then bringing these two monolayers into contact in air. These manipulations allow the position of $D = 0$ to be pinned down in each experiment which is also required to obtain the distance range of the short-range hydration force, i.e. the distance between $D = 0$ and $D = D_0$ in Fig. 4. At $D = D_0$, the two curved surfaces jump apart from each other under a pull-off force. Then according to Eq. (40)

$$\begin{aligned} \frac{\partial F(D)/R}{\partial D} &= 2\pi\left(\frac{\partial E(D)}{\partial D}\right)_{D=D_0} \\ &= 2\pi P_{FS}(D_0) \\ &= 0. \end{aligned} \tag{41}$$

$P_{FS}(D_0)$ is the interaction pressure between flat bilayers in contact with each other at a distance $D = D_0$. In adhesive contact there exists a balance between the repulsive hydration forces and the attractive van der Waals forces. Hence the distance $D = D_0$ is equivalent to the equilibrium separation between planar bilayers where the net interaction pressure is zero. It also corresponds to the difference between the (by X-ray or neutron diffraction) measured repeat spacings in multibilayer systems at 100% hydration and at 0% hydration (after an adjustment for the change in the anhydrous bilayer thickness itself) which has been used by Le Neveu et al. (1976, 1977) and Lis et al. (1982a) to establish the distance range of the hydration force in zwitterionic multibilayer systems, and by McDaniel in DGDG multibilayer systems.

3.2.3 Van der Waals Forces and Hydration Forces between Galactolipid Bilayers

Since galactolipids are uncharged, there is no electrostatic double-layer force to be expected. This was indeed confirmed in the experiments. The absence of electrostatic interaction also proves that the mica does not interfere with the measured surface forces. This is due to the fact that when a monolayer is deposited on the mica, the mica is raised through the air/water interface into the air where the whole system has to be

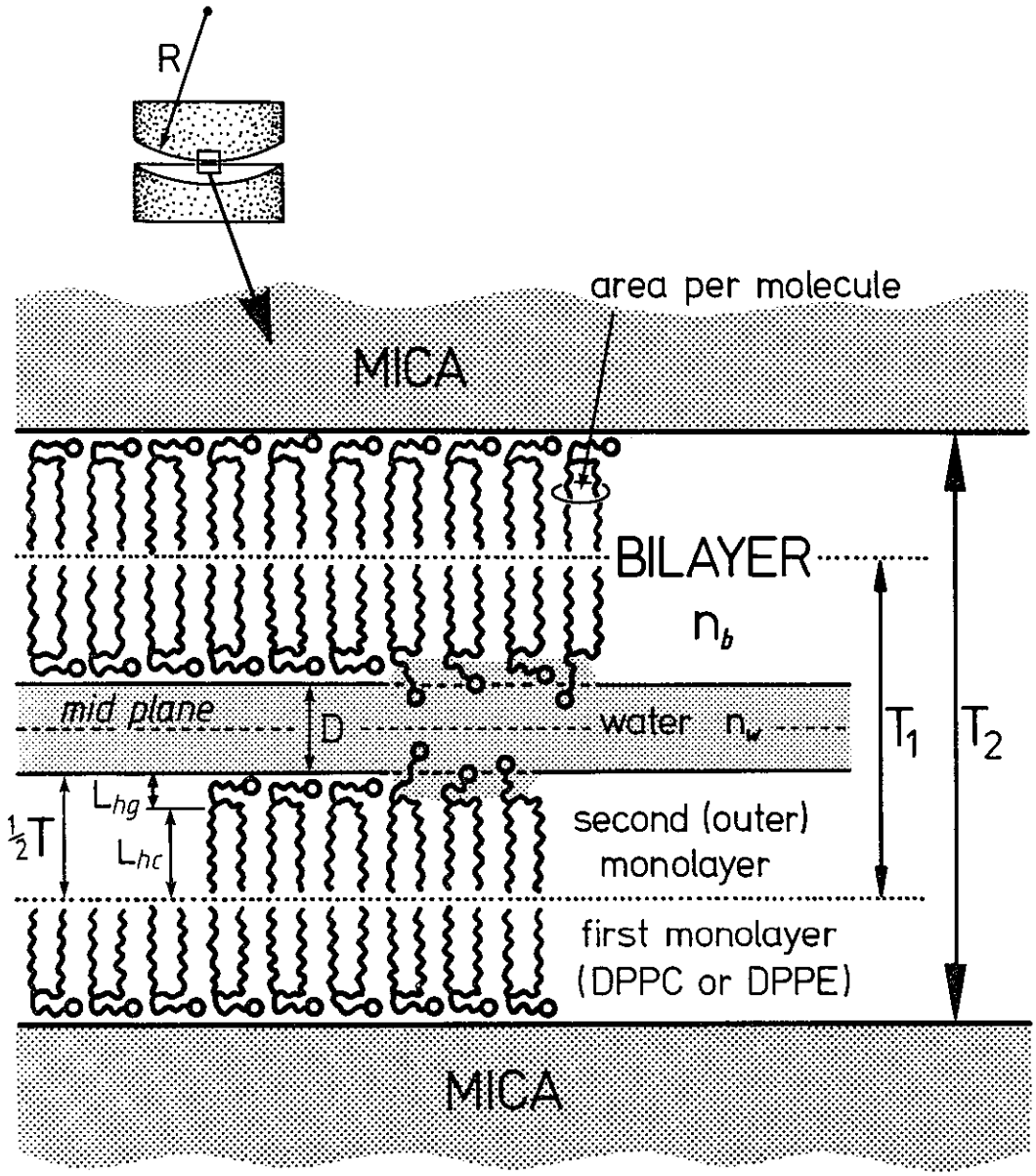

Fig. 7: Definition of distances and refractive indices for two planar surfaces with an adsorbed or deposited bilayer on each. For two cylindrically curved surfaces of radius R at a distance D apart, the force F(D) between them is related to the interaction energy per unit area E(D) between two planar surfaces by $E(D) = F(D)/2\pi R$ (Derjaguin, 1934).

electrostatically neutral. The counterions of the initially charged mica surface are trapped between the mica and the monolayer. When brought back into the water phase to deposit a second layer, the mica can not become dissociated any more since ions from the mica surface are unable to cross the lipid bilayer. Hence, surface forces essentially originate from the bilayer surfaces.

The van der Waals forces were measured using the variable spring method which, as discussed in the previous Chapter, allows the measurement of the gradient of the surface force with respect to bilayer separation. The spring stiffness could be varied over about three orders of magnitude. Taking the (non-retarded) van der Waals interaction according to Eq. (33) and applying Eq. (40), it follows that for each spring constant K, an inward jump occurs at

$$D_j = \left(\frac{AR}{3K}\right)^{1/3}. \tag{42}$$

Strictly, D_j represents the distance from where the surfaces jump relative to the van der Waals plane $D_{VDW} = 0$. In the case of two interacting mica surfaces, the definition of $D_{VDW} = 0$ where the attraction becomes infinitely large, presents no problem. However, as we have seen, the lipid/water interface is not unambiguously defined and it is not obvious either that the van der Waals plane should coincide with $D = 0$, because of the very possibility of headgroup penetration into the aqueous region beyond $D = 0$. Hence, the best thing to do at this stage is to define the van der Waals plane as an effective lipid/water interface with respect to the van der Waals interaction, and which is to be determined experimentally.

The distance D_j can also well be different from the distance over which the surfaces jump before coming to rest (see Fig. 4). This arises when short-range repulsive forces begin to dominate the interbilayer interaction beyond $D_{VDW} = 0$. Because the location of $D_{VDW} = 0$ is unknown beforehand, the distances D_j were measured relative to $D = 0$. Then a plot of $(R/3K)^{1/3}$ versus D_j yields A from the slope (independent of $D_{VDW} = 0$), and $D_{VDW} = 0$ relative to $D = 0$ is obtained from the extrapolated intercept with the horizontal axis (infinite spring constant).

Of course, this procedure is only justified provided Eq. (33) holds for all distances down to $D_{VDW} = 0$. Rigorously, Eq. (33) is only valid for two interacting uniform halfspaces. In our system, the bilayers have a thickness of about 45 Å. Besides, the influence of the van der Waals interaction from the mica on which the bilayers are deposited has to be taken into consideration. However, according to Ninham and Parsegian (1970), when the bilayer separation is less than the bilayer thickness, the

influence of the underlaying medium is small and can be ignored in a first approximation, at the same time taking the bilayers as halfspaces. This approximation holds the better, when the Hamaker constants of the two media across water are not too different from each other (the non-retarded Hamaker constant for mica across water is about three times larger (Israelachvili, 1985a) than the one for hydrocarbon across water, which should not be too serious).

Fig. 8 gives the distances between DGDG bilayers from which they jump into contact in pure water as a function of $(R/3K)^{1/3}$. The same figure also gives the jump distances in the presence of 0.2 M NaCl. It is seen that below D = 4 nm a straight line can be drawn through the experimental points which indicates that in that region the interaction indeed can be described by Eq. (33).

Extrapolation of the straight lines to $(R/3K)^{1/3} = 0$ cuts the distance axis at D = 6 Å, both in pure water and in the presence of 0.2 M NaCl. As discussed above, this is the location of the effective van der Waals plane of origin $D_{VDW} = 0$.

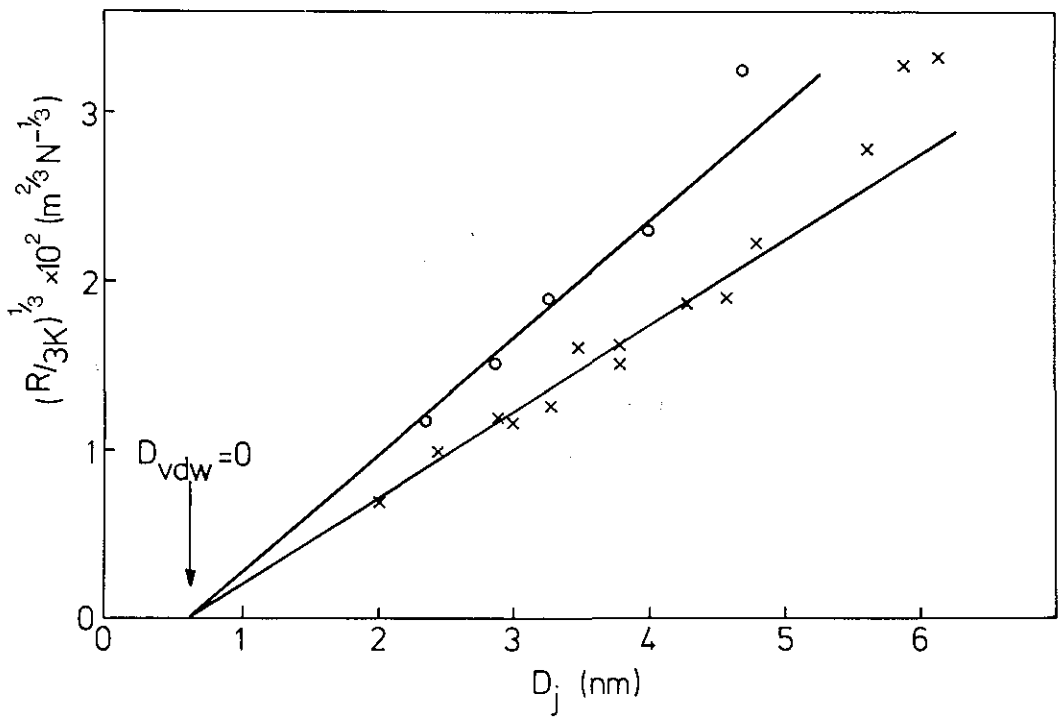

Fig. 8: Inward jump experiments between two deposited DGDG bilayers. The crosses (×) represent the jumps in pure water. The open symbols (o) represent the jumps in the presence of 0.2 M NaCl. In each case, the effective plane of origin of the van der Waals force is located at D = 6 Å.

From the slope of the two curves in Fig. 8, the Hamaker constants were calculated to be $A = 7.5 \pm 1.0 \times 10^{-21}$ J in pure water and $A = 3.1 \pm 0.6 \times 10^{-21}$ J in 0.2 M NaCl. The decrease of the Hamaker constant upon addition of NaCl is most likely due to the screening of the temperature-dependent contribution to the van der Waals interaction as predicted by Lifshitz theory (Davies and Ninham, 1972; Mitchell and Richmond, 1973). At jump distances exceeding D = 50 Å, it is seen in Fig. 8 that the experimental points begin to deviate from the straight line which is likely to be the result of retardation of the van der Waals force at large surface separations and might be related to the breakdown of Eq. (33) at these distances.

When the bilayers jump into contact, a short-range repulsion is experienced. Fig. 9 gives the short-range interaction between DGDG bilayers and MGDG bilayers. For DGDG bilayers, the calculated van der Waals force is also shown using the experimental $A = 7.5 \times 10^{-21}$ J, the measured location of $D_{VDW} = 0$ and Eq. (33). For MGDG bilayers, the location of $D_{VDW} = 0$ was not investigated, hence only the short-range repulsive force is given.

Upon separation of the bilayers under a pull-off force, the DGDG bilayers jumped apart at a separation $D_0 = 13$ Å with an adhesion force $(F/R)_{D_0} = -1.8 \pm 0.4$ mN/m. The jump-apart distance between MGDG bilayers was at $D_0 = 6$ Å with an adhesion force $(F/R)_{D_0} = -3.0 \pm 0.5$ mN/m. Because the van der Waals plane is at D = 6 Å for DGDG bilayers, the distance $D_0 = 13$ Å corresponds to $D_{VDW} = 7$ Å. With the help of Eq. (33), the Hamaker constant A_{Adh} can now be calculated from the force of adhesion. The result $A_{Adh} = 5.3 \pm 1.5 \times 10^{-21}$ J agrees reasonably with the Hamaker constant found from the inward jump experiments. It must be noted however, that the force of adhesion gives a minimum value for the van der Waals attraction at $D = D_0$, since any repulsive contribution from the short-range forces at D_0 is not included. But because short-range forces are strongly dependent on the bilayer separation (see Fig. 9) and fall off rapidly near D_0, it is not expected that this contribution is significant.

3.3 DISCUSSION

The Hamaker constants deduced from the inward jump measurements and

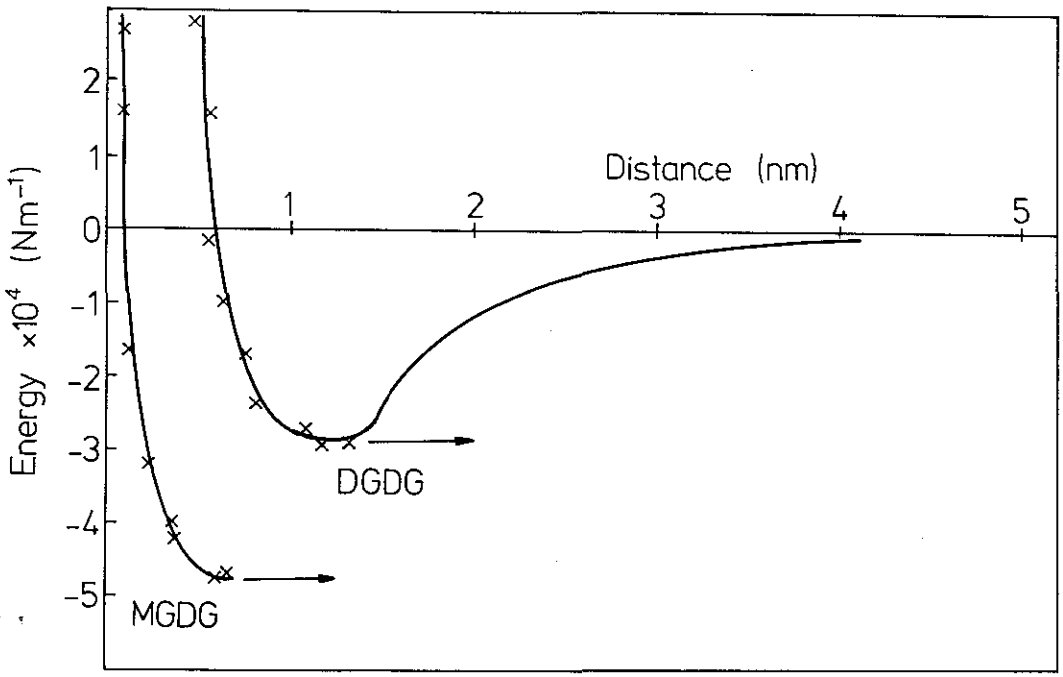

Fig. 9: Interaction energy E(D) between galactolipid bilayers in water (no salt) as a function of the bilayer separation. DGDG bilayers (right curve) have an energy minimum at $D_o \simeq 1.3$ nm; MGDG bilayers (left curve) have a deeper energy minimum at $D_o = 0.6$ nm. Beyond D = 1.3 nm, the long-range van der Waals attraction between DGDG bilayers is also given. Below D = 1.3 nm (DGDG) or D = 0.6 nm (MGDG), the bilayer interaction is strongly repulsive due to the short-range hydration/steric interaction.

adhesion force measurements on DGDG bilayers in pure water ($7.5 \pm 1.0 \times 10^{-21}$ J and $5.3 \pm 1.5 \times 10^{-21}$ J, respectively) agree well with the theoretically predicted value $A = 6 \times 10^{-21}$ J for hydrocarbon interacting across water (Parsegian and Ninham, 1970). According to Lifshitz theory (Mahanty and Ninham, 1976), the magnitude of the Hamaker constant results from two contributions: the temperature-dependent contribution and the dispersion contribution. Both contributions are of roughly equal magnitude ($\sim 3 \times 10^{-21}$ J).

Lifshitz theory predicts a screening of the temperature-dependent contribution upon addition of electrolyte. In 0.2 M NaCl the temperature-dependent contribution is predicted to be almost completely absent (Davies and Ninham, 1972; Mitchell and Richmond, 1973) which is confirmed (for the first time) in the present experiments, showing a Hamaker constant of only $3.1 \pm 0.6 \times 10^{-21}$ J.

Following our definition of $D = 0$, the distance D_0 is equivalent to a layer of hydration water between the bilayers of thicness D_0. This however should not be taken to imply that there is no headgroup penetration into this hydration layer. A clear indication for this is the location of $D_{VDW} = 0$ at a separation $D = 6$ Å, which can only be obtained if the digalactosyl diglyceride headgroups protrude somewhat into the water phase instead of lying flat on the bilayer surface. The bilayer separation where $D_{VDW} = 0$ can be considered as the effective van der Waals separation of hydrocarbon in water which at least in this system is seen to be different from what was assumed by Lis et al. (1982a) who identify $D_{VDW} = 0$ with $D = 0$. Their assumption also implied that the short-range repulsion energy at a particular bilayer separation was identical to the free energy necessary to dehydrate the bilayers in order to bring them to that particular bilayer separation. This cannot be completely true when the headgroups protrude into the water phase because in that case there will be an extra steric (or entropic) interaction between the mobile headgroups which is additional to the hydration interaction (see also Chapter 4).

The measured thickness of the hydration layer between MGDG bilayers is 6 Å, between DGDG bilayers this is 13 Å. The latter value agrees reasonably with the reported 10 Å by McDaniel (unpublished). These thicknesses clearly show that a doubling of the number of galactose units on the bilayer surface doubles the amount of hydrated water on the bilayer surface, which is expected intuitively.

A consequence of the difference in hydration is that the force of adhesion between MGDG bilayers is about twice that between DGDG bilayers. This is an example of the indirect modulation of the van der Waals interaction at small surface separations through the presence of short-range interactions which determine the equilibrium separation between bilayers. The more hydrated DGDG bilayers must have their equilibrium separation farther away from $D_{VDW} = 0$ than MGDG bilayers. That the DGDG headgroup is more hydrated than the MGDG headgroup is also consistent with the larger headgroup area of DGDG (cf. Fig. 5) as well as the different molecular packing geometries of the respective lipids in photosynthetic thylakoid membranes

(Murphy, 1982). In these assemblies, MGDG lipids are especially abundant in the highly curved concave inner thylakoid margins indicating a stabilization of the membrane curvature through a cone-shaped molecular geometry, whereas DGDG lipids are believed to be mostly located in the convex marginal surfaces of thylakoids (wedge-shaped molecular geometry). It is likely that high concentrations of MGDG lipids (40% in Zea mays chloroplasts) also serve to locally stabilize the many concave deformities in the thylakoid membranes.

CHAPTER 4

FORCES BETWEEN BILAYERS OF THE ZWITTERIONIC PHOSPHOLIPIDS PC AND PE IN AQUEOUS SOLUTIONS

4.1 INTRODUCTION

The zwitterionic phospholipids phosphatidylcholine (PC) and phosphatidylethanolamine (PE) are the main lipid constituents in animal cell membranes. It is interesting to see that like the galactolipids which are the most abundant lipids in plant cell membranes, they are intrinsically uncharged. However, unlike galactolipids, they can acquire a net charge through the binding of divalent ions as has been shown by electrophoresis, conductance and NMR studies on PC vesicles (Grasdalen et al., 1977; McLaughlin et al., 1978; Altenbach and Seelig, 1984) and the swelling of a PC multilamellar system (Lis et al., 1981; Ohshima et al., 1982) in divalent electrolyte solutions.

The interesting properties of zwitterionic dipoles on the bilayer surface have been the subject of several studies, using techniques like NMR (Hauser et al., 1981; Finer and Darke, 1974), X-ray (Franks, 1976; Lewis et al., 1983) and neutron diffraction (Hauser et al., 1981; Worcester and Franks, 1976; Buldt et al., 1978). They have yielded valuable insight concerning the conformation and mobility of the dipoles, which will be used later in this chapter when the results of force measurements between the bilayers are discussed.

Although the chemical structure of the PC headgroup is not very different from the PE headgroup (see Fig. 1), the hydration properties are quite different. This has been evident for a long time from the observation that anhydrous PC bilayers swell much more (Le Neveu et al., 1976, 1977; Parsegian et al., 1979; Lis et al., 1982a) than

PE bilayers (Seddon et al., 1984) on addition of water. The work of Le Neveu, Rand, Lis and Parsegian has emphasized the importance of hydration forces in PC lamellar systems. The presence of PE has been found to promote the fusion of phospholipid vesicles (Sundler et al., 1981). On the other hand, PC strongly inhibits fusion. These observations are likely to be related to the differences in the hydration and hence the geometrical packing properties of these lipids.

Horn (1984) has investigated PC interbilayer interactions and observed their fusion using the direct force measurement technique of Israelachvili after letting lecithin bilayers adsorb onto mica from a vesicle solution. However, this method proved not to be completely satisfactory. Apart from reproducibility problems, electrostatic double-layer interactions originating from the supporting mica surfaces could not be suppressed which obscured the interactions existing between the bilayers alone.

This chapter will discuss the interbilayer interactions when the PE and PC bilayers are deposited on mica using the Langmuir-Blodgett technique. A number of detailed studies has already been published (see Discussion) concerning various properties of zwitterionic bilayers which together with the results of the present study allows a detailed picture to emerge of the complicated nature of the zwitterionic surface. For instance, an interesting circumstance of the present work is that the bilayers are essentially fixed in their position on the mica surfaces whereas in the lamellar system studied by Lis et al. (1982a) the bilayers are free (and hence subject to thermal thickness fluctuations and undulations of the bilayers as a whole). A comparison of the interactions measured in the two systems allows us to investigate the importance of surface fluctuations and undulations on the total interaction and to obtain a better insight into the molecular mechanism responsible for the short-range repulsion.

4.2 RESULTS

4.2.1 Monolayer Compression Isotherms of PC and PE

Monolayer compression isotherms of four different phospholipid monolayers at the air-water interface are shown in Fig. 10. The isotherms were measured at 16 °C (DMPC), 20 °C (DPPC) and 21 °C (DPPE, DLPC).

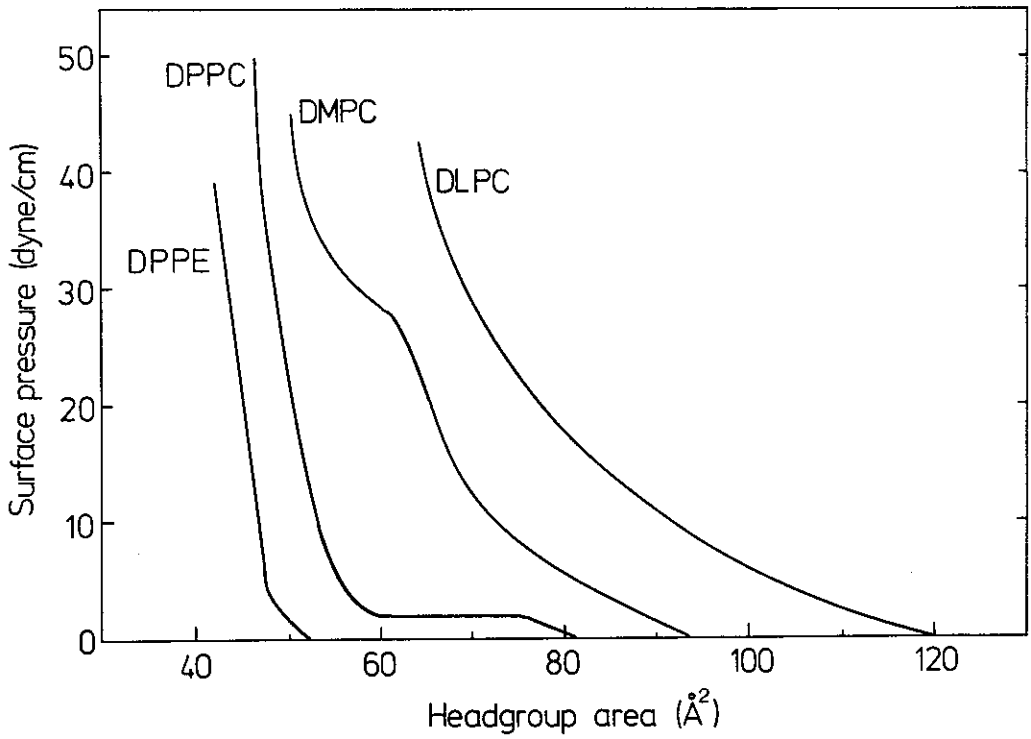

Fig. 10: Monolayer compression (Π-A) isotherms of DPPE, DPPC, DMPC and DLPC.

The DPPC and DMPC isotherms show the characteristic features of phase transitions described by several authors (Phillips et al., 1968; Albrecht et al., 1978). For example, at 20 °C, the DPPC monolayer is in the liquid-expanded state below $\Pi = 2$ dyne/cm, in the liquid-condensed state between $\Pi = 2$ dyne/cm and $\Pi = 13$ dyne/cm and in the solid state beyond $\Pi = 13$ dyne/cm. The transition between the liquid-expanded and the liquid-condensed state is first order; the transition between the liquid-condensed state and the solid state is of second order.

Regions of the Π-A curves of particular interest are the parts in the neighbourhood of headgroup areas which correspond to the expected headgroup areas of lipids in a fully hydrated bilayer at the same temperature. The headgroup areas are (Lis et al., 1982a; Lewis and Engelman, 1983): DPPE - 42 Å^2 (solid state); DLPC - 70 Å^2 (liquid-expanded state); DMPC - 52 Å^2 (liquid-condensed state) and DPPC - 52 Å^2 (solid state). These headgroup areas are approximate ones. Because of stability problems, there is hardly any information available about headgroup areas of lipids in bilayers which are in the gel phase.

At 16 °C, DMPC bilayers are in the pretransition phase and go over into the

liquid phase at the chain melting temperature T = 24 °C. This T = 24 °C is also the Krafft point of DMPC and the temperature beyond which the monolayer compression isotherm is completely of the liquid-expanded type. At 16 °C, the monolayer is in the liquid-condensed state when compressed to a lipid headgroup area of 52 $Å^2$. For DPPC bilayers, the situation is qualitatively the same. At 20 °C, the bilayer is in the gel phase while the monolayer at a headgroup area of 52 $Å^2$ is in the solid state. Between 32 and 42 °C, the bilayer is in the pretransition phase while the monolayer at a headgroup area of 52 $Å^2$ is in the liquid-condensed state. At T = 42 °C (Krafft temperature of DPPC), the bilayer goes over to the liquid phase and the monolayer becomes completely of the liquid-expanded type. At room temperature, the DLPC and DPPE bilayers exist in the liquid phase and the solid phase, respectively, while the monolayers are in the liquid-expanded state and the solid state.

We see that in the region where the monolayer is compressed to a lipid headgroup area that corresponds to the headgroup area in the bilayer, there exist parallel physical states and transitions in the monolayer and the bilayer. In the monolayer, the solid, liquid-condensed, and liquid-expanded states correspond to the gel phase, pretransition phase and liquid phase in the bilayer, respectively.

4.2.2 Deposition of PE and PC Bilayers onto Mica

Fig. 11 gives the deposited headgroup area of DPPE as a function of the applied surface pressure. One curve gives the deposition of the first lipid layer on mica, and the second curve of the second layer on the first layer. For the first layer, there was always a 1:1 correspondence between the surface area of the mica sheets and the area swept by the barrier in the Langmuir trough in order to keep the surface pressure constant during deposition. For the second layer of DPPE, this was only true for surface pressures exceeding 25 dyne/cm. Deposition at $\Pi = 33$ dyne/cm was done to deposit bilayers in force measurement experiments, because this gives a lipid headgroup area of 42 $Å^2$.

Fig. 12 gives the deposition results for DLPC. Deposition of the first layer of DLPC on mica gave no problems. It was noticed that the headgroup area of deposited DLPC at most surface pressures was about 10% smaller than the DLPC headgroup area

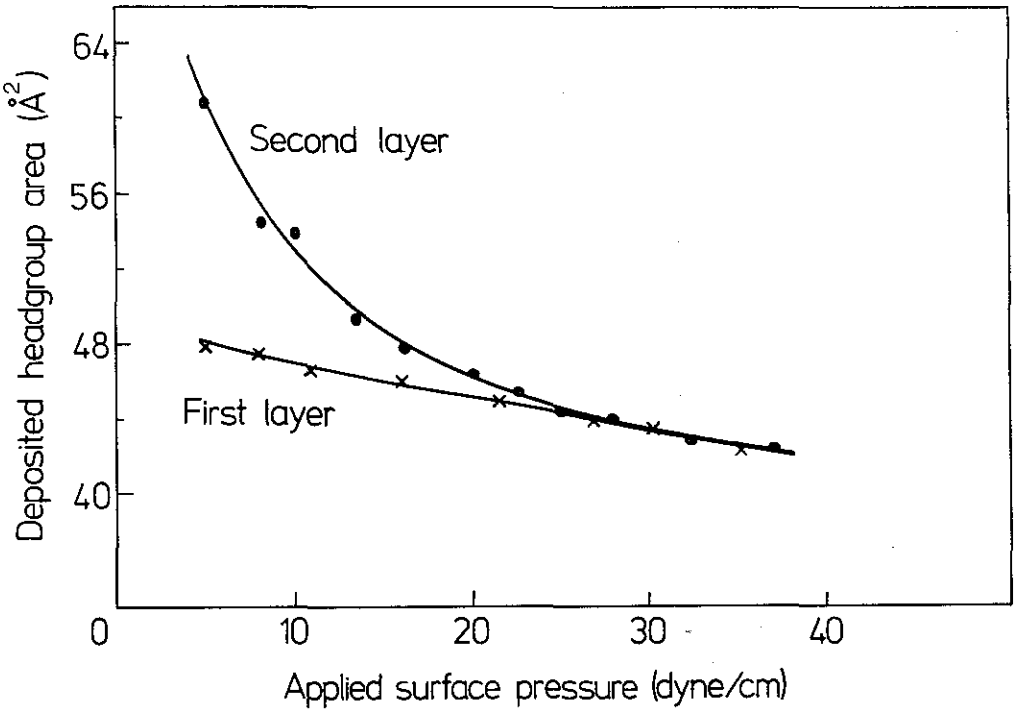

Fig. 11: Deposition onto mica of a DPPE monolayer ((×), first layer), and a DPPE bilayer (•), second layer on the first layer), as a function of the applied surface pressure in the Langmuir trough. Beyond $\Pi = 26$ dyne/cm, the deposited headgroup area in the second layer is identical to the deposited headgroup area in the first layer.

in the spread monolayer on the Langmuir trough at the same pressures. This indicates that the monolayer contracts upon deposition, probably a consequence of headgroup dehydration. Deposition of a second layer of DLPC on the first deposited DLPC layer was very difficult. The deposited amount of lipid was very sensitive to the applied surface pressure which caused a considerable scatter in the average headgroup area. However, it was found that when the second layer of DLPC was deposited onto mica already covered with a monolayer of DPPE (with a headgroup area of 42 $Å^2$), deposition could be controlled more accurately. Deposition of DLPC on a first layer of DPPE at $\Pi = 35$ dyne/cm gives the required headgroup area in the bilayer of 70 $Å^2$.

Considering this observation, it was decided to use this hydrophobic surface also for deposition of a second layer of the other lipids described below.

Fig. 13 gives the results of the deposition of DPPC and DMPC (16 °C) on mica covered with a monolayer of DPPE. Final deposition of DMPC at $\Pi = 36$ dyne/cm and

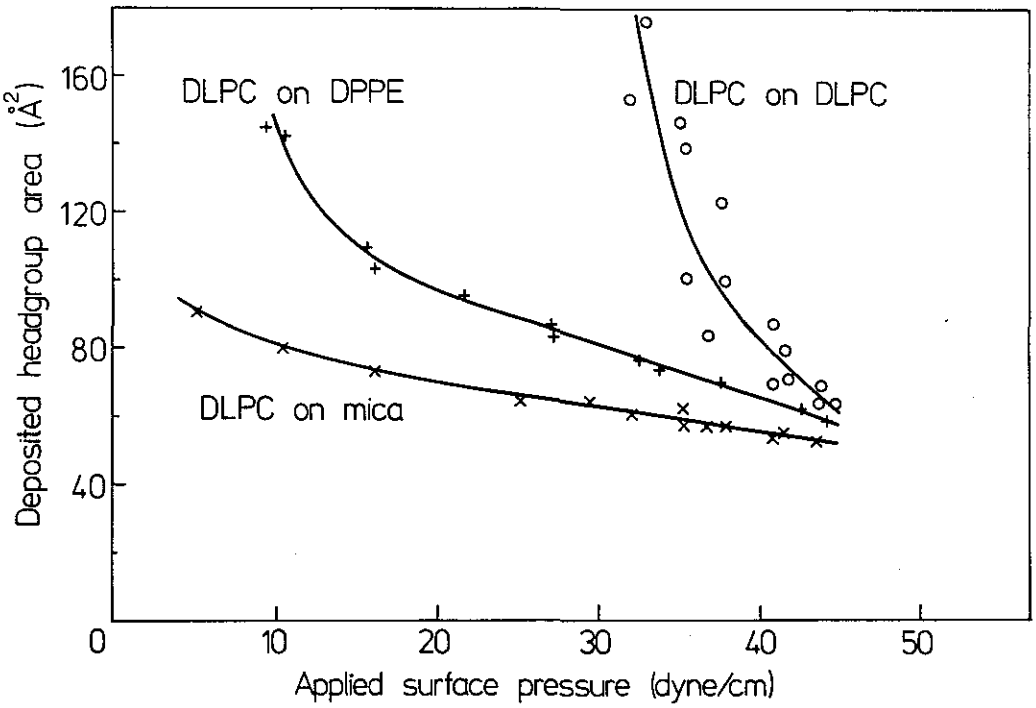

Fig. 12: Deposition onto mica of a DLPC monolayer (×) and of a second DLPC layer on a first layer of DLPC, both deposited at the same surface pressures (o), the (+) symbols give the deposition of a DLPC layer on a first layer for DPPE, where the DPPE is always deposited at a headgroup area of 42 Å^2.

DPPC at $\Pi = 19$ dyne/cm gives in both cases a headgroup area of 52 Å^2. It is seen that deposition on a first layer of DPPE is never particularly sensitive to the applied surface pressure.

Because it is necessary to check whether the type of lipid used in the first layer will influence forces between bilayers, the deposition of a second layer of DPPC was investigated when the first layer was also a DPPC layer. When deposition of DPPC as a first layer is done at a surface pressure $\Pi = 19$ dyne/cm, the deposited headgroup area per lipid becomes 46 Å^2. As with DLPC, this is about 10% smaller than the headgroup area at the air/water interface, reflecting headgroup dehydration upon deposition. Results of the deposition of a second DPPC layer on this first layer of DPPC at various surface pressures are also given in Fig. 13. Deposition at $\Pi = 23$ dyne/cm gives a headgroup area of 52 Å^2 in the second layer. It was found that when the surface forces were measured (see following Sections), there was no difference in the measured surface forces when the first layer was a DPPE layer rather than a DPPC layer.

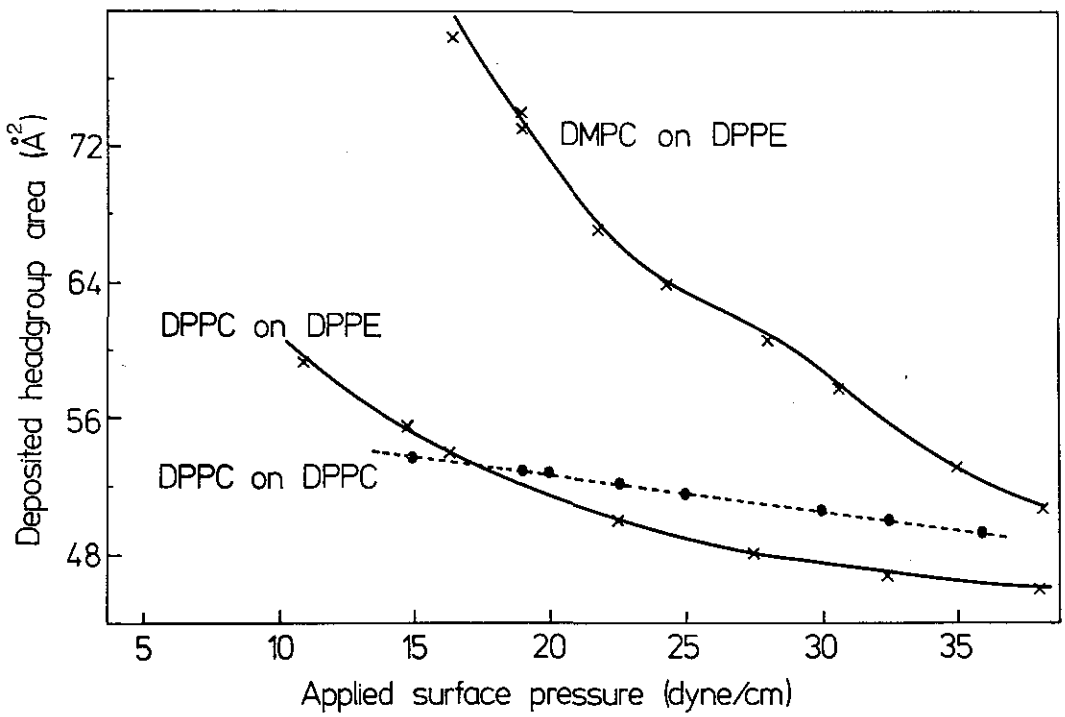

Fig. 13: Deposition of a second layer of DMPC (top curve) and DPPC (bottom curve) as a function of the surface pressure on a first layer of DPPE, where the DPPE always has a headgroup area of 42 $Å^2$. The dotted curve gives the deposition of a second DPPC layer on a first DPPC layer, where the first layer is deposited with a headgroup area of 46 $Å^2$.

4.2.3 The Bilayer-Water Interface and the Bilayer Thickness

As with the section on galactolipid bilayers, it is appropriate at this stage to discuss the location of the anhydrous bilayer/water interface which will be taken as the location of D = 0 (see Fig. 7).

Table I shows the areas per lipid molecule deposited in the second (outer) monolayers and the corresponding anhydrous bilayer thickness T as determined from the volumes occupied by the hydrocarbon chains and headgroups. The volume of a saturated chain in the gel state is $(27.4 + 26.9\ n)Å^3$ per n-carbon chain (Tanford, 1972), which corresponds to a density of 0.87 gm/cm^3, while for chains in the fluid state a density of 0.75-0.77 gm/cm^3 was used (the values for dodecane-hexadecane). The polar headgroup volumes were taken as 324.5 $Å^3$ for PC and 243 $Å^3$ for PE (Small, 1967). For example, for DPPC with area = 52 $Å^2$ we calculate $T = 2 \times [2(27.4 + 26.9 \times 15) + 324.5]/52 = 45.6$ Å. These thicknesses are given in the 5th column in Table I, where the accuracy is estimated at about ±1 Å.

Table I: AREAS AND THICKNESSES OF ADSORBED BILAYERS

Phospholipid Deposited	Temp. (°C)	Phase State	Area Deposited (nm^2)	Anhydrous Bilayer Thickness, T (nm)	
				Deposited (± 0.1 nm)	From Refractive Index Measurements[a] (± 0.3 nm)
DLPC	22	Fluid	0.70	3.1	3.6
DMPC	16	Pre-trans.	0.52	4.15	4.2
	30	Fluid	0.68	3.5	3.8
DPPC	21	Gel	0.52	4.6	4.6
DSPC	21	Gel	0.52	5.0	5.1
DPPE	21	Gel	0.42	5.3	-
Adsorbed from solution[b]					
DLPC	20	Fluid			3.6
Egg-PC	20	Fluid			4.0

[a] $n_b = 1.464$ assumed for all lecithins (Cherry and Chapman, 1969).
[b] R.G. Horn (unpublished results).

As mentioned before, from measurements of the mean refractive index of the medium between the two surfaces at some particular separation, one can determine the amount of material (other than water) present between the surfaces. The only additional information needed is the tangential component of the refractive index of the adsorbed material, which in the present study is the lecithin bilayer whose refractive index will be taken as $n_b = 1.464$, the value obtained for egg-PC (Cherry and Chapman, 1969). R.G. Horn (unpublished results) measured the refractive index of egg-PC and DLPC bilayers after they had adsorbed onto mica surfaces from a dilute solution of vesicles. In the egg-PC solution, Horn obtained for the total mean refractive index: $n = 1.440 \pm 0.006$ at $T_2 = 9.6$ nm and $n = 1.451 \pm 0.007$ at $T_2 = 8.9$ nm (see Fig. 7). The thickness of each bilayer T and their separation D is therefore given by solving

$n = [2Tn_b + Dn_2]/T_2$, and $D = (T_2 - 2T)$, using $n_b = 1.464$ and $n_w = 1.334$. This gives $T = 3.9$ nm at $D = 1.8$ nm and $T = 4.0$ nm at $D = 0.9$ nm, and the results for n *vs* D at larger separations, up to $D = 40$ nm, were all consistent with there being two bilayers of constant thickness ~ 4 nm between the surfaces. Likewise, for DLPC a value of 3.6 nm was obtained for the bilayer thickness.

In the present study, the thickness $\frac{1}{2}$ T of the outer two deposited monolayers was measured (since the first monolayer was usually DPPE to ensure its stability). Accordingly, the mean refractive index was here measured across T_1 rather than T_2 (see Fig. 7). The calibration of $T_1 = 0$ was, like what was done with the galactolipids, accomplished by slowly draining the apparatus of water which removes the second monolayer. Table I (last column) shows the results obtained for T from such measurements. The two values obtained by Horn for the bilayers adsorbed from solution are also given. Most of these readings were made at aqueous separations D in the range 1-2 nm which covered the range over which the short-range hydration forces were measured.

Note from Table I, that within experimental error, there is excellent agreement between the bilayer thickness deduced from the areas deposited and from the refractive index measurements. The slightly higher value obtained for the bilayer thicknesses of DLPC in the last column may be due to its having a higher intrinsic refractive index than that assumed (1.464) arising from the larger relative contribution of the polar headgroup for this short-chained lipid. It was observed that so long as the aqueous solution was saturated with lipid monomers at the CMC, the deposited bilayers remain stable with time (up to at least 24 hrs) and show no tendency to desorb.

4.2.4 Forces in Pure Water

Fig. 14 shows the measured force-laws for DLPC, DPPC and DPPE at 21-22 °C. The force-laws of DSPC and DMPC (at 15 °C) were practically indistinguishable from that of DPPC, while DMPC (at 30 °C) was very similar to DLPC. For the lecithins, the equilibrium separations D_0, and the adhesion forces F_0/R, were found to fall into two distinct groups: for bilayers in the gel state ($T < T_c$), the equilibrium separations

are smaller and the adhesions larger than for the fluid bilayers ($T > T_c$), while for DPPE bilayers ($T < T_c$), the equilibrium separation is much smaller and the adhesion much larger than for any of the lecithins (Table II). More significantly, we may note the general trend that the closer two curved bilayers come at equilibrium, the greater the adhesion force (or - equivalently - the adhesion energy E_0 between two planar bilayers).

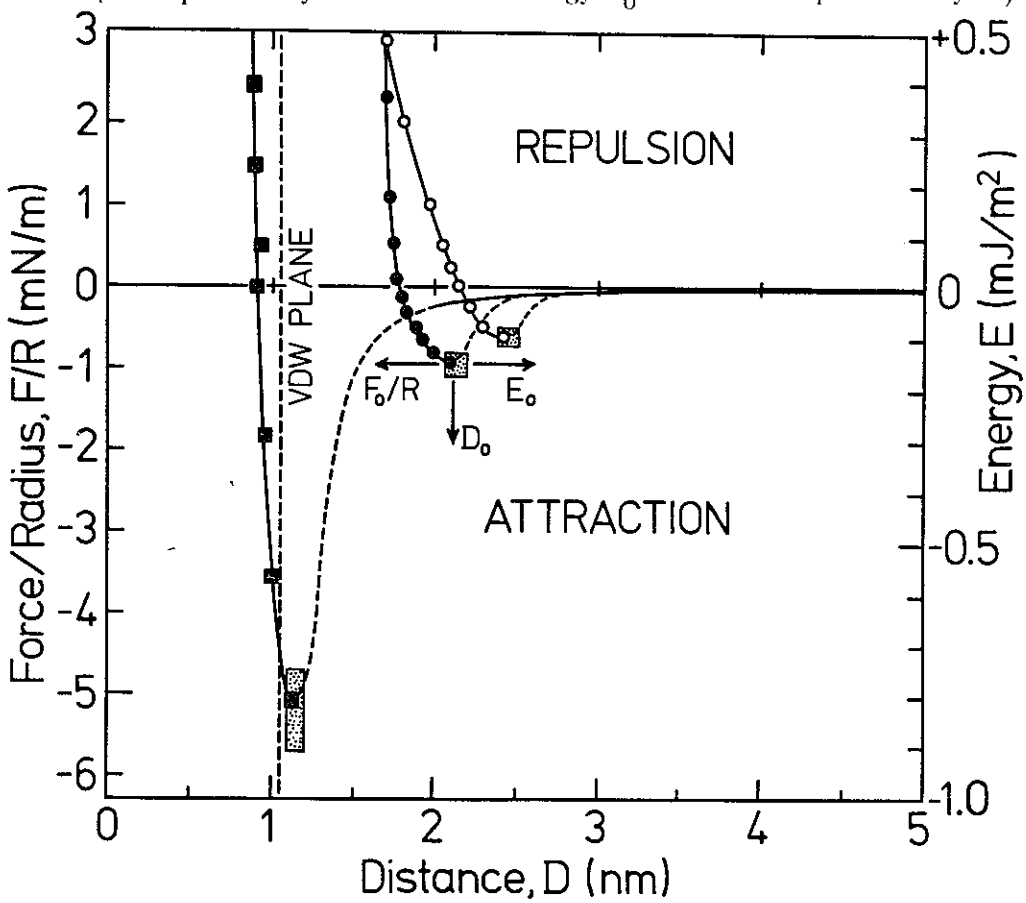

Fig. 14: Measured force laws between adsorbed phospholipid bilayers in water around the equilibrium region. (○) Lecithins in the fluid state ($T > T_c$), DLPC at 22 °C and DMPC at 30 °C; (●) lecithins in the gel or pretransition state ($T < T_c$), DPPC and DSPC at 21 °C and DMPC at 15 °C; (■) DPPE in the gel state at 22 °C. The van der Waals forces beyond 2 nm were measured accurately only for DPPE and DPPC (see Fig. 15). The squares around the force minima enclose the limits of error of the adhesion force F_0/R at separation D_0.

In order to measure the much weaker attractive van der Waals forces beyond D_0, the variable spring facility was employed but only for DPPC and DPPE. Fig. 15 shows the distances D_j from which the two surfaces jumped in as a function of the spring constant K (see Eq. (42)).

Table II: ADHESION PARAMETERS IN PURE WATER

Phase State	Bilayer Lipids	Equilibrium Separation, D_0 (range of hydration force) (nm)	Adhesive Force F_0/R (mN/m)	Adhesive Energy $E_0=F_0/2\pi R$ $(mJ/m^2)^a$	Hamaker Constant[b] A (J)
$T > T_c$	DLPC(22 °C)	2.4-2.5	0.6 ±0.1	0.1	$(7\pm1)\times10^{-21}$
	DMPC(30 °C)[c]				
$T < T_c$	DMPC(15 °C)	2.1-2.2	0.95±0.15	0.15	$(7\pm1)\times10^{-21}$
	DPPC(21 °C)				
	DSPC(21 °C)				
	DPPE(21 °C)	1.2	5.2 ±0.5	0.8	-

[a] $mJ/m^2 \equiv erg/cm^2$.

[b] Deduced from adhesion forces, Eqs. (33) and (40). In high concentrations of monovalent electrolyte, the Hamaker constant is reduced (see later).

[c] Same results obtained for DMPC when deposited at 30 °C or after heating from 15 °C ($T < T_c$) to 30 °C.

We see that also here a plot of $(R/3K)^{1/3}$ against D_j yields a straight line. According to Eq. (42), the slope gives the Hamaker constant A and the intercept with the horizontal axis the van der Waals plane from which the van der Waals force effectively originates. Since the distances over which the van der Waals force was measured were less than the bilayer thickness, we expect the simple expression of Eq. (33) to apply. It must be emphasized that for bilayers the plane of origin of the van der Waals force may well be a diffuse one, rather than a sharp well-defined interface as for perfectly smooth solid surfaces. The application of Eq. (33) to the results must therefore be viewed as a first approximation. From Fig. 15, we find that for both the DPPC and DPPE bilayers the effective van der Waals plane is at $D = 1.05 \pm 0.10$ nm, which is shown by the vertical dashed line in Fig. 14. If the van der Waals plane $D_{VDW} = 0$ is indeed beyond $D = 0$, it indicates that the thermal motions of the headgroups must take them out by at least 0.5 nm beyond each surface; the significance and implications of this will be discussed later.

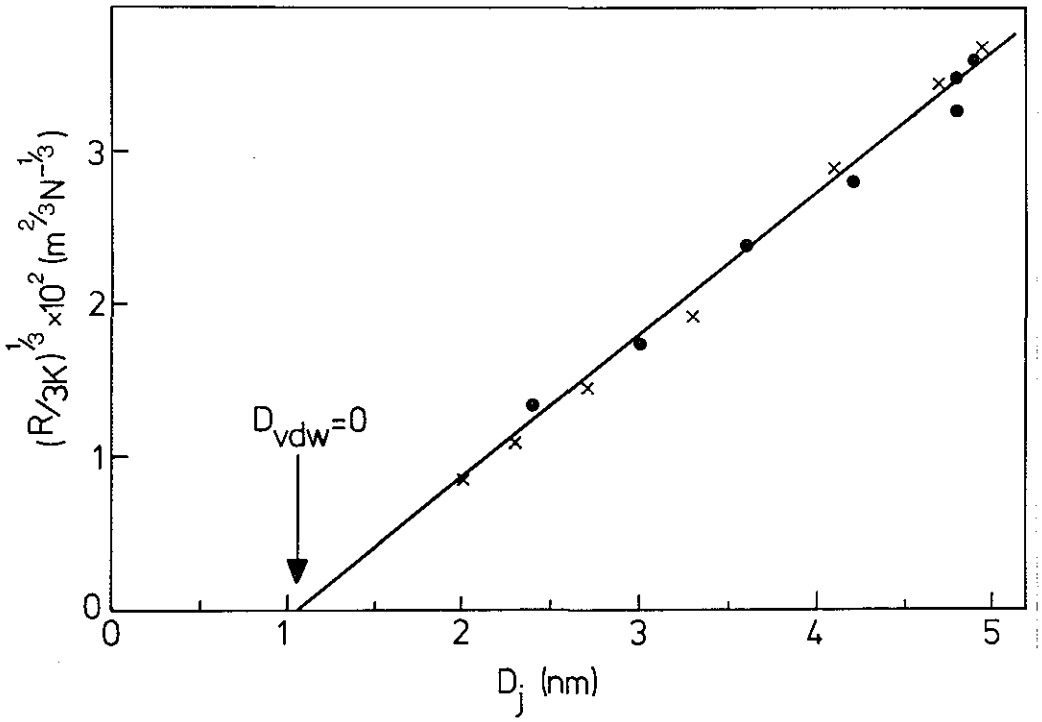

Fig. 15: Inward jumps between DPPE bilayers (× symbols) and DPPC bilayers (o symbols) in pure water. The effective origin of the van der Waals forces is for both phospholipids located at D = 1.05 nm.

In Table II, the values for the interfacial energy per unit area, E_0, of two planar bilayers at their equilibrium separation and the corresponding Hamaker constants A deduced from the adhesion forces are also given. These quantities are related to the adhesion force F_0 by

$$E_0 = F_0/2\pi R$$

$$F_0/R = A/6D_{VDW}^2 = A/6(D_0 - 1.05nm)^2. \tag{43}$$

For DPPE, since the adhesion, at $D_0 \approx 1.2$ nm, occurs so close to $D_{VDW} = 0$ it was not possible to obtain a reliable estimate for the Hamaker constant at these small separations. Returning to Fig. 15, it is clear that at long-range the van der Waals interaction is well described by Eq. (33) with a Hamaker constant of $(1.3 \pm 0.2 \times 10^{-21})$ J, i.e. a factor of five smaller than the values deduced from the adhesion forces. Possible reasons for this discrepancy will be presented in the Discussion section.

Fig. 16 shows the measured repulsive forces for all the lipids studied, plotted on a

log-linear graph. The repulsive forces for DSPC, DPPC and DMPC (at $T < T_c$) all fell within the narrow shaded band (Fig. 16A) while for the DLPC and DMPC (at $T > T_c$) within another shaded band, slightly farther out (Fig. 16B). For comparison, in Fig. 16C the previous measurements of the repulsive forces F_R per molecule for DSPC and DLPC by Lis et al. (1982a) between planar bilayers are reproduced and compared with the derivative with respect to distance of the interaction energy ($F_R = \partial E/\partial D$) between curved bilayers given in Figs. 16A and 16B. The open arrows and the closed arrows on the horizontal axis give the equilibrium bilayer separations D_0 for deposited and free bilayers (in lamellae), respectively. Fig. 16C shows (as previously also found by Horn (1984) for egg-PC and DLPC) that the repulsive forces between free bilayers in lamellae have a longer range than those between adsorbed (immobile) bilayers. This is especially true for bilayers whose lipids are in the fluid state where the equilibrium separations of the free bilayers are in the range 2.8-3.3 nm (2.8-2.9 nm for DLPC and DMPC) compared to 2.4-2.5 nm for adsorbed bilayers, while for gel state bilayers the equilibrium separations are much the same, viz. 2.0-2.2 nm for free bilayers of DPPC and DSPC compared to 2.1-2.2 nm in the present study. Closer in, however, both types of measurements appear to yield similar values for the forces (except for DPPE where both the repulsive forces, as well as the equilibrium separation of $D_0 = 1.1$-1.2 nm, are much smaller for the adsorbed bilayers than those measured by Lis et al. (1982a) for egg-PE, where $D_0 = 2.05$ nm was reported. Note that Seddon et al. (1984) obtained equilibrium spacings D_0 in the range 0.8-1.3 nm for a variety of different PE bilayers in both the gel and fluid states consistent with the present finding.

4.2.5 Forces in Monovalent Electrolyte Solutions

Since monovalent ions are believed to bind only very weakly if at all to the neutral headgroups of PC or PE, one should not expect there to be any significant repulsive double-layer force between these bilayers in the presence of salts such as NaCl. The van der Waals force, however, is expected to be reduced in the presence of high concentrations of electrolyte where the temperature dependent contribution to the Hamaker constant is screened at distances beyond the Debye screening length (Mahanty

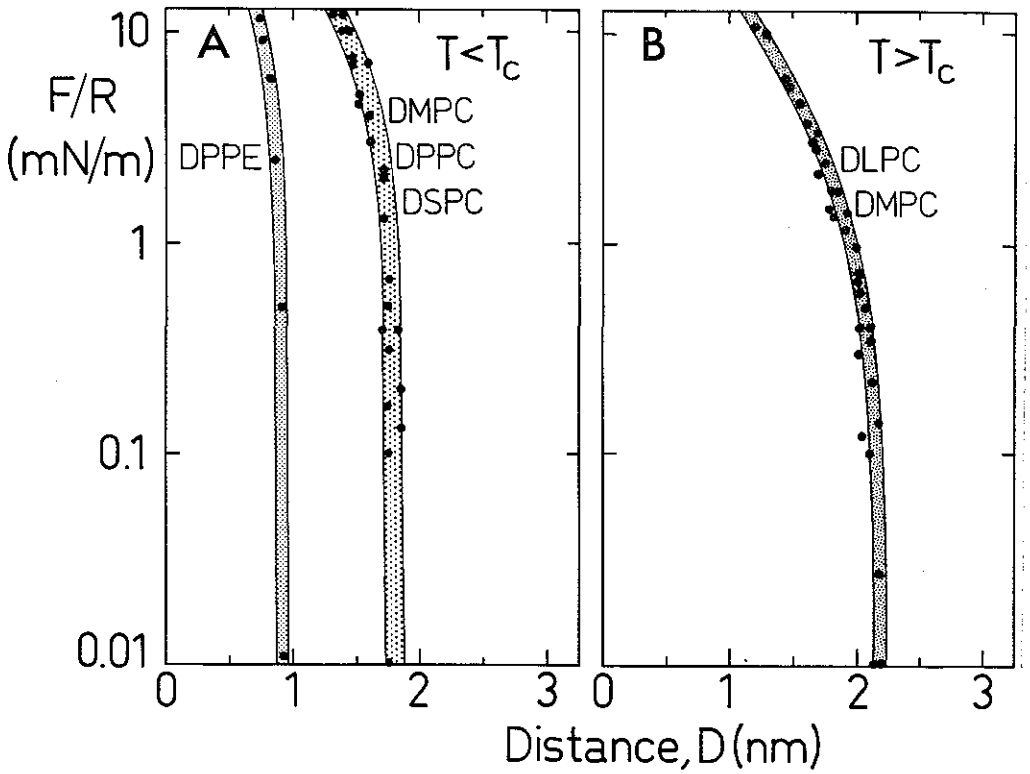

Fig. 16A and 16B: Repulsive forces at separations below equilibrium separations (continued from Fig. 14). (A) Bilayers in the gel or pretransition state ($T < T_c$): DPPE, DPPC, and DSPC at 21 °C and DMPC at 15 °C. (B) Lecithin bilayers in the fluid state ($T > T_c$): DLPC at 22 °C and DMPC at 30 °C. At F/R values above 10 mN/m and up to 10^3 mN/m, the initially curved surfaces flatten, but the bilayers do not fuse, even at pressures up to 40 atm.

and Ninham, 1976). Thus if only the van der Waals force was responsible for the adhesion, we should expect decreased adhesion at increasing concentrations of electrolyte, while any ion binding should lower the adhesion even more.

Fig. 17 shows results obtained for the variation of the adhesion forces between the two DPPC bilayers in the presence of various 1:1 electrolytes. Three regimes could be identified. In regime A (0 to 50 mM salt) the adhesion forces fell to 50-70% of the value in pure water, while in regime B (50-200 mM salt) the adhesions reached a minimum, then rose again. So far, the effects are small and the initial decrease could be qualitatively understood for the reasons given above. However, in regime C, above 200 mM salt, the adhesion forces varied considerably depending on the electrolyte, and the results can not be explained using simple concepts in terms of van der Waals and/or double-layer forces. Thus, from Fig. 17 it is seen that in LiCl the adhesion rose

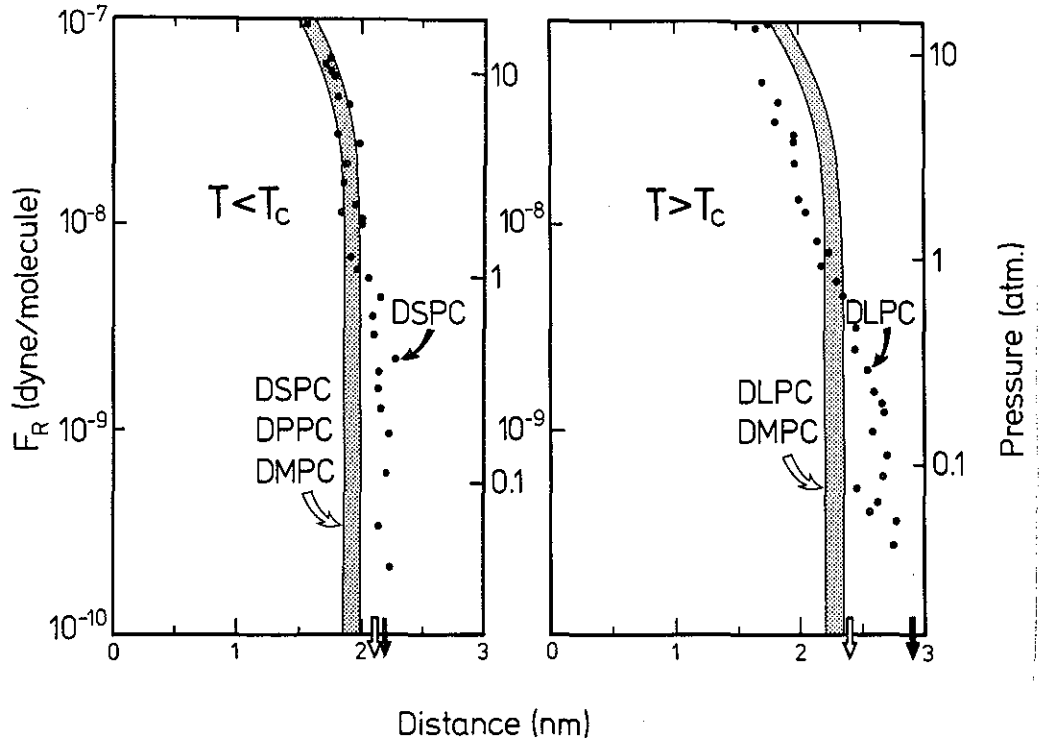

Fig. 16C: Comparison between the calculated repulsive force per molecule F_R from Figs. 16A and 16B, as given by the shaded band, and the measured force F_R by Lis et al. (1982a) between free bilayers of DSPC and DLPC in lamellae ((•) symbols). The vertical arrows on the horizontal axis indicate the equilibrium bilayer separations D_0.

dramatically (an effect that was also found with DLPC); in NaCl it levelled off (an effect that was also found with DLPC, and with NaI), while in CsCl it fell rapidly to zero. In order to pursue this further, full force curves were measured in concentrated solutions of LiCl, NaCl and CsCl, shown in Fig. 18. The results show that changes in the adhesion forces correlate with the equilibrium bilayer separation, D_0, viz. larger adhesions at smaller equilibrium separations. It is also apparent that changes in the adhesion are due not to any increase or decrease in the attractive forces but rather to changes in the repulsive short-range forces. Thus using Eq. (33), the Hamaker constant estimated from the adhesion forces at the equilibrium separations do not vary very much with the equilibrium separations. The only systematic correlation that was found is a slight fall in the Hamaker constants at higher electrolyte concentrations, viz. $A = 7 \pm 1 \times 10^{-21}$ J in 0-150 mM salt, decreasing to $A = 3.5 \pm 1.5 \times 10^{-21}$ J in 1300 mM salt. We therefore note the disappearance of the temperature-dependent contribution of $\sim 3 \times 10^{-21}$ J in high salt, as expected theoretically.

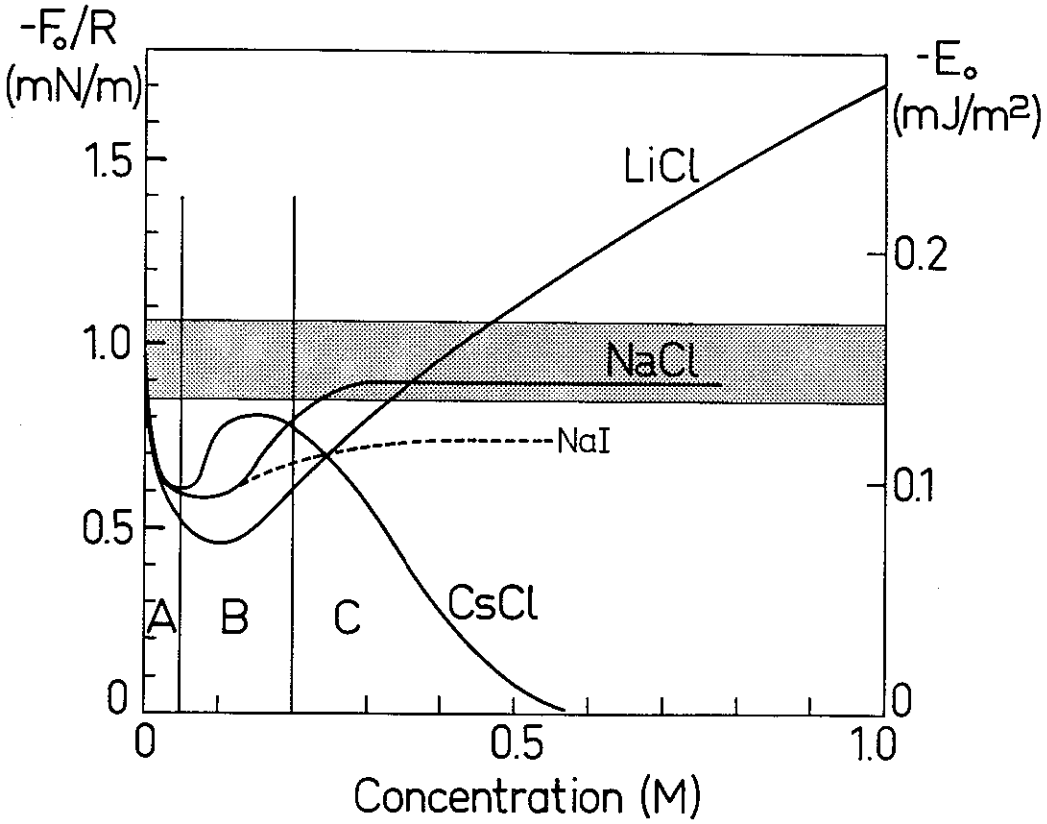

Fig. 17: Adhesion force (F_0/R) and energy (E_0) for DPPC bilayers at 21 °C as a function of salt concentration. (Note that the direction of increasing adhesion is upward.) Qualitatively similar results were obtained for DLPC bilayers. The shaded band gives the range of values in pure water, included for comparison.

As regards the large effects of high concentrations of electrolytes on the short-range repulsive forces, the consideration of this is reserved for the Discussion section; but note here that the equilibrium aqueous separation follows the order CsCl > NaCl ≈ NaI > pure water > LiCl, which follows the hydration of the cations, and which is the same order as that previously reported by Gottlieb and Eanes (1972) for the maximum uptake of concentrated solutions of these electrolytes by multilamellar lecithin bilayers.

4.2.6 Forces in Divalent Electrolyte Solutions

While PC lamellae do not swell in monovalent salt solutions, they swell many hundreds of angstroms in mM $CaCl_2$ and $MgCl_2$ solutions due to the long-range double-layer force brought about by the binding of these ions onto the otherwise neutral surfaces.

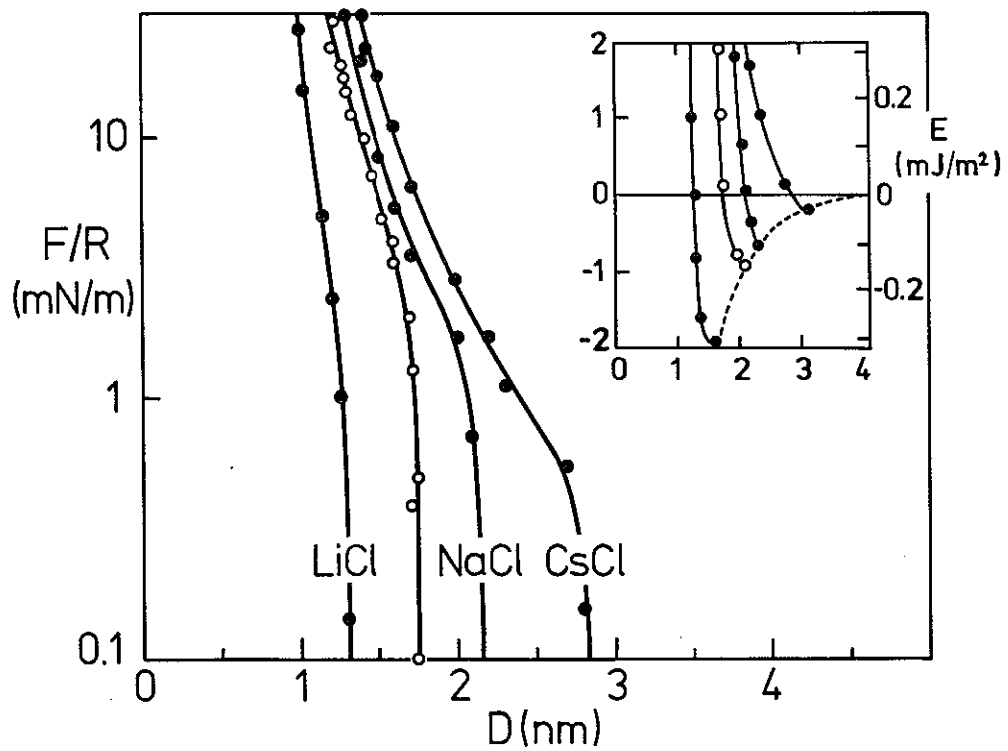

Fig. 18: Force curves for DPPC bilayers at 21 °C in various concentrated salt solutions (see also Fig. 17). From left to right, 1300 mM LiCl, pure water (reference), 150 mM NaCl, and 430 mM CsCl. No long-range double-layer forces were ever measured in water or in monovalent salt solutions with any of the lipids studied. However, at these high concentrations, some short-range repulsive double-layer force contribution due to ion binding can not be excluded, especially in the NaCl and CsCl solutions, but which is undetectable because it is swamped by the attractive van der Waals force.

In this section, results of force measurements are given between PC and PE bilayers in $CaCl_2$ and $MgCl_2$ solutions in the range ~ 1 mM to above 30 mM. In all, more than 100 force curves were measured and it is not proposed to plot them all in detail, except in Fig. 19 where the forces between DPPC bilayers in ~ 1 mM $CaCl_2$ and $MgCl_2$ are shown. Note the expected longer range of the double-layer forces in the more dilute solutions and the larger repulsions in the $CaCl_2$ solutions reflecting the stronger binding of Ca^{2+} to the phosphate group. Since the forces measured between different lipids at different salt concentrations all exhibit the same trends, only a detailed quantitative analysis of the results in Fig. 19 will be given.

When Ca^{2+} ions bind to a neutral surface such as PC, the surfaces become

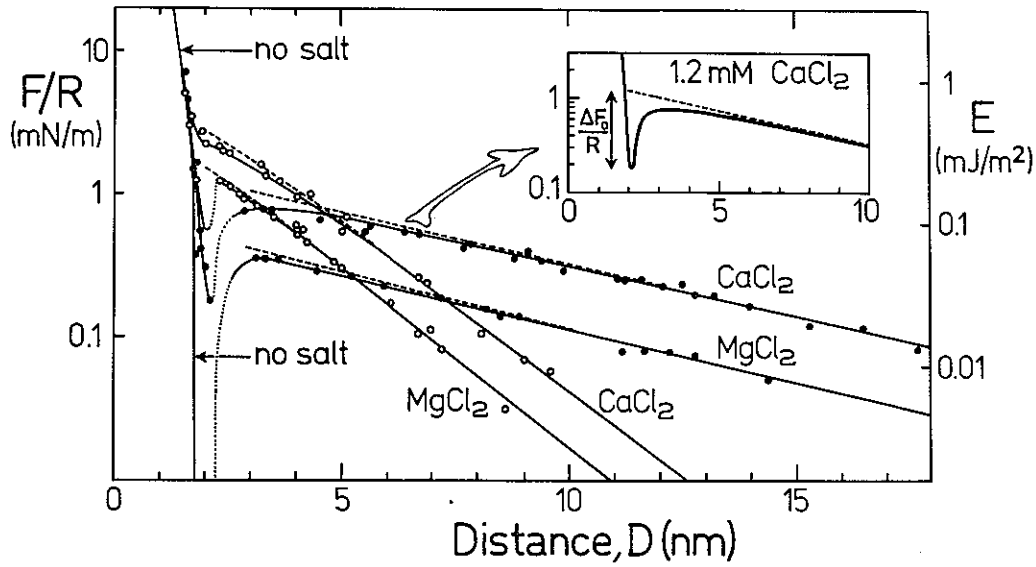

Fig. 19: Forces between DPPC bilayers in $CaCl_2$ and $MgCl_2$ solutions at 22 °C: (•) 1.2 mM $CaCl_2$ and 1.2 mM $MgCl_2$; (o) 10.8 mM $CaCl_2$ and 10.9 mM $MgCl_2$. Dashed curves: theoretical double-layer interaction with charge regulation; solid curves, experimental force curves showing the effect of the van der Waals force at smaller separations. In pure water (no double-layer force), the adhesion force was $F_0/R \approx -1.0$ mN/m; the inset shows that in 1.2 mM $CaCl_2$ the dip in the repulsion ($\Delta F_0/R$) is the same, and similarly in 1.2 mM $MgCl_2$.

positively charged and the double-layer interaction then takes place in an electrolyte where the counterion is the anion. For such systems the surface potential ψ_0^∞ or surface charge density σ_0^∞ of the isolated surfaces (or two surfaces at infinite separation) can be obtained by fitting the theoretical double-layer force curve to the tail end of the measured force curve. (Closer in, the surface potential and surface charge will of course both change due to charge regulation and double-layer overlap as outlined in Chapter 1). When this is done to the four curves in Fig. 19, we obtain the potentials ψ_0^∞ and charge densities σ_0^∞ shown in Table III. Note that ψ_0^∞ and σ_0^∞ are related via the Grahame equation Eq. (31), which for 2:1 electrolytes can be rewritten as

$$\sigma_0^\infty = 0.118\, sinh\left(\frac{\psi_0^\infty}{50.9}\right)\left(2+e^{-\psi_0^\infty/25.4}\right)^{1/2}\sqrt{c}. \tag{44}$$

at 22 °C, where ψ_0^∞ is in mV, σ_0^∞ in C/m^2, and the bulk electrolyte concentration C in moles/litre. Table III also shows the fraction α of lipid headgroups that have bound a cation, calculated form an adsorption site area of 52 $Å^2$ per molecule (the headgroup area per DPPC lipid).

Table III: DOUBLE-LAYER PARAMETERS FOR DPPC AT 22 °C (Fig. 19)

Electrolyte	Conc. C (mM)	Surface Potential ψ_0^∞(mV)	Surface Charge σ_0^∞ C/m^2	nm^2/Ca^{2+}	Fraction bound α	Assoc. Constant K (M^{-1})
$CaCl_2$	1.2	37	0.0048	67	0.008	118
	10.8	47	0.0190	17	0.031	114
$MgCl_2$	1.2	21	0.0028	116	0.004	20
	10.9	30	0.0118	27	0.019	19

The binding constants for the adsorption of the cations have been determined following the procedure outlined in Section 1.2. The theoretical double-layer force curves (with charge regulation when the surfaces approach) are shown by the dashed lines in Fig. 19. It was noted that the theoretical curves were hardly different from the predicted force curves when the surfaces were supposedly interacting at constant surface potential. However, for the constant charge case, always too large a force was predicted, especially at small bilayer separations. The solid lines are the experimental force-laws which include the attractive van der Waals forces, though this fitting procedure must be approached with some caution at small bilayer separations. It has been predicted by Kjellander and Marcelja (1985a) that adsorbed ions on two approaching surfaces can correlate with each other, giving rise to an extra attractive interaction, and we also expect discreteness of charge effects to become important at surface separations less than the average distance between two adsorbed cations.

The adhesion minima in Fig. 19 were found to be at the same separations D_0 as in pure water but raised from their values in pure water (i.e. in the absence of any double-layer repulsion) by just the amount of the expected double-layer force at D_0. This is illustrated in the inset of Fig. 19 where the value of $\Delta F_0/R$ is practically the same as F_0/R in pure water. Clearly, the binding of the divalent cations, while affecting the electrostatic interactions between these bilayers, does not affect the short-range 'hydration' repulsion nor the intrinsic adhesion force except by reducing it by just the

amount corresponding to the double-layer force at the equilibrium separation. The lack of any drastic effect of Ca^{2+} or Mg^{2+} binding on the short-range forces is understandable, considering that the fraction α of the lipids binding these ions never exceeds a few per cent (Table III).

The general features of the results of Fig. 19 were found to apply to all the lipids studied at all concentrations of both $CaCl_2$ and $MgCl_2$. In particular, it was found that for each lipid the surface potential, charge, and double-layer interaction could be described by a single association constant over the whole range of $CaCl_2$ and $MgCl_2$ concentrations studied (see Table IV). The results are shown in Figs. 20-23, where the solid and dashed lines are now the experimental and theoretical DLVO curves, respectively. At higher electrolyte concentrations, where the Debye length is small and the double-layer forces are of relatively short-range, it becomes critical where the outer Helmholtz plane (OHP) be placed, viz. the plane of origin of the diffuse double-layer interaction. In all cases, good agreement between theory and experiment was obtained at all concentrations with a single association constant by placing the OHPs as indicated by the arrows in Figs. 20-23 (also tabulated in Table IV). As will be discussed later, the positions of the OHPs so deduced all lie within about 1 Å of the negatively charged outer oxygen atoms of the phosphate groups. (Note that the theoretical curves in each figure are plotted for the same value of the binding constant K and position of the OHP; much better agreement could of course be obtained if these were fitted separately for each force curve).

Figs. 20-23 cover the interactions of bilayers in their three different phase states: the gel phase (DPPC and DSPC in Fig. 20, and DPPE in Fig. 23), the pretransition phase (DMPC in Fig. 21) and the fluid or liquid-crystalline phase (DLPC in Fig. 22). They show that: (i) Ca^{2+} ions always bind more strongly than Mg^{2+} ions (an effect that is more pronounced for bilayers in the gel state); (ii) at ambient temperatures the strength of Ca^{2+} binding is in the order gel phase > pretransition phase > liquid phase; and (iii) DPPE bilayers bind less than DPPC bilayers.

The dependence of Ca^{2+} binding on the phase state of DPPC and DMPC bilayers

Table IV: DOUBLE-LAYER PARAMETERS FOR ALL PHOSPHOLIPIDS

Bilayer Lipid	Association Constant K (M^{-1})		Location of OHP[a] Relative to D = 0, per surface (± 0.1 nm)
	Ca^{2+}	Mg^{2+}	
DPPC (22 °C, gel phase)	120	20	0.1
DMPC (16 °C, pretransition phase)	46	8.6	0.2
DLPC (22 °C, liquid phase)	15	10	0.1
DPPE (21 °C, gel phase)	12	4	0.15

[a] OHP: Outer Helmholtz Plane, or plane of origin of diffuse double-layer charge.

was further investigated as a function of the temperature. With DMPC (main transition: $T_c = 24$ °C) in 3.6 mM $CaCl_2$, the surface potential remained at $\psi_0^\infty = 33$ mV at T = 14 °C to 23.5 °C (cf. Fig. 21). On heating above 25 °C (and up to 30 °C) the value of ψ_0^∞ gradually fell and settled at 20 mV, which is identical to that measured for DLPC in 3.6 mM $CaCl_2$ at 22 °C, i.e. in the liquid phase (Fig. 22). The same result was obtained when DMPC was deposited at 30 °C with a headgroup area of 68 $Å^2$, and the double-layer forces then measured at 30 °C. With DPPC (pretransition temperature: $T_p = 35$ °C) in 1.2 mM $CaCl_2$, the potential remained constant at $\psi_0^\infty = 37$ mV at 20-36 °C, then above 36 °C and up to 40 °C it slowly fell to ~ 30 mV, close to that measured for DMPC in the pretransition phase (Fig. 21). These results clearly show that the binding of divalent ions to lecithins does not depend so much on the temperature per se but on the phase state of the bilayers, and they confirm the indications of Figs. 20-23 that the binding falls abruptly on going from the gel phase to the pretransition phase, and again on going from the pretransition phase to the liquid phase. The results also indicate that (at least the outer monolayers of) the deposited bilayers go through their pretransition and main transition at the same temperatures as they do in water (to within about 1 °C).

Finally, experiments were also carried out with DPPC and DLPC in

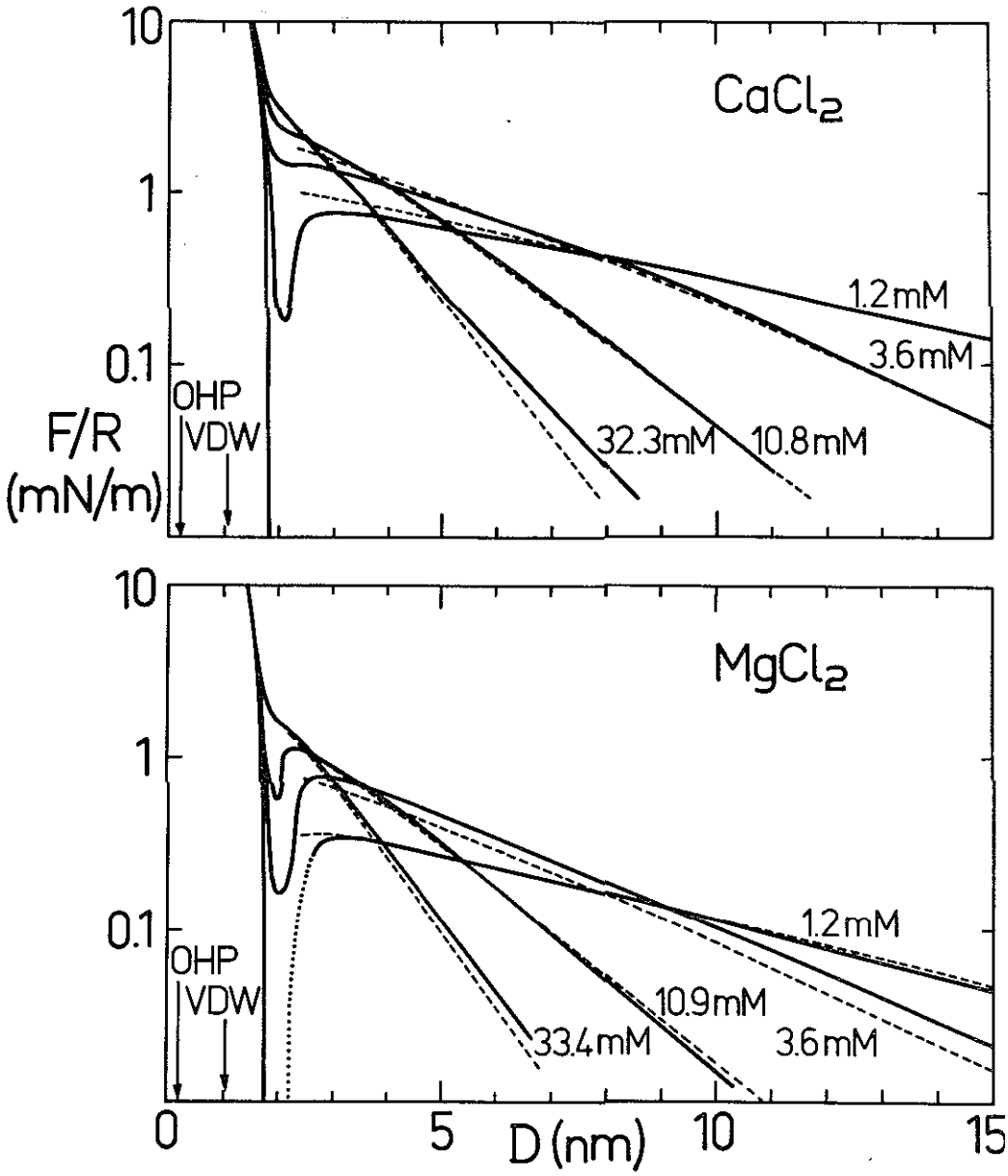

Fig. 20: Forces between DPPC bilayers in $CaCl_2$ and $MgCl_2$ solutions at 22 °C (bilayers in the gel phase, $T < T_c$). Solid curves, experimental; dashed curves, theoretical curves based on the association constants given in Table IV, a Hamaker constant of $A = 1.3 \times 10^{-21}$ J, and $D_{VDW} = 0$ at D = 1.05 nm. Results for DSPC were very similar.

140 mM NaCl in addition to varying concentrations of $CaCl_2$ (at 22 °C). In both systems, the surface potentials were typically well below 30 mV so that the double-layer forces were always weak and, because they were screened by the high concentration of NaCl, also of very short-range. The double-layer forces could not therefore be accurately measured as a function of D. For DLPC, and $CaCl_2$ concentrations in the range

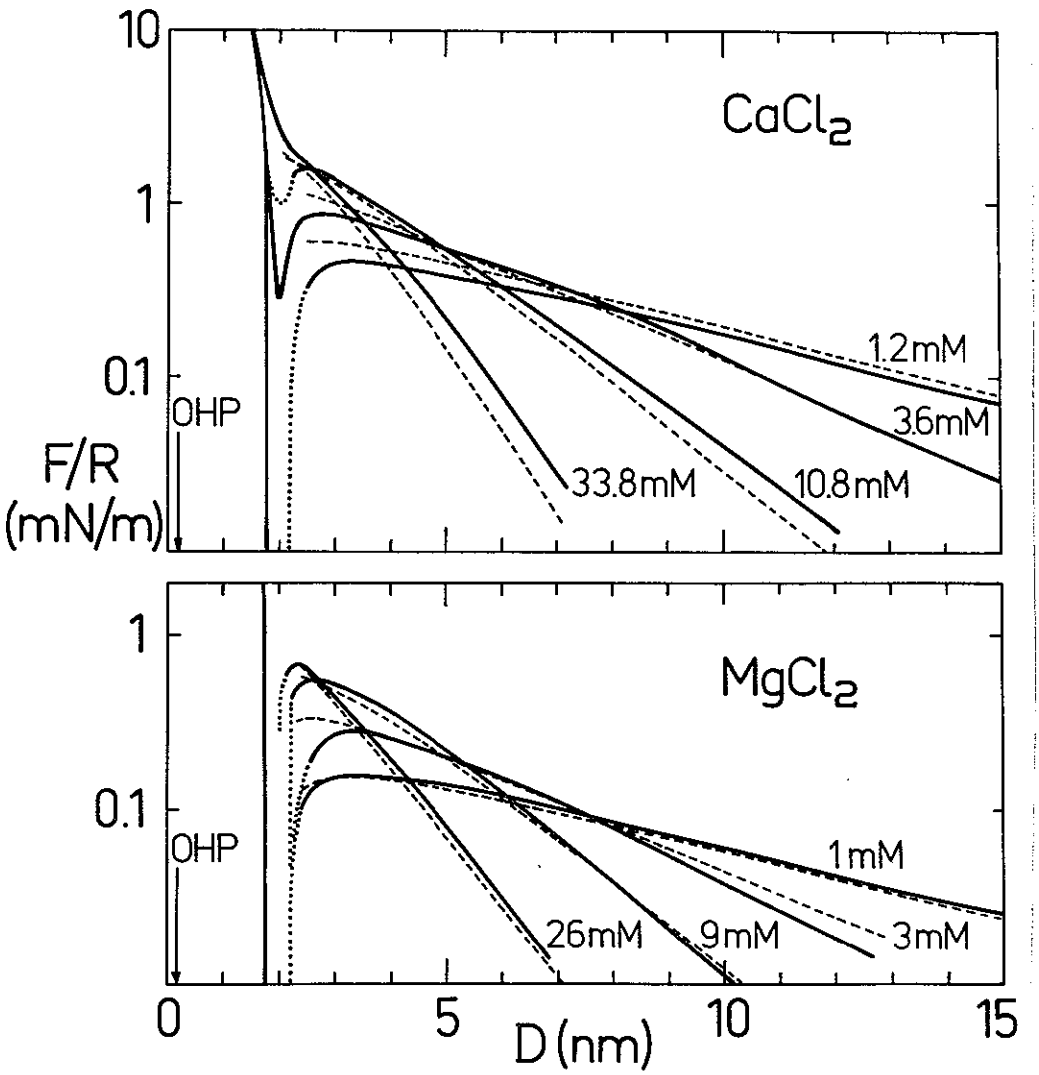

Fig. 21: As in Fig. 20 but for DMPC at T = 16 °C (pretransition phase, $T_p < T < T_c$).

0-90 mM, the interactions were found to be determined essentially by the attractive van der Waals forces; the main effect arising from the addition of $CaCl_2$ was a small progressive reduction in the strength of the adhesion force by about 30%. With DPPC, since the Ca^{2+} binding is much greater, the effect of $CaCl_2$ on the adhesion force was more pronounced, and F_0/R fell roughly linearly from about -0.8 mN/M (in the absence of $CaCl_2$) to zero at $\sim$ 10 mM $CaCl_2$.

4.2.7 Fusion

No fusion was observed in any of the experiments described so far. Even at the highest forces applied (giving rise to pressures exceeding 30 atmospheres), the two initially curved surfaces simply flattened locally but did not fuse. As already mentioned,

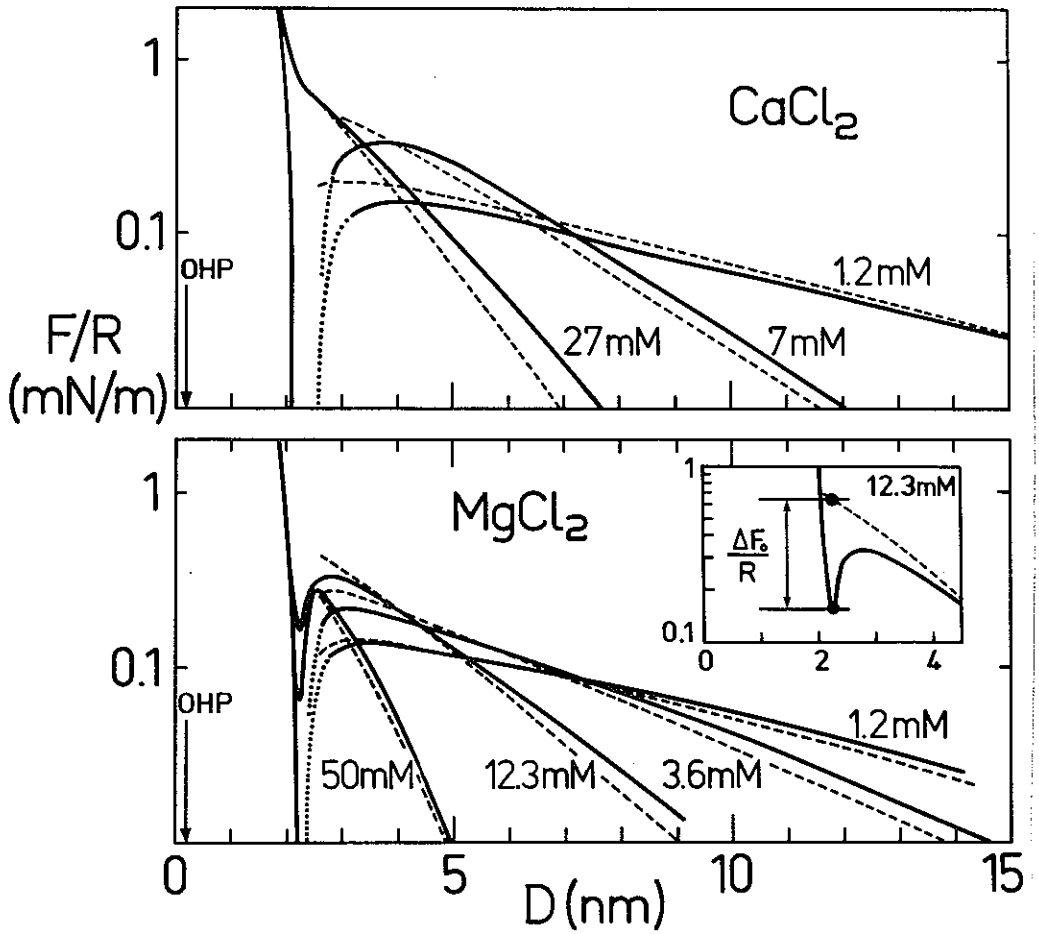

Fig. 22: As in Fig. 20 but for DLPC at 22 °C (liquid-crystalline phase, $T > T_c$). In pure water (no double-layer force), $F_0/R = -0.53$ mN/m. The inset shows the dip in the repulsion in 12.3 mM $MgCl_2$ relative to the pure double-layer force (dashed) where $\Delta F_0/R \approx 0.50$ mN/m. Likewise at 50 mM $MgCl_2$.

so long as the solution was fully saturated with phospholipid monomers, the deposited bilayers did not desorb. In pure water, it was found that an outer DLPC monolayer desorbs after about 1 hour but that in a partially saturated solution, desorption takes many hours (as monitored by the thinning of the bilayers with time). Clearly, as thinning progresses the headgroup area (i.e. the hydrophobic area exposed to water) per lipid must increase. In one such experiment (Fig. 24), after two hours the DLPC bilayer had thinned by about 15%, since the adhesion minimum D_0 now occurred ~ 0.5 nm farther in; and the adhesion force increased by a factor of three. But more importantly, the two thinned bilayers now spontaneously fused into one bilayer once they were brought to a separation of 1-1.5 nm, at which point the pressure between the two bilayers was still well below 2 atm (whereas for two full DLPC bilayers no fusion was

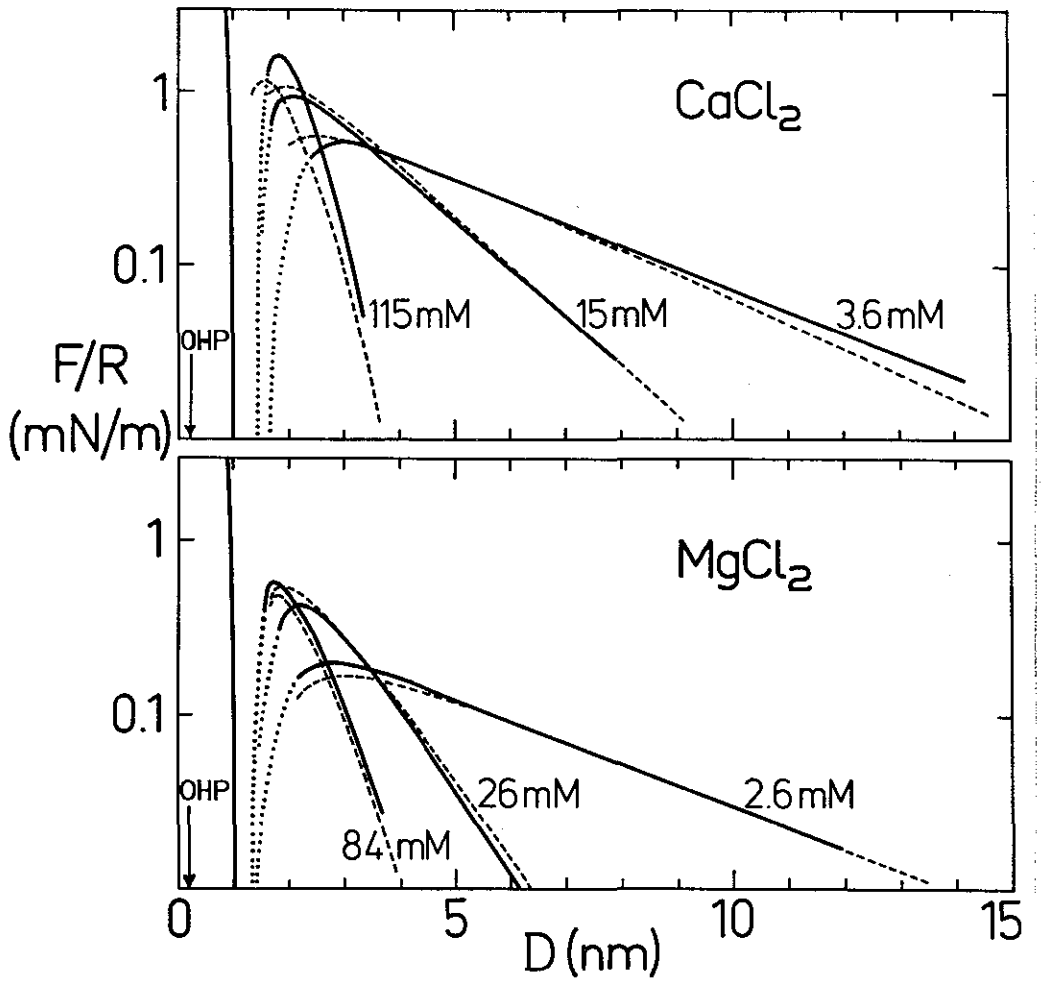

Fig. 23: As in Fig. 20 but for DPPE at 22 °C (gel phase, $T < T_c$).

observed even at pressures up to 20 atm). For a graphic illustration of the molecular events occurring during the fusion process, see Horn (1984).

4.3 DISCUSSION

Many of the results presented in the previous sections are self-explanatory and require no further discussion. Broadly speaking, the results show that there are three types of forces operating between phospholipid bilayers: at long range we find the expected repulsive double-layer and attractive van der Waals forces, while at short range below 1-3 nm, a strongly repulsive steric-hydration force balances the van der Waals attraction.

The measurements of the double-layer and van der Waals force laws have allowed us to locate the planes of origin of these two interactions which, when taken together with X-ray and neutron scattering data, provide a consistent picture of bilayer structure

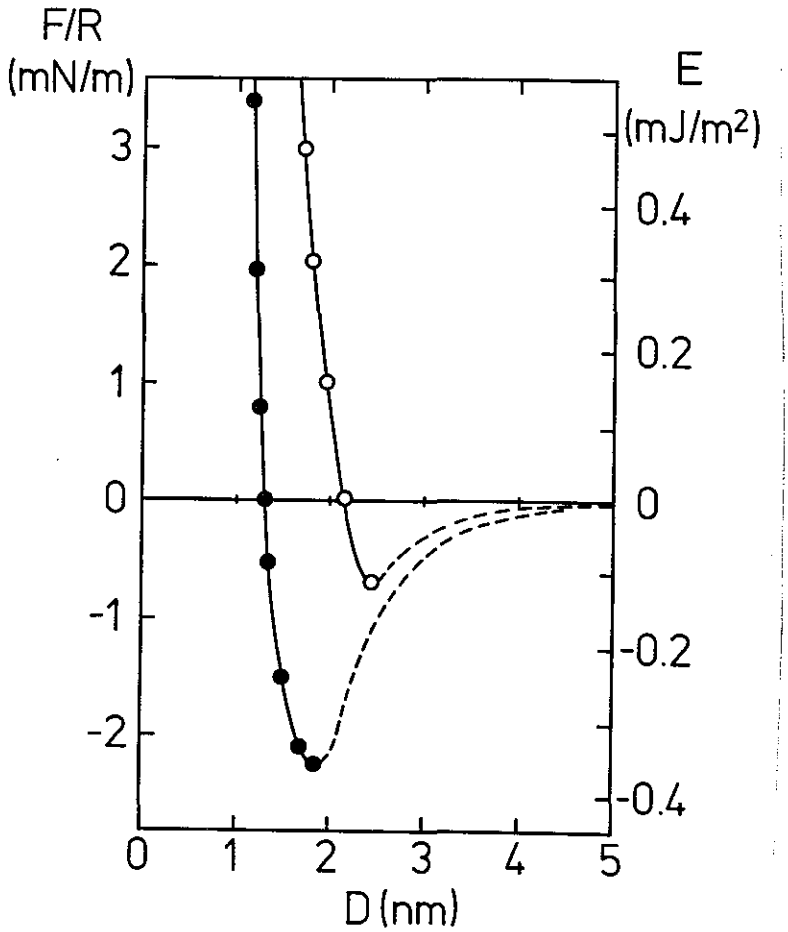

Fig. 24: Forces between DLPC in water at 22 °C ($T > T_c$). [o] Full bilayer (as in Fig. 14); (•) ~ 85% of full bilayer. In both cases, D = 0 refers to that of the original full bilayer.

as illustrated in Fig. 25. Thus the position of the outer Helmholtz plane, at D ≃ 0.1 nm for all the lipids, gives us the effective plane of diffuse double-layer charge and hence the likely location of cation binding. Not surprisingly, this coincides with the mean positions of the outer negative phosphate oxygens as obtained from neutron scattering and X-ray data on electron density profiles. For example, neutron diffraction measurements (Buldt et al., 1978) show that for DPPC the outer phosphate oxygens are 2.4 nm for the bilayer centre which, from Table I corresponds to about 0.1 nm beyond D = 0. The data of Lewis and Engelman (1983) lead to a similar result for DLPC in the fluid state.

The effective plane of origin of the van der Waals forces was also found to be at much the same distance from D = 0 for all the lipids and to be located at D = 0.5 nm per surface. A possible explanation for this is that the headgroups are not immobilized

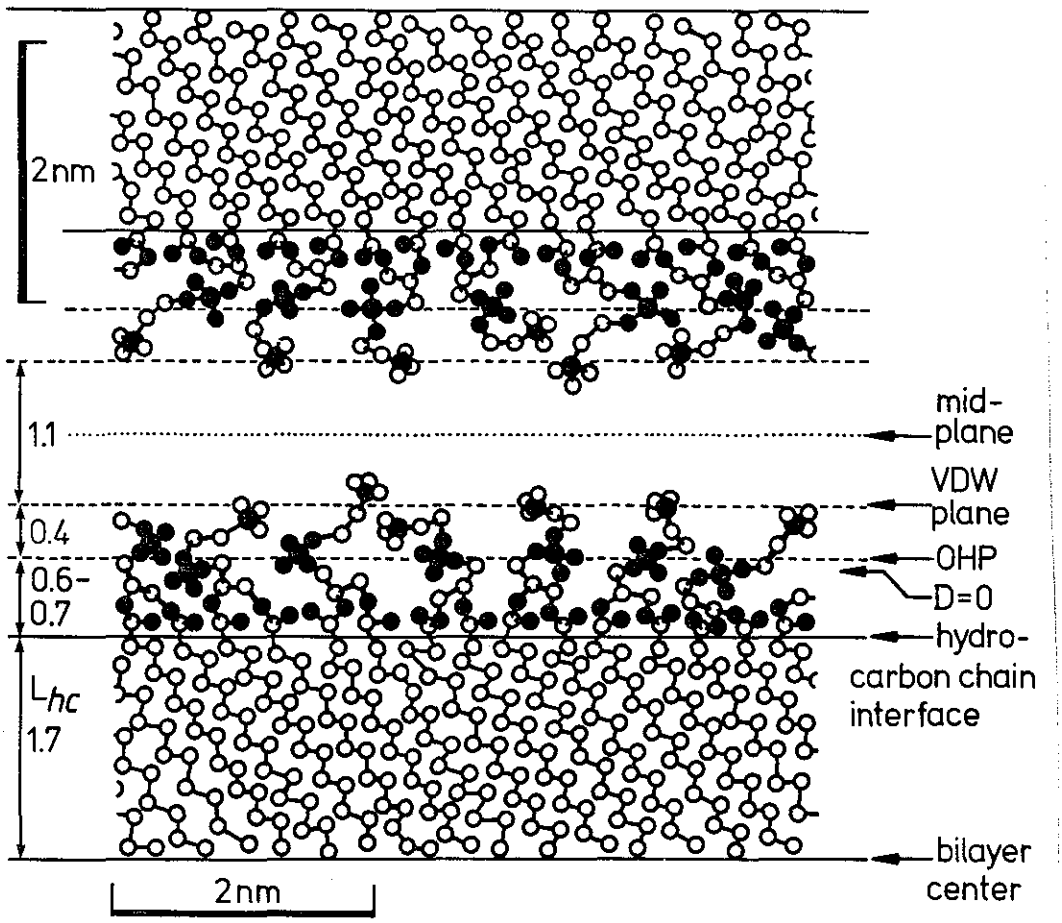

Fig. 25: Schematic view of planar DPPC bilayers at 21 °C with various structural dimensions and interaction distances drawn to scale. The position of the OHP - the plane of charge and probable site of ion binding - coincides with the position of the PO^- group; the plane of origin of the van der Waals interaction probably coincides with the mean position of the thermally mobile trimethylammonium groups. For different PCs and PE in different phase states, while L_{hc} will vary depending on the hydrocarbon chains, the OHP and VDW planes do not appear to change by more than 0.1 nm relative to the hydrocarbon-water interface. For free bilayers in the fluid state, additional thermal motions of the hydrocarbon-water interface could modify some of the above parameters and increase the range of the steric repulsion between bilayers.

in a flat orientation on each surface, but that the terminal parts of the headgroups are extended on average by about 0.5 nm beyond the anhydrous headgroup configuration (which defines D = 0). This is in agreement with the neutron scattering data of D.L. Worcester (unpublished experiments) who found that the terminal (deuterated) methyl groups of fully hydrated egg lecithin bilayers sample the whole aqueous interspace during

their motion, with the peak in the distribution occurring at a spacing of about 1.1 nm across the water space. Independent confirmation of this phenomenon comes from other neutron scattering measurements of the number density distribution of water molecules across the aqueous regions of partially and fully hydrated lecithin bilayers, which show (at a resolution of 0.7 nm and positional accuracy of 0.1 nm) that the water density in the region between two bilayers in adhesive contact nowhere attains its bulk value, even at the centre of the aqueous region [see Fig. 6 in Worcester and Franks, 1976; Worcester, 1976].

From the adhesion force F_0 between the two cylindrically curved surfaces, each of radius R, the value of F_0/R quoted in all the results is convenient for two reasons. First, $E_0 = F_0/2\pi R$ where E_0 is the energy, or work of adhesion, per unit area of two planar surfaces. This value is also needed for calculating the total adhesion free energy of two curved deformable bilayers, e.g. two large vesicles (Israelachvili, 1985c). Second, it gives the force needed to separate a vesicle of radius R = 1 m from 'contact' with a planar surface, or twice the force to separate two vesicles each of radius R = 1 m. For other radii, the force of adhesion simply scales by R.

The measured adhesion forces and energies ($E_0 \approx 0.1$ mJ/m^2 for PCs in water) are much higher, by a factor of about 4, than would be obtained if one assumes that the van der Waals plane is at D = 0. This is important for estimating interbilayer and intervesicle adhesion energies and has important implications for theoretical considerations of fusion and the relative stability of vesicles and multibilayer liposomes (Israelachvili et al., 1980). From the adhesion forces it was deduced that the effective Hamaker constants at short-range are all within $A = 6 \pm 2 \times 10^{-21}$ J, when referred to $D_{VDW} = 0$ at $D = 1.05 \pm 0.1$ nm (Fig. 25). For hydrocarbons such as hexadecane across water, we expect $A = 5\text{-}7 \times 10^{-21}$ J, and since the headgroup region contains water, one might expect even lower values. The slightly higher values obtained could be due to the higher contributions from the polar headgroup and/or to some residual hydrophobic attraction (Israelachvili and Pashley, 1984) in addition to the van der Waals contribution.

At longer range, beyond the adhesive minima, but still below distances where retardation becomes important, the value of A is much less than expected, viz. $A = 1.3 \pm 0.2 \times 10^{-21}$ J. It is possible that this lower value arises from the screening of the temperature-dependent contribution to A which theoretically is about 3×10^{-21} J for hydrocarbon across water (Mahanty and Ninham, 1976). This is expected to occur at large distances but only in high salt (see Section 1.4); here, the presence of high concentrations of the negative and positive charges of the zwitterionic headgroups between the two surfaces may already act to reduce the Hamaker constant at distances beyond the adhesive minima. In the previous chapter, the screening of the van der Waals attraction in high salt was demonstrated for the non-ionic galactolipid bilayers.

Thus for PE and PC, while the adhesion force appears to be well given by a reasonable Hamaker constant, the complete force law cannot be described by a single power law, or a single Hamaker constant, over the whole distance regime.

Likewise, the short-range repulsive forces can not be described by a simple equation, such as a single exponential function. In some cases, the repulsion closer in could be fitted by an exponential function (see Figs. 16 and 18) but farther out, towards the equilibrium separations D_0, the repulsive forces always fell much more steeply.

There is a definite correlation between the range of the repulsive forces and the phase state of the bilayers: the range being greater for bilayers in the fluid state ($T > T_c$) than in the gel state ($T < T_c$). At this point, it is worth comparing the results with the repulsive forces previously measured using the osmotic pressure technique (Lis et al., 1982b) (see Fig. 16C) where the agreements are quite good. In Fig. 16, both experiments find that the repulsive forces are of longer range for bilayers above T_c than below T_c.

As already noted in the previous chapter, the molecular mechanism responsible for the short-range repulsion is complicated. It can not be simply a pure 'hydration force' due solely to water structure effects, since, as already discussed, the aqueous region is not pure water but contains the thermally mobile headgroups (see also Zaccai et al., 1979). As proposed by Huh (1979), these must contribute their own entropic 'steric

repulsion' in the same way that surfaces with adsorbed polymers repel each other (Dolan and Edwards, 1974). Indeed, it is noteworthy that both theoretically and experimentally this type of steric repulsion is in general expected to be exponentially repulsive at short range, but decaying more rapidly at larger distances (Dolan et al., 1974; Israelachvili, 1985b; Klein and Luckham, 1984). It is proposed that this type of interaction is the main cause of the 'hydration forces' so far measured between lipid and surfactant bilayers, where the role of the hydration shell around each headgroup comes into the picture in determining the excluded volume of the headgroups which will extend the range of the repulsion (Dolan and Edwards, 1975). This interpretation in terms of a coupled 'steric-hydration interaction' is consistent with all the force measurements reported so far on such systems. Furthermore, it explains the increased range of these forces between free bilayers above T_c, due to the increased thermal fluctuations and undulations of the now fluid bilayers.

Clearly, the steric contribution to the total repulsion is complex, and made up of at least three interactions: a (polymer-type) steric repulsion as discussed above, a contribution from long wavelength undulations of bilayers (Helfrich, 1978; Sornette and Ostrowsky, 1984), and a contribution from local fluctuations in bilayer thickness (Lis et al., 1982b). Further insight into the relative contributions of these three interactions may be gleaned by comparing the results on adsorbed bilayers with those using the osmotic pressure technique on free bilayers (cf. Fig. 16C). First, it is seen that the range of the repulsive forces in pure water are the same for PC bilayers below T_c, with D_0 in the range 2.0-2.2 nm in both systems. This suggests that the steric-hydration interaction of the headgroups is mainly responsible for this repulsion. For PC bilayers in the fluid state, where additional thermal thickness fluctuations and undulations of whole bilayers should be expected, the repulsion between free bilayers is now of longer range than that between adsorbed bilayers (cf. equilibrium separations D_0 in the range 2.7-3.3 nm for the free bilayers with 2.4-2.5 nm for adsorbed bilayers). Clearly, the restricted possibilities for undulations of adsorbed bilayers has reduced the range of the steric-hydration repulsion compared to that for free bilayers (Israelachvili, 1985b).

Thus, above T_c, there is a significant contribution to the repulsion from all three types of steric-hydration interactions.

What can be said about the relative importance of the steric and purely hydration force contributions? Can they be separated? As described earlier, the refractive index results show that there is no measurable extrusion of the bilayers as they are forced together (at least over the range of compressive forces of these experiments). Consequently, the repulsive forces reflect the simultaneous entropic compression and dehydration of the headgroups. These two effects may be coupled so intimately as to be inseparable. It may be possible to consider the interaction as a steric one, with the hydration of the protruding hydrophilic headgroups treated simply as an excluded volume effect, increasing their effective volumes above their van der Waals radii (Dolan and Edwards, 1975). It is also possible that the fundamental hydration interaction is oscillatory (Pashley et al., 1984) but that the inherent roughness of bilayer surfaces and the thermal motions of the headgroups and hydrocarbon-water interfaces smear these out and extend the range of interaction (D. Sornette and N. Ostrowsky, unpublished results) so that there remains only a smooth overall repulsive force.

Further insight into the hydration force contribution comes from the effects of high concentrations of LiCl, NaCl and CsCl. The reduced range of the steric-hydration force in 1.3 M LiCl may be due to a 'salting out' effect, whereby the highly hydrated Li^+ ion now competes with the headgroups for water. The reverse occurs with the very weakly hydrated Cs^+ ion, while Na^+ is intermediate, giving a hydration force and adhesion similar to that in pure water. We also conclude that there is no significant binding of monovalent ions to PC and PE bilayers (unless both the anions and cations bind equally).

With Ca^{2+} and Mg^{2+} chloride solutions, significant cation binding already occurs below 1 mM. This results in a long-range double-layer repulsion but does not affect the short-range steric-hydration repulsion. For any particular lipid system, a single binding constant is enough to describe quantitatively the bindings at all electrolyte concentrations from 1-100 mM, and the double-layer forces are also excellently described

by theory. At shorter range, the attractive forces cause the surfaces to jump into adhesive contact, but the question is whether it is only the van der Waals force responsible for the attraction. When the experimentally determined Hamaker constant $A = 1.3 \times 10^{-21}$ J (in pure water) is used, the theoretical force curves in Figs. 20-23 appear to be somewhat too repulsive at short bilayer separations. Of course, below 20 Å it may well be questioned whether continuum double-layer theory still holds and whether the simple charge regulation model developed in Chapter 1 is adequate enough. It is quite possible that discreteness of charge effects begin to play a role, since below 20 Å, the bilayer separation is much less than the mean distance between two adsorbed Ca^{2+} ions on the bilayer surface (see Table III). Also, Kjellander and Marcelja (1985a) predicted that through ion-ion correlation effects on both surfaces, an extra attraction comes in comparable to the conventional van der Waals interaction. However, their theory has not been worked out completely and especially the deconvolution of charge-regulation effects and the ion-ion correlation effects is unknown. Whatever the precise cause may be, a range of A from 3 to 6×10^{-21} J would account for all the data near the force maxima in Figs.20-23.

As in many colloidal and biocolloidal systems, the binding of Ca^{2+} was always greater (by up to a factor of 2) than that of Mg^{2+} - a consequence, no doubt, of the lower hydration of Ca^{2+}. Binding of both cations (especially that of Ca^{2+}) was also sensitive to the phase states of PC bilayers, in the order: gel state > pretransition state > liquid state. These trends are entirely consistent with those previously reported by Lau et al. (1980) and Lis et al. (1981). The binding constants measured in the present study for Ca^{2+} and Mg^{2+} to DPPC and DMPC in the absence of NaCl (Table IV) are about a factor of two larger than those measured using electrophoresis by MacDonald and McLaughlin (personal communication). Concerning calcium binding to bilayers in the fluid state, the value of $K = 15\ M^{-1}$ of Ca^{2+} binding to DLPC is very close to that of $K = 19\ M^{-1}$ measured by Akatsu and Seelig (1981) for DPPC at 59 °C (fluid state) using deuterium magnetic resonance, while in a later study with POPC (1-palmitoyl-2-oleoyl-5n-glycero-3-phosphocholine) at 40 °C, the binding measured by Altenbach and Seelig (1984; Table I) in dilute $CaCl_2$ solutions was again very similar.

Finally, the fusion between two bilayers was observed only once they were about 15% thinner than their equilibrium thickness, i.e. exposing a larger hydrophobic area than when in the natural state. Fusion is initiated at one point via a local deformation involving the parting of headgroups followed by a breakthrough and meeting up of the hydrocarbon chains of apposing bilayers, as described by Horn (1984), and earlier suggested by Hui et al. (1981). Interestingly, the shape of the force-law between the two thinned bilayers at distances down to the point of fusion was not obviously different from some of the other force-laws measured when there was no fusion: the long-range attraction and adhesion was greater than for unthinned bilayers - perhaps due to some additional hydrophobic interaction, and the repulsive wall was less steep - perhaps due to the weakened, softer bilayers. While more work needs to be done in this area, it does appear that a knowledge of the interbilayer force-law alone does not allow us to deduce when a fusion will occur. The intrabilayer forces involved in the local stresses and deformations accompanying the fusion process must also be considered.

CHAPTER 5

FORCES BETWEEN MOLECULES IN MONOLAYERS AND BETWEEN BILAYERS OF PHOSPHATIDYLGLYCEROL

5.1 INTRODUCTION

The previous chapters have dealt with the interactions between intrinsically uncharged lipid bilayers. It is a natural extension to proceed with investigations on charged lipid bilayers. The present chapter reports the results of force measurements between DSPG bilayers and DMPG bilayers. Phosphatidylglycerol (PG) is the major negative lipid in bacterial and plant membranes (Lehninger, 1975). It carries a single charged phosphate group (see Fig. 1), and has a phase behaviour which is fairly well understood (Findley and Barton, 1978). In animal membranes, phosphatidylglycerol is usually replaced by phosphatidylserine.

A few studies on PG monolayers at the air-water interface have been published (Tocanne et al., 1974; Sacre and Tocanne, 1977). They have shown that protons, monovalent cations and divalent cations all show some degree of binding to the PG headgroups. The presence of divalent cations can also have a profound influence on the phase separation behaviour of PG molecules in bilayers composed of mixtures of lipids (Findley and Barton, 1978). An important bilayer study on the adsorption of divalent ions to PG has been published by Lau et al. (1981) using electrophoresis and NMR. A knowledge of the degree of ion binding is essential for understanding the interbilayer interactions, as we have seen in the case of PE and PC bilayers.

Cowley et al. (1978) have measured the repulsive force between PG bilayers (without added electrolyte) using the osmotic stress technique. Apart from the expected double-layer force, they also report the existence of an additional short-range hydration repulsion below 30 Å bilayer separation.

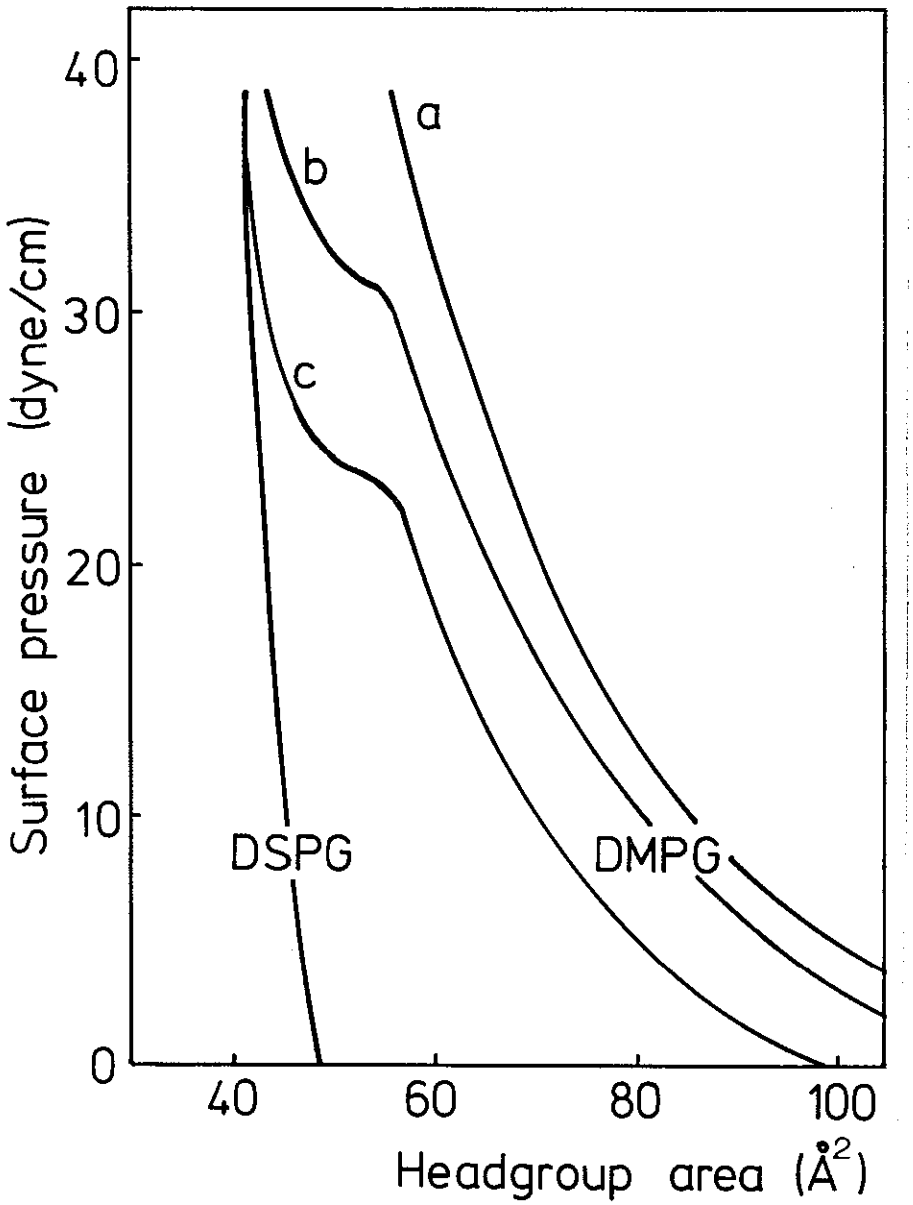

Fig. 26: Monolayer isotherms of DSPG and DMPG on various electrolyte solutions: (a) 1 mM phosphate buffer, pH = 6.9; (b) 100 mM NaCl + 1 mM $CaCl_2$, pH = 5.5; (c) 1 mM NaCl + 1 mM $CaCl_2$, pH = 5.5.

In this chapter, the full force-laws will be given between fluid-phase DMPG bilayers and gel-phase DSPG bilayers. The binding of Na^+, H^+, and Ca^{2+} ions is investigated as well as the force of adhesion and the possible existence of a hydration force. Furthermore, the contraction of a PG monolayer at the air-water interface following addition of NaCl and/or $CaCl_2$ is given attention. A comparison is made between the experimentally observed monolayer contraction and the theoretically predicted contraction using the theory of the diffuse double-layer. This comparison gives

an insight into the lateral interactions between PG lipids in monolayers and bilayers as a function of the electrolyte species present in the aqueous solution. The results shed new light on the interbilayer and intrabilayer interactions of PG and identify possible factors responsible for the morphological behaviour of PG aggregates.

5.2 RESULTS

5.2.1 Monolayer Compression Isotherms of DMPG and DSPG

Fig. 26 shows the monolayer compression isotherm of DSPG (22 °C) and DMPG (27 °C) at various electrolyte concentrations. The DSPG monolayer is clearly in the gel phase, remains unaffected by changing the electrolyte concentration, and has a limiting headgroup area of 42 $Å^2$.

The DMPG monolayer isotherm on a 1 mM phosphate (pH = 6.9) subphase is of the liquid-phase type and shows only a minor contraction of about 1.5 dyne/cm upon raising the electrolyte concentration to 100 mM NaCl (isotherm not shown). However, a pronounced contraction and a first order phase transition is observed following addition of 1 mM $CaCl_2$ (no buffer added; pH = 5.5). Clearly, Ca^{2+} raises the phase transition temperature of the DMPG monolayer, which is 24 °C when no divalent ions are present. The effect of Ca^{2+} furthermore depends on the NaCl concentration. A quantitative analysis of the effect of Ca^{2+} will be carried out later when from an analysis of the force measurements, the binding affinities of Na^+ and Ca^{2+} to the DMPG headgroups have been determined.

5.2.2 Langmuir-Blodgett Deposition of PG on Mica

Fig. 27 shows the deposited headgroup areas of DSPG and DMPG on a first layer of DPPE. Because in pure water, both the mica and the PG molecules are negatively charged, a deposition of PG as a first layer on mica is impossible. Hence, the choice to take DPPE as a first deposited layer is again particularly suitable.

In experiments where the interbilayer forces were to be measured, DSPG was deposited at a surface pressure Π = 32 dyne/cm giving a deposited headgroup area of 42 $Å^2$. DMPG was deposited at Π = 38 dyne/cm, which leads to a deposited headgroup

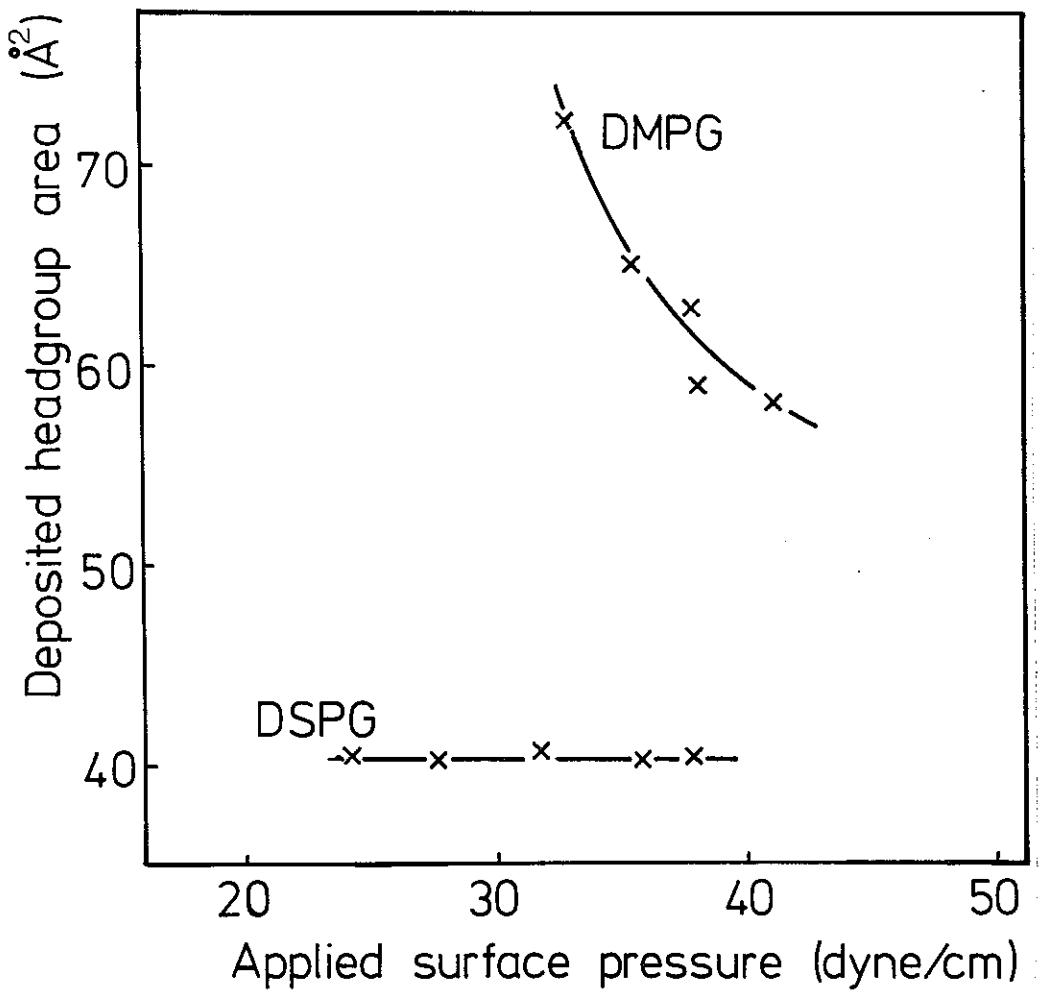

Fig. 27: Deposited headgroup areas on a hydrophobic DPPE monolayer of DMPG (27 °C, pH = 6.9) and DSPG (22 °C, pH = 5.5) as a function of the applied surface pressure in the Langmuir trough.

area of 60 Å^2. Because the deposition was carried out in a 1 mM phosphate buffer at pH = 6.9 (27 °C), the outer layer of DMPG lipids is in the liquid phase.

5.2.3 Forces between DSPG Bilayers

Forces between DSPG bilayers deposited on mica were measured in electrolyte solutions with concentrations up to 100 mM for NaCl and 10 mM for $CaCl_2$. This range includes the physiologically interesting ionic environment of 100 mM monovalent electrolyte with about 1 mM divalent electrolyte.

Monovalent ions are known to have a much lower binding affinity for the charged phosphate groups than divalent ions. The previous measurements on PC and PE bilayers failed to show a detectable monovalent ion binding, but demonstrated

substantial Ca^{2+} and Mg^{2+} binding. In those systems, the double-layer force increased in strength when the divalent ion concentration was increased (increase in the surface charge), but its range decreased due to the enhanced ionic screening of the surface charge. In the present system, the initial charge density on the DSPG surface is 1 elementary charge per 42 $Å^2$ which only can decrease due to ion binding. Hence, when the electrolyte concentration is increased, both the strength and range of the double-layer forces are expected to decrease.

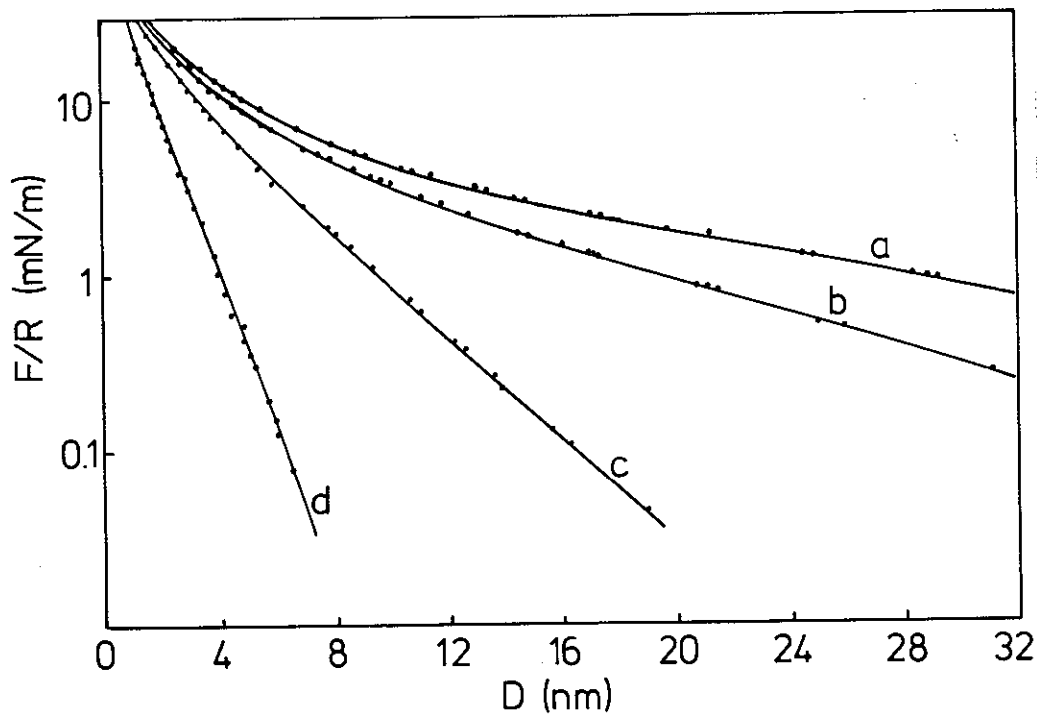

Fig. 28: Measured forces between two DSPG bilayers (22 °C, pH = 6.9) at various NaCl concentrations. See also Table I. The solid lines are the theoretically predicted forces assuming fully charged bilayers and a Hamaker constant $A = 6 \times 10^{-21}$ J. (a) 0.3 mM NaCl; (b) 1.1 mM NaCl; (c) 9.2 mM NaCl; (d) 100 mM NaCl.

Fig. 28 gives the forces in 10^{-4} M to 10^{-1} M NaCl as a function of the bilayer separation. Note the expected longer range of the double-layer forces in the more dilute solutions. An important problem in these experiments is the determination of D = 0: the outer Helmholtz plane (OHP). It is evident in Fig. 28 that contact at D = 0 can never be attained in a monovalent electrolyte solution. At surface separations less than 20 Å, the double-layer repulsion becomes so strong that the supporting curved mica

surfaces locally begin to flatten. The van der Waals attraction is completely dominated by the electrostatic repulsion and no adhesion was ever observed. However, when at the end of an experiment a small amount of $CaCl_2$ was added, there was a drastic reduction in the double-layer force (see below) and at close separation a sudden jump into adhesive contact. This contact was chosen as D = 0 for the following reasons:

(i) When forcing the two adhering surfaces further together under a large load, they appear to behave essentially as a hard wall: no hydration force was observed.

(ii) Draining the apparatus of water removes the outer DSPG monolayers from the mica surfaces, exposing only the hydrophobic first DPPE layers which can be brought into contact again in air. A comparison of the surface contacts before and after the drainage with the FECO interferometry gave for the thickness of the two outer monolayers (one DSPG bilayer) a value of 59 ± 1 Å. A theoretical calculation for the thickness of a DSPG bilayer was carried out using Tanford's formula for the volume v of an alkane hydrocarbon chain in the gel phase containing n carbon atoms (Tanford, 1972): $v = (2 \times 27.4 + n \times 26.9)$ Å^3. Choosing the PG headgroup volume as 300 Å^3 (Small, 1967) and using the deposited headgroup area of 42 Å^2, the thickness T of the bilayers is calculated as $T = 2 \times [2(27.4 + 26.9 \times 17) + 300]/42 = 60$ Å. Now, this is identical to the experimental thickness, which means that the observed hard wall is due to the lipid headgroups and that there is almost no hydration region near the bilayer surfaces, contrary to what has been found for PE and PC bilayers in the previous chapter. Assuming that the PG headgroups are laying flat on the surface when two bilayers adhere to each other, the charged phosphate groups must be exposed to this surface, which leads us to locate the position of D = 0 at the contact between the two bilayer surfaces. It follows that the outer Helmholtz plane and the van der Waals plane, defined as the effective hydrocarbon/water interface are expected to be both virtually identical to D = 0.

An analysis of the force curves in Fig. 28 can now be carried out by fitting the curves to the theoretical double-layer repulsion with charge regulation as described in

Chapter 1. This makes it possible to fit the intrinsic binding constant K_{Na} for Na^+ ions and to obtain the surface charge σ_0^∞ and the surface potential ψ_0^∞, existing when the bilayers are well separated. Due to the charge regulation, both the surface charge and the surface potential will change to some extent when the bilayers approach each other.

While analysing the force-laws between DSPG bilayers, it became evident that K_{Na} was very low indeed ($< 0.4\ M^{-1}$) and that all the force curves could be fitted adequately by assuming a fully charged bilayer surface. Both the range and magnitude of the measured double-layer force are in excellent agreement with theory. However, with the present technique, an accurate determination of very small binding constants is not possible, since in the limit of high charge density, the double-layer force becomes fairly insensitive to a small reduction of the surface charge through ion binding. The results given in Table V for the values of ψ_0^∞ and σ_0^∞ should therefore not be taken too literally and are probably somewhat too high.

Fig. 29 gives the force-laws between DSPG bilayers in the presence of 10^{-5} - 10^{-3} M of $CaCl_2$ only. Fig. 30 gives the forces in mixtures of NaCl and $CaCl_2$. It is seen that the magnitude of the double-layer force is much reduced compared to that in a NaCl solution. Not only screening but also substantial binding of Ca^{2+} has to be taken into account in order to fit the results with theory. Values for K_{Ca}, ψ_0^∞, σ_0^∞, and the surface area per elementary charge for various electrolyte mixtures are given in Table V.

In Fig. 29, it was noted that in 10^{-5} M $CaCl_2$ solution, the decay of the double-layer force with distance is somewhat more rapid than according to theory. This observation is in agreement with the results of earlier measurements of double-layer forces between mica surfaces in dilute $CaCl_2$ solutions (Israelachvili and Adams, 1978) and might reflect inadequacies of the double-layer theory. In a 100 mM NaCl + 10 mM $CaCl_2$ solution, no repulsion could be measured any more.

Figs. 29 and 30 show that the van der Waals attraction becomes apparent below 30 Å bilayer separation. The bilayers jump into adhesive contact from that distance where the gradient of the force equals the spring constant. Taking the van der Waals

Table V: DOUBLE LAYER AND ADHESION RESULTS FOR DSPG BILAYERS AT 22 °C; ($K_{Na} = 0$)

Electrolyte Concentration NaCl (mM)	$CaCl_2$ (mM)	Surface Potential ψ_0^∞ (mV)	Surface Charge σ_0^∞ (C/m^2)	($Å^2$/charge)	Binding Const. K_{Ca} (M^{-1})	Adhesion Energy E_0 (dyne/cm)
0.3	-	-310	-0.381	42	-	-
1.1	-	-265	-0.381	42	-	-
9.2	-	-212	-0.381	42	-	-
100	-	-154	-0.381	42	-	-
~0.03	0.01	-93	-0.0075	2130	60	0.48
~0.03	0.12	-64	-0.0080	2000	48	0.56
~0.03	1.2	-37	-0.0083	1930	40	0.64
1	0.1	-69	-0.0109	1470	40	0.40
1	1.2	-37	-0.0088	1820	40	0.64
100	0.1	-65	-0.0623	257	40	-
100	1.0	-38	-0.0315	508	40	-
100	10.0	-	-	-	-	0.80

force law Eq. (33), the forces below D = 20 Å can be fitted when a Hamaker constant of about $8 - 10 \times 10^{-21}$ J is used. This value is slightly higher than the theoretically expected value of $5 - 7 \times 10^{-21}$ J for two hydrocarbon slabs interacting across water (Parsegian and Ninham, 1970). A similar small discrepancy was found in the previous chapter when the measured force-laws between PC or PE bilayers were analysed (see Section 4.2.6); the same possible reasons as the ones given in Section 4.2.6 might apply in the present case to explain this matter.

Upon pulling the bilayers out of adhesive contact, an adhesion force F_0 is needed to separate the surfaces. This adhesion force F_0 is related to the interfacial free energy per unit area, E_0, of two planar bilayers at their equilibrium separation D_0 according to Eq. (40). Values for E_0 at various electrolyte concentrations are given in Table V. We

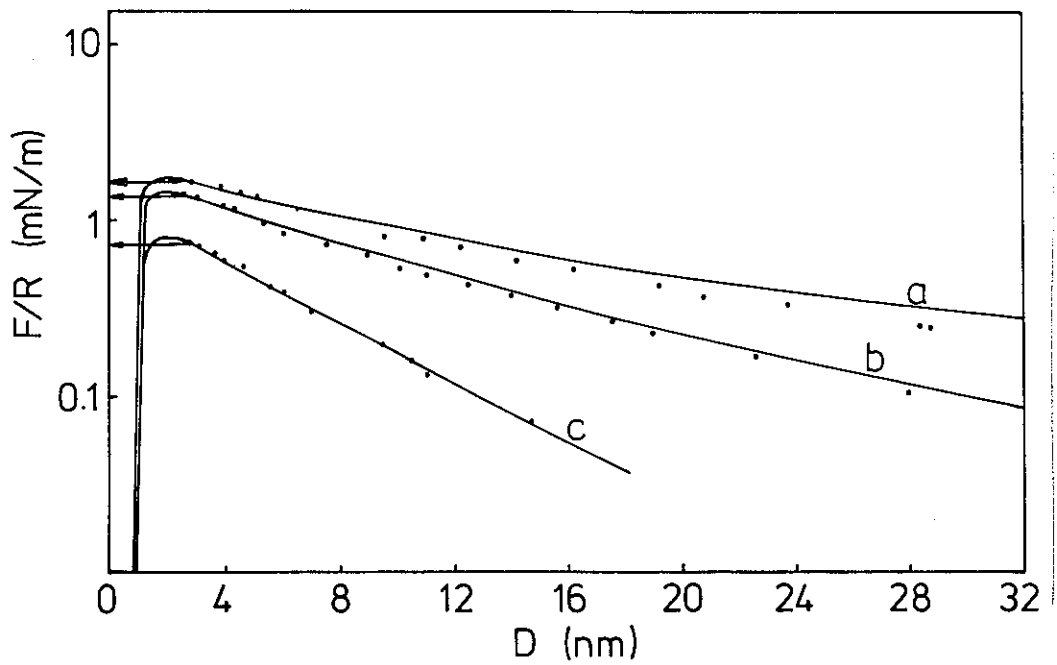

Fig. 29: Measured forces between two DSPG bilyers (22 °C, pH = 5.5) at various $CaCl_2$ concentrations. The arrows give the surface separations from where a jump into adhesive contact occurred. The solid lines are the theoretically predicted force curves using the binding constants given in Table V and assuming a Hamaker constant $A = 6 \times 10^{-21}$ J. (a) 0.01 mM $CaCl_2$; (b) 0.12 mM $CaCl_2$; (c) 1.2 mM $CaCl_2$.

see that E_0 has a limiting value of about 0.8 dyne/cm when the double-layer force becomes small. Using Eqs. (33) and (40) with $A = 6 \times 10^{-21}$ J, a calculation shows that the corresponding equilibrium bilayer separation should be $D_0 = 4$ Å. This agrees with the measured D = 3-5 Å where the curved bilayers jumped apart from each other under a pull-off force. Whether this non-zero distance can be called a hydration layer or not remains subjective. After all, when the two bilayers are at their equilibrium separation, a layer of Ca^{2+} ions is present between the surfaces and is expected to have an effect on D_0 through the finite size of the Ca^{2+} ions.

The proton dissociation from the DSPG headgroups was investigated by measuring the interlayer forces at different values of the pH. The measured force-laws are given in Fig. 31.

The same formalism used to describe the binding of Na^+ ions with the charge regulation model was applied to evaluate the binding of protons. At pH = 4.7 and 4.2,

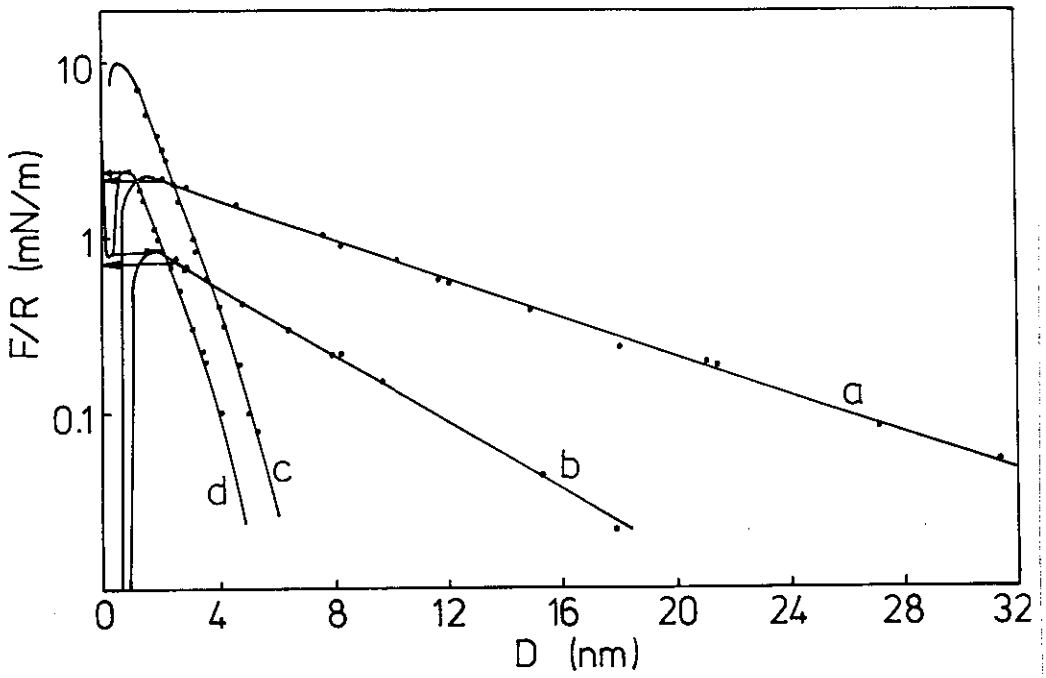

Fig. 30: Measured forces between two DSPG bilayers (22 °C) in mixtures of NaCl and $CaCl_2$ (see also legend of Fig. 29). In a 100 mM NaCl + 1 mM $CaCl_2$ solution, an outward jump from D = 4 Å to D = 20 Å was observed. (a) 1 mM NaCl + 0.1 mM $CaCl_2$; (b) 1 mM NaCl + 1.2 mM $CaCl_2$; (c) 100 mM NaCl + 0.1 mM $CaCl_2$; (d) 100 mM NaCl + 1 mM $CaCl_2$.

the intrinsic binding constants K_H were $K_H = 120\ M^{-1}$ and $150\ M^{-1}$, respectively. These values should be compared with the literature value for the dissociation of $H_2PO_4^-$ in solution (25 °C), i.e. $K_H = 132\ M^{-1}$ (Handbook of Chemistry and Physics).

At pH > 5, the proton concentration becomes relatively very low and the difference between the force curve of the fully charged bilayer and the partly protonated bilayer becomes relatively small. Under these circumstances, the constants K_H can not be determined accurately any more. On addition of 10 mM NaCl to a solution of pH = 4.7, the force curve became indistinguishable from the force curve in a 10 mM NaCl solution at pH = 6.9. Below pH = 4.0, it is expected that the phosphate groups are hydrolyzed on the bilayer surface.

5.2.4 Forces between DMPG Bilayers

A DMPG bilayer in a monovalent electrolyte solution (pH $\simeq$ 7) exists in the fluid state above T = 24 °C. The present experiments were performed at T = 27 °C.

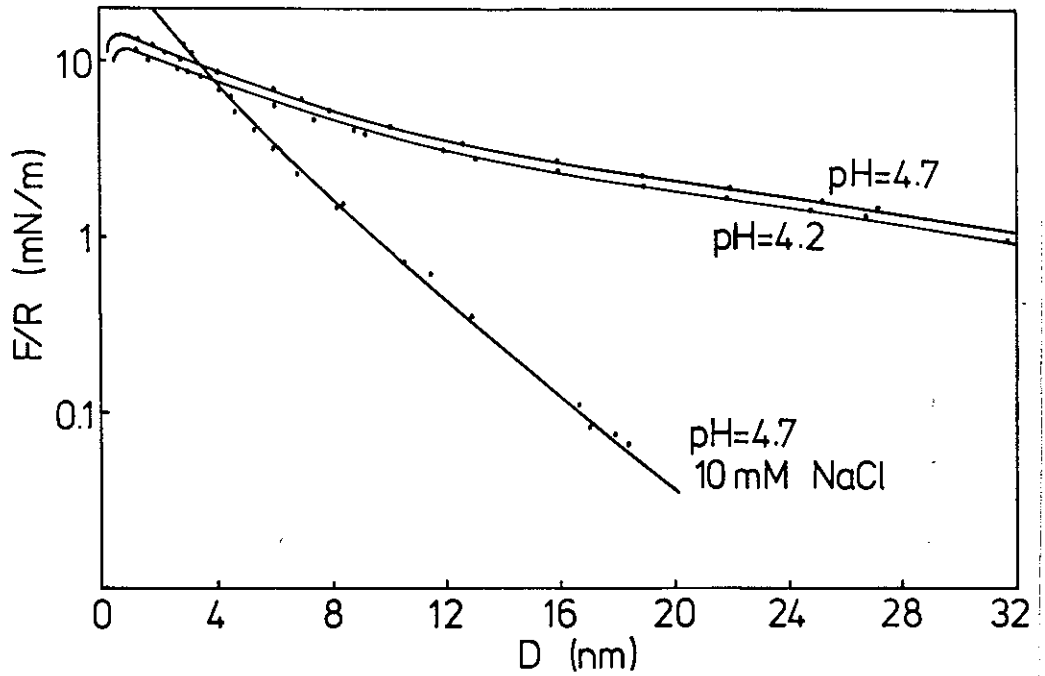

Fig. 31: Measured forces between two DSPG bilayers (25 °C) at pH = 4.7 and 4.2. The solid lines are the theoretically predicted forces using a binding constant $K_H = 120\ M^{-1}$ (ψ_0^∞ = -221 mV) or $K_H = 150\ M^{-1}$ (ψ_0^∞ = -191 mV) at pH = 4.7 and pH = 4.2, respectively. Background electrolyte concentration $\approx 10^{-5}$ M monovalent electrolyte. In a 1 mM NaCl, pH = 4.7 solution, the experimental (and theoretical) force curve is virtually indistinguishable from the predicted force curve between two fully charged bilayers. No adhesion was observed.

Following addition of $CaCl_2$, the phase transition temperature rises because of the decrease of the electrostatic free energy of the surface (Trauble et al., 1976). Note on the other hand, that with a headgroup area of 60 $Å^2$ at which the DMPG bilayer was deposited, the monolayer at 27 °C remains in the fluid state in the presence of $CaCl_2$ (Fig. 26) and shows a liquid-gel phase transition only below a headgroup area of 56 $Å^2$.

When a bilayer goes through a phase transition, it should contract to a smaller headgroup area and at the same time thicken. However, since the DMPG layer is deposited on top of a DPPE monolayer, the DMPG layer cannot contract to a headgroup area of 42 $Å^2$ without exposing a large hydrophobic DPPE surface area to water, which is energetically extremely unfavourable. Of course, extra DMPG monomers from solution can be incorporated but in regard to the very small DMPG equilibrium concentration (< 10^{-6} M), this must be a very slow process. The

experiments were carried out in a matter of hours and the headgroup area is expected to be fixed at 60 $Å^2$, leaving the DMPG layers to remain in the fluid phase whether this is the equilibrium phase or not. Indeed, no indication of a thickening of the bilayers became apparent during the experiments.

Fig. 32 gives the forces between two DMPG bilayers in 1.5 mM NaCl and mixtures of NaCl and $CaCl_2$, all at about pH = 6. As was found for the DSPG bilayers, also the DMPG bilayers showed no hydration force in the presence of $CaCl_2$ when they came into adhesive contact. Results from the analysis of the force curves are presented in Table VI.

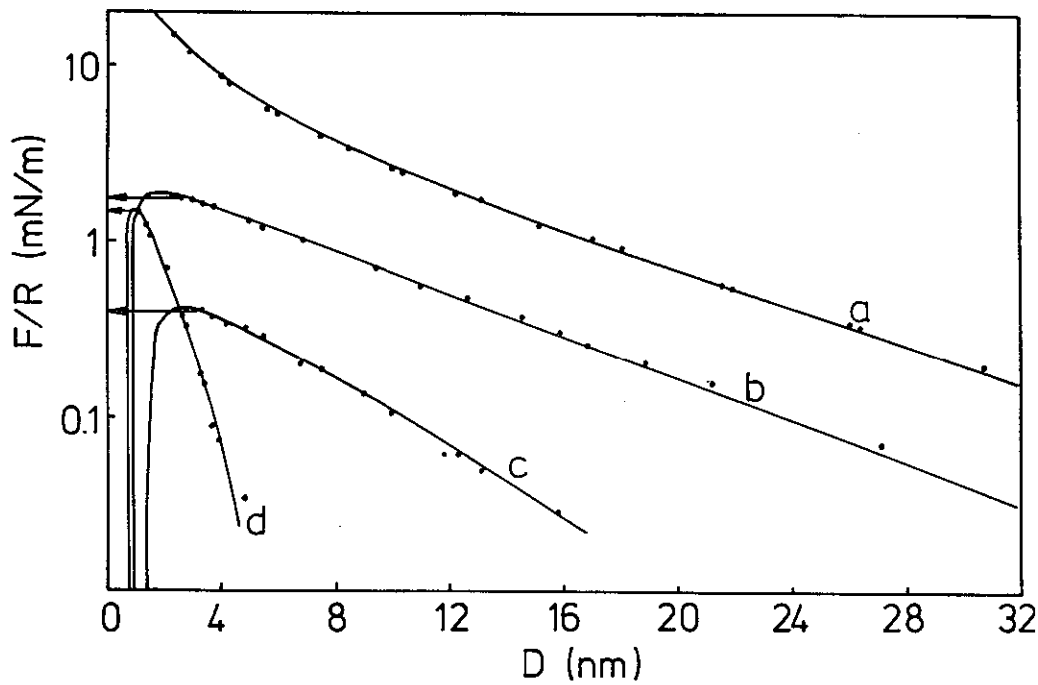

Fig. 32: Measured forces between two DMPG bilayers (27 °C) in a 1.5 mM NaCl solution (pH = 6.9) or in solutions containing a mixture of NaCl and $CaCl_2$ (pH = 5.5). The solid lines give the theoretical force curves using the binding constants given in Table VI and assuming a Hamaker constant $A = 6 \times 10^{-21}$ J. The arrows give the surface separations from where a jump into adhesive contact occurred. (a) 1 mM NaCl; (b) 1.5 mM NaCl + 0.08 mM $CaCl_2$; (c) 1.5 mM NaCl + 1 mM $CaCl_2$; (d) 100 mM NaCl + 1 mM $CaCl_2$.

It is apparent that the binding of both Na^+ and Ca^{2+} to DMPG is stronger than to DSPG. The forces between DMPG bilayers in a 1.5 mM NaCl solution are smaller than those between fully charged bilayers and can be fitted with an intrinsic binding

Table VI: DOUBLE LAYER AND ADHESION RESULTS FOR DMPG BILAYERS AT 27 °C.

Electrolyte Concentration NaCl (mM)	$CaCl_2$ (mM)	Surface Potential ψ_0^∞ (mV)	Surface Charge σ_0^∞ (C/m^2)	Surface Charge σ_0^∞ ($Å^2$/charge)	Binding Const. K_{Na} (M^{-1})	Binding Const. K_{Ca} (M^{-1})	Adhesion Energy E_0 (dyne/cm)
1.5	-	-191	-0.0970	165	0.6	-	-
1.5	0.08	-60	-0.0088	1820	0.6	100	0.64
1.5	1	-28	-0.0056	2857	0.6	100	0.96
100	1	-32	-0.0260	615	0.6	60	0.25

constant $K_{Na} = 0.6\ M^{-1}$, a value often quoted in the literature for phosphatidylglycerol bilayers (Lau et al., 1981). A consequence of the stronger ion binding is that in a 100 mM NaCl + 1 mM $CaCl_2$ solution, a significant adhesion energy $E_0 = 250$ mdyne/cm exists, whereas no adhesion was observed between two DSPG bilayers in the same electrolyte solution. Using the binding constants given in Table VI, excellent agreement with theory is obtained at large surface separations, but like what was found for DSPG bilayers, the theoretically predicted force-law is slightly too repulsive at small bilayer separations. Finally, the value of K_{Ca} decreases by almost a factor of two when the NaCl concentration is increased.

5.2.5 The Contraction of a DMPG Monolayer at the Air-Water Interface following Addition of $CaCl_2$

With the results on the surface potentials and binding constants of DMPG bilayers, we can now return to the monolayer compression isotherms in Fig. 26 and analyse the observed changes in the surface pressure Π as a function of the electrolyte concentration. Because the compression isotherms give an idea about the lateral interactions existing between adjacent lipid molecules in monolayers or bilayers, this analysis should provide insight into the importance of electrostatic interactions on the total lateral interaction.

The equations in Section 1.3 are used to evaluate the diffuse double-layer

contribution Π^{el} to the total surface pressure Π of the charged monolayer. The data in Table VI are used to calculate ψ_0^{∞} at a headgroup area of 60 $Å^2$ in the monolayer. The results on the differences in Π^{el} at various electrolyte concentrations are given in Table VII and a comparison is made with the experimentally observed changes in Π.

Table VII: MONOLAYER DATA OF DMPG (27 °C)

Electrolyte Concentration (mM) NaCl	$CaCl_2$	Π^{el} (theor.) (dyne/cm)	$\Delta\Pi^{el}$ (theor.) (dyne/cm)	$\Delta\Pi$ (exptl.) (dyne/cm)
1	-	4.7	1.3	1.4
100	-	3.4		
100	-	3.4	3.0	5
100	1	0.4		
1	-	4.7	4.6	13
1	1	0.07		
100	1	0.4	0.3	6
1	1	0.07		

It is apparent that good agreement with theory is only obtained when the subphase does not contain $CaCl_2$. When $CaCl_2$ is added, the observed decreases of the surface pressure are significantly larger, especially at low NaCl concentrations, than the theoretical predictions in which only the diffuse double-layer contribution is taken into account. The results indicate that changes in the chemical interactions between lipids accompanying ion binding are important as well and can be much larger than the change in the double-layer interactions alone.

5.3 DISCUSSION

The interbilayer force measurements have shown that there are only two types of forces operating between ionic bilayers: at long range the repulsive double-layer force and at shorter range the attractive van der Waals force (though some additional attraction at small bilayer separations can not be ruled out). No repulsive hydration or

steric force is observed, contrary to what has been claimed by Cowley et al. (1978). It follows that if adhesion and/or fusion is to occur between negatively charged bilayers or vesicles, the only repulsion that needs to be overcome is the double-layer force.

Also, no hydration forces were measured between bilayers of the cationic dioctadecyldimethylammonium surfactants (see next Chapter). Certainly, it is not the specific nature of the individual phosphate and methylated ammonium groups that is responsible for the hydration force found between PC and PE bilayers. In the latter bilayers, it must be the dipolar character of the zwitterion in the lipid headgroup which causes the hydration force, as proposed by Kjellander and Marcelja (1985b). According to their theory, the electric field between the oppositely charged groups on the PC or PE bilayers strongly orientates the water molecules in the vicinity of the surface (Pashley, 1981). When these bilayers are brought together, the water structure becomes disturbed which is energetically unfavourable. A hydration repulsion is the consequence.

Experiments on bare mica surfaces have shown that hydration forces are intimately associated with the adsorption of ions on the surface (Pashley, 1981). Because there, the negative surface lattice charge is known to be located a small distance below the basal plane of the mica/water interface, the adsorbed ions form dipoles with these lattice charges and a hydration force is observed when the mica surfaces are brought together.

However, in the present experiments on PG bilayers, no hydration force is observed in $CaCl_2$ solutions although almost 50% of the lipids carry an adsorbed Ca^{2+} ion. Assuming that the range of the hydration force is somehow a function of the dipole moment of the ionic species on the surface, the absence of a hydration force could be due to the intimate association of the Ca^{2+} ions with the phosphate groups, creating only a small dipole moment. Another possibility is that the adsorbed cations are simply not 'seen' when the bilayers come into contact because they sit between the headgroups, and probably bridge-bind between two adjacent headgroups (see below).

A phase transition in a PG bilayer appears to influence the binding affinity of ions. Bilayers in the fluid phase (DMPG) bind ions stronger than bilayers in the gel phase

(DSPG). This is also apparent from the observation that the adhesion between DMPG bilayers is stronger than the adhesion between DSPG bilayers in the same electrolyte solution. The magnitude of the adhesion force can be explained approximately from the sum of the van der Waals force and the double-layer force at the equilibrium bilayer separation. No bilayer fusion was ever observed to take place in this system. Note that the binding constants in Tables V and VI for Ca^{2+} with PG and the binding constants in Table IV for Ca^{2+} with PE and PC, which had values between 12 and 120 M^{-1}, are of comparable magnitude.

The intrinsic binding constants K_{Ca} in 100 mM NaCl (40 M^{-1} and 60 M^{-1} for DSPG and DMPG, respectively) are larger than the binding constant $K_{Ca} \simeq 8.5\ M^{-1}$ in a 100 mM NaCl solution (PG in the fluid phase) reported by Lau et al. (1981), who used the same adsorption model. Also, their reported zeta potential ψ_0 = -41 mV measured by electrophoresis in a 100 mM NaCl + 1 mM $CaCl_2$ solution, is clearly higher than the value of ψ_0^∞ = -32 mV at the OHP, found for DMPG bilayers in the present study. The latter comparison can be made because the OHP should be very close to the plane where the zeta potential is measured, a view held by most colloid scientists (Hunter, 1981).

A possible source of the discrepancy might be that Lau et al. (1981) used PG derived from egg-PC, which has a different hydrocarbon composition than synthetic DMPG. It is difficult to say to what extent a different hydrocarbon interior (unsaturation, etc.) changes the properties of the headgroup region, and a straightforward comparison between the two studies might not be possible. Another circumstance which should be considered is that in the present system, the potential at the OHP has been obtained using the theory of the diffuse double-layer. It is not obvious that this theory holds very close to the surface (where the zeta potential is measured), since discrete ion effects are not accounted for (i.e. Stern layer effects). This might affect the decay and magnitude of the potential up to a few Å from the surface.

Inspection of Table V shows that for a DSPG bilayer, the values for K_{Ca} are independent of the electrolyte concentration (except in 10^{-5} M $CaCl_2$ but that value is somewhat uncertain since the experimental decay of the double-layer force does not

agree with theory), suggesting that the Langmuir adsorption model is quite adequate here.

Table VI shows that the Langmuir adsorption model holds less well for the fluid DMPG bilayers. The values K_{Ca} decrease with an increase in the electrolyte concentration, a trend also found by Lau et al (1981). A possible reason is that the assumed 1:1 binding mode only is too simplistic and that 2:1 binding also occurs where Ca^{2+} bridges two neighbouring lipids. A 2:1 binding mode on phospholipid bilayers has been shown to exist by Altenbach and Seelig (1984), but a 1:1 binding mode is certain to occur as well, since by electrophoresis, PG membranes have been shown to reverse charge in concentrated $CaCl_2$ solutions (Lau et al., 1981).

An adsorption model in which both binding modes are considered is readily developed (but also increases the number of adjustable parameters). This has been done recently by Ohshima and Ohki (1985) who analysed their binding studies on PS monolayers with such a model. Like what was found for PG monolayers here, they also found that upon addition of $CaCl_2$, the surface pressure of a PS monolayer decreased much more than could be accounted for by pure double-layer effects only. According to them, the main cause of the decrease in the surface pressure following addition of $CaCl_2$ is a conformational change of the lipid headgroups due to the bridge-binding of divalent ions. A similar explanation can be given for the results presented here. (Note that possible Stern layer effects have always been ignored.)

Of relevance is also the work of Verkley et al. (1974), and Van Dyck et al. (1975, 1978) who studied the morphological characteristics and phase transitions of synthetic PG aggregates. They found a drastic increase in the phase transition temperature near surface neutralization by Ca^{2+} adsorption, and a morphological change from liposomal structures to cylindrical or lamellar structures.

These observations indicate that Ca^{2+} has a marked effect on the nature of the bilayer surface. The present results on PG monolayers show that apart from double-layer interactions, other more specific short-range factors like bridge-binding and/or conformational changes also play an important role.

CHAPTER 6

EFFECTS OF COUNTERION SPECIFICITY ON THE INTERACTIONS BETWEEN QUATERNARY AMMONIUM SURFACTANTS IN MONOLAYERS AND BILAYERS

6.1 INTRODUCTION

Recently, a strong interest has grown around the phenomenon of the spontaneous formation of vesicles of dialkyldimethylammonium salt surfactants (Ninham et al., 1983; Brady et al., 1984). Many of the surfactant salts such as the fluoride, acetate and hydroxide salts are very soluble in water, give isotropic solutions up to high surfactant concentrations and form stable vesicles spontaneously. This is in sharp contrast to the extensively studied vesicle systems of phospholipids (Fendler, 1983) which usually require sonication to facilitate vesicle formation, are often unstable, eventually reverting to a liquid-crystalline lamellar phase. In general, these vesicles are not monodisperse either.

As the theory concerning the equilibrium statistical mechanics of self-assembly of dilute surfactant solutions is well established (Israelachvili et al., 1976, 1977; Carnie et al., 1979; Evans et al., 1986), it is important to have access to equilibrium systems which can be subjected to intensive scrutiny. The dialkyldimethylammonium salt surfactants provide such a system.

The theory of the assembly of surfactants can be characterized in terms of the geometric parameter v/al. Here v is the volume of the hydrocarbon region of the surfactant, a is the optimal headgroup area and l is an optimal hydrocarbon chain length related to its maximum extended length. The theory relates the shape of the aggregates to the value of v/al: (1) spherical micelles: $v/al < \frac{1}{3}$; (2) globular or cylindrical micelles:

$\frac{1}{3} < v/al < \frac{1}{2}$; (3) vesicles or bilayers: $\frac{1}{2} < v/al \leq 1$. These criteria demand that if vesicles are the desired structure, one is normally restricted to double-chained surfactants (larger v). Single-chained surfactants form micellar structures.

The relationship between aggregate geometry and surfactant structure has received considerable attention, but specific counterion effects have remained largely unexplored (Brady et al., 1985). The present study deals with specific counterion effects. Attention is given to the possible influence which counterion adsorption and Stern layer effects can have on the aggregate geometry (via its effect on the optimal headgroup area a). Note that Stern layer effects were ignored in analysing the results given in the previous chapters.

In general, counterions will adsorb to some extent to the surfactant headgroups. This not only alters the electrostatics on the aggregate surface, but also might change the hydrophobic-hydrophilic nature of the surface through specific interactions of a non-electrostatic kind (Ohshima and Ohki, 1985) (dehydration of the surfactants, conformational changes in the surfactant headgroups, etc.). In the case of quaternary ammonium surfactants, there is some evidence that Stern layer effects, where the distance of closest approach of an unbound counterion to the surface is considered (Ninham et al., 1983; Brady et al., 1985; Stigter, 1975; Beunen et al., 1983), must be given special attention. Here, the size of the ion becomes important because it determines the thickness of the Stern layer and the actual surface potential (Hunter, 1981).

Specific interactions can also greatly change the lateral interactions between surfactants in a monolayer or bilayer. This has been shown in the previous chapter with the work on PG, and by Ohshima and Ohki (1985) with work on PS. In those systems, the specific influence of bridge-binding of Ca^{2+} seemed to be most important (the significance of Stern layer effects is completely unknown). Specific effects have been found to exist in the spontaneous formation process of vesicles of quaternary ammonium salt surfactants (Ninham et al., 1983; Hashimoto et al., 1983; Talmon et al., 1983) and are evidently responsible for the phenomenon of counterion-dependent CMCs and

aggregation numbers in micellar solutions (Brady et al., 1985; Porte and Appell, 1982). They also have shown up dramatically in three-component ionic microemulsions (Evans and Ninham, 1986). An understanding of these processes enables one to elucidate specific counterion effects other than counterion valency.

A logical way to attack this problem is first to establish the amount of ion adsorption by the direct force measurement technique and second its consequences on the lateral interactions between adjacent surfactant molecules by recording the surface pressure of the monolayer as a function of the electrolyte species present in the subphase, as has also been done with PG lipids. Changes in the lateral interactions between the surfactants are expected to be related to the equilibrium headgroup area and hence the curvature of a surfactant aggregate through the geometrical factor v/al.

Direct force measurements between (planar) bilayers are also of use in the evaluation of the interaggregate interactions. The latter can be obtained by a simple scaling of the measured bilayer interaction as long as the aggregates are large compared to the range of the interaggregate interaction (Israelachvili, 1985a). The interaggregate interactions are important to explain the phase behaviour of surfactant solutions as a function of the surfactant concentration (Brady et al., 1985).

Using the direct force measurement technique, Pashley et al. (1986) investigated the interactions between bilayers of dihexadecyldimethylammonium acetate surfactants. Because these surfactants are soluble in water, they could be adsorbed from solution as a bilayer on the mica surfaces. The advantage of this adsorption from solution method is that the adsorbed bilayers and the surfactants in solution necessarily form an equilibrium system. A disadvantage is that at low electrolyte concentrations, the aggregates in solution have an influence on the measured double-layer force between the adsorbed bilayers, which is hard to quantify, especially when the geometry of the aggregates is unknown. Using the Langmuir-Blodgett deposition technique for an insoluble surfactant like dioctadecyldimethylammonium bromide (DOABr), the solution can be saturated with monomers without containing any aggregates and provides an infinite reservoir of electrolyte.

Finally, it can be expected that the general binding behaviour of anions to the quaternary ammonium headgroups responsible for the electrostatics on the amphiphilic surfaces, will not depend sensitively on the precise length of the hydrocarbon tails and the results obtained here with DOA salt surfactants should be of relevance to shorter chained surfactants as well. Of course, the packing of the surfactants and the geometry of the aggregates do depend on the hydrocarbon chain length, but this can be accounted for as long as the optimal headgroup area remains approximately the same.

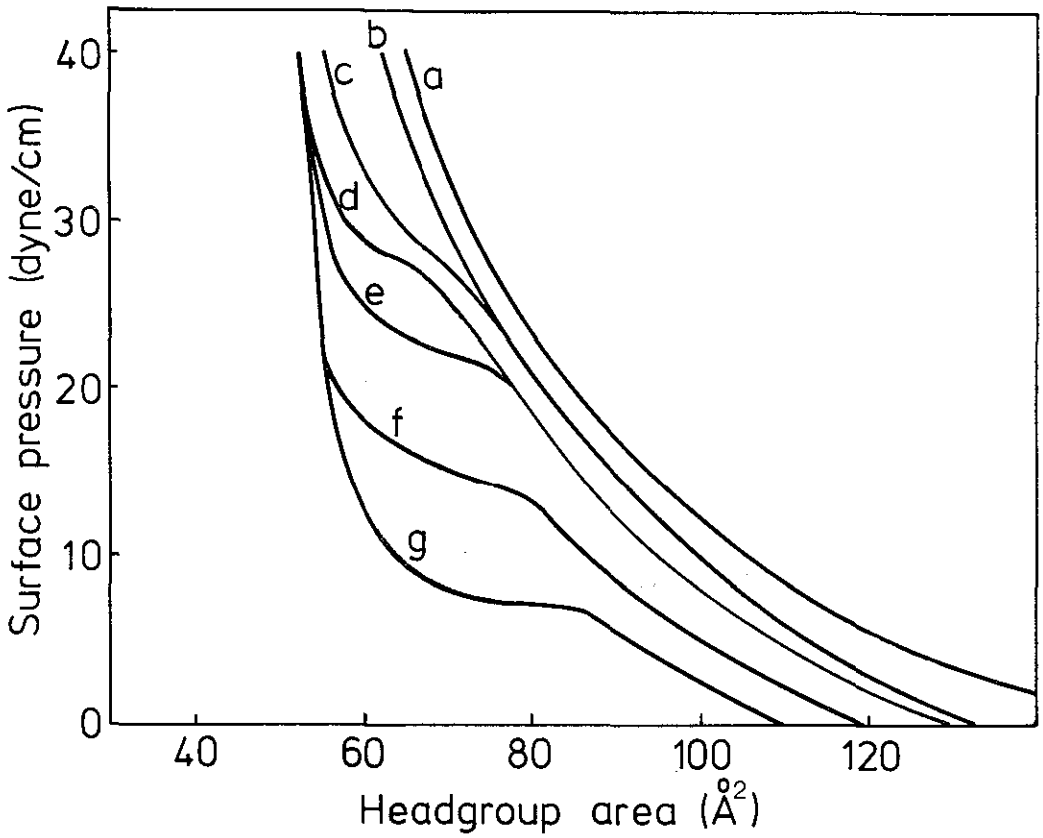

Fig. 33: Monolayer compression isotherms of DOA (at 22 °C) on different electrolyte solutions: (a) 1 mM NaAc or 1 mM NaF; (b) 1 mM NaOH + 2×10^{-5} M Na_2CO_3 or 1 mM NaOH + 1 mM Na_2CO_3; (c) pure water; (d) 1 mM Na_2SO_4; (e) 1 mM NaCl + 1 mM Na_2SO_4; (f) 1 mM NaCl; (g) 1 mM NaBr.

6.2 RESULTS

6.2.1 Monolayer Compression Isotherms

Fig. 33 gives the monolayer compression isotherms of DOA salts at T = 22 °C for different electrolyte species present in the subphase. (The concentration of the original

Br^- counterions becomes negligible as soon as the monolayer is spread on water.) The subphase containing 1 mM Na_2CO_3 also contained 1 mM NaOH to ensure the complete ionization of the CO_3^{2-} ion.

It is clear that the properties of DOA depend strongly on the type of counterion, indicating a pronounced ion specificity. The fluoride, acetate and carboxylate surfactant monolayers are completely of the liquid-expanded type whereas the sulphate, chloride, and bromide surfactant monolayers all show a phase transition from the liquid phase to the condensed phase. Because this phase transition occurs at different surface pressures for the various counterions, the critical temperature T_c beyond which no phase transition occurs must depend on the type of counterion. An interesting observation is that the ability of the anions to contract the monolayer follows a lyotropic series in the order $Br^- > Cl^- > F^-$. This is also the order in which the anions become decreasingly hydrated, suggesting that the specificity of the counterions is directly related to their hydration. The monolayer contraction on a subphase containing a mixture of Na_2SO_4 and NaCl is intermediate between the observed contractions in the presence of only NaCl or Na_2SO_4.

6.2.2 The Deposited Headgroup Area

Before the forces between DOA bilayers in various electrolyte solutions could be measured accurately, a problem arose concerning the deposited headgroup area. When the deposition was carried out in pure water, which gave a deposited headgroup area of 60 $Å^2$ (1:1 transfer ratio at a surface pressure of 32 dyne/cm, see Fig. 33), and 1 mM NaF was subsequently added, some of the surfactant molecules seemed to get pushed out of the bilayers. This became apparent when the interbilayer forces were measured: at a surface separation $D \simeq 30$ Å, the repulsion became much stronger than was expected from the double-layer forces alone. On application of the force $F/R \simeq 60{,}000$ mdyne/cm, a layer of material was rapidly squeezed out and the bilayers came to the position $D = 0$, where bilayer contact occurred before addition of NaF. Subsequent force versus distance measurements gave much less repulsive forces, but some additional repulsion at short bilayer separations remained. The same phenomenon, but to a lesser

extent, was observed when 1 mM NaOH was added into the apparatus. Then the material between the bilayers was squeezed out at a force $F/R \simeq 10{,}000$ mdyne/cm.

These observations are not surprising when the monolayer compression isotherms in Fig. 33 are studied again. At a headgroup area of 60 $Å^2$, the surface pressure and hence the surface energy, increases substantially when NaOH and especially when NaF is added to the subphase. The pressure can be reduced when the headgroup area becomes larger, which in the case of a deposited bilayer is only possible when a number of surfactant molecules is pushed out of the bilayer. Indeed, no additional bilayer repulsions were observed when the disposition was carried out from a 1 mM NaF subphase, which gave a deposited headgroup area of 70 $Å^2$ at a disposition pressure of 32 dyne/cm.

Following these preliminary investigations, it was decided to deposit bilayers from a subphase containing 1 mM NaF when forces in NaF or alkaline solutions were to be measured. In all other cases the deposition was done in pure water, choosing a headgroup area of 60 $Å^2$.

6.2.3 Forces between DOA Bilayers

Figs. 34 and 35 give the forces between DOA bilayers as a function of their separation in pure water, solutions of the monovalent ions NaCl, NaF, NaOH, and solutions of the divalent ions Na_2SO_4 and Na_2CO_3. At large separations, only a repulsive double-layer force is measured. At shorter range, typically less than 30 Å, the interaction becomes attractive: at the surface separation where the gradient of the surface force equals the spring constant, an instability occurs and the bilayers jump into adhesive contact. The position $D = 0$ where the surfaces come into adhesive contact, appeared to be essentially a hard wall. No hydration force was observed in any of the electrolyte solutions considered. Because the DOA headgroups are exposed at the bilayer surface, a logical choice is to take $D = 0$ as the outer Helmholtz plane, and also as the van der Waals plane where the van der Waals interaction of hydrocarbon across water becomes infinitely large.

With this reference distance, the force-laws in Figs. 34 and 35 can now be analysed

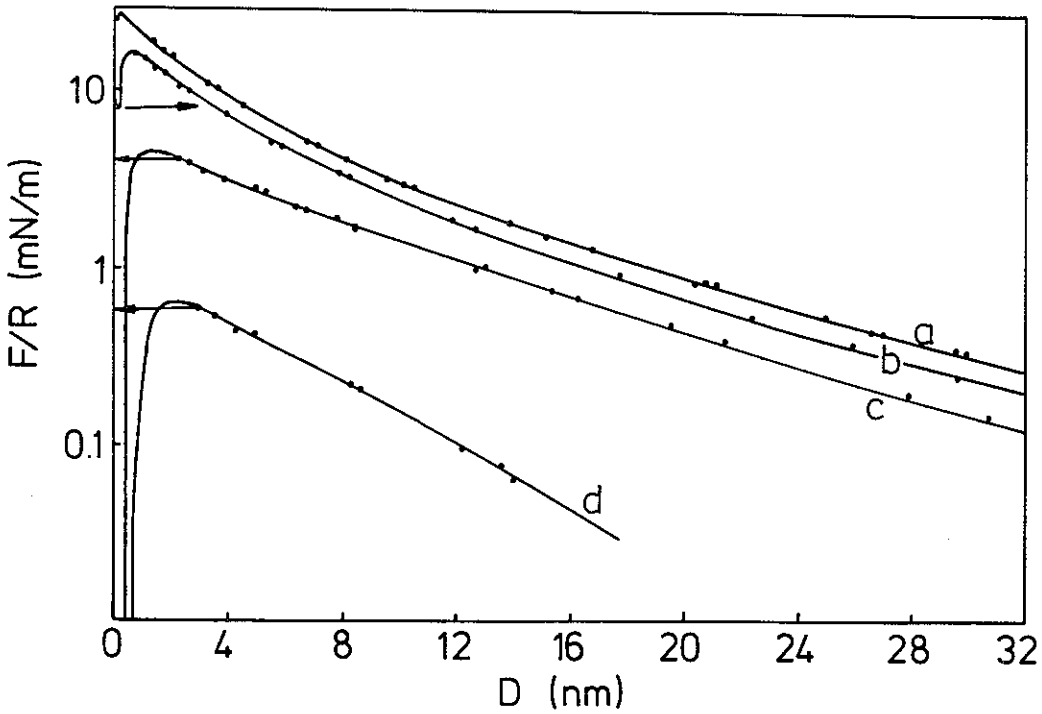

Fig. 34: Measured forces between DOA bilayers in various electrolyte solutions at 22 °C: (a) 1 mM NaF; (b) 1 mM NaCl; (c) 1 mM NaOH + 2×10^{-5} M Na_2CO_3; (d) 1 mM Na_2SO_4. The inward and outward jumps are indicated by inward and outward arrows. The solid curves are the theoretical curves with charge regulation in which a Hamaker constant of 6×10^{-21} J has been used.

by fitting the curves to the theoretical double-layer repulsion with charge regulation. It appeared that the fitted surface charge density was always well below its value for the fully charged bilayer. Even in "pure" water, a considerable amount of ion binding to the bilayers had to be taken into account. From the measured Debye length, the ionic concentration in pure water seems to be about 3×10^{-5} M (assumed to be monovalent) and must mainly stem from dissolved CO_2 and ions leaking out of the glass-ware, and the stainless steel force measurement apparatus. This effect is disturbing, but can be separated out by assigning a separate binding constant to the background electrolyte. When this is taken into account, the binding of the other electrolyte species can be investigated independently. The analysed double-layer parameters ψ_0^∞, σ_0^∞ , and the binding constants are given in Table VIII. It was noted that the theoretical force curves calculated with charge regulation were very close to the predicted force curves at constant surface potential, whereas the force curves at constant surface charge were always clearly too repulsive.

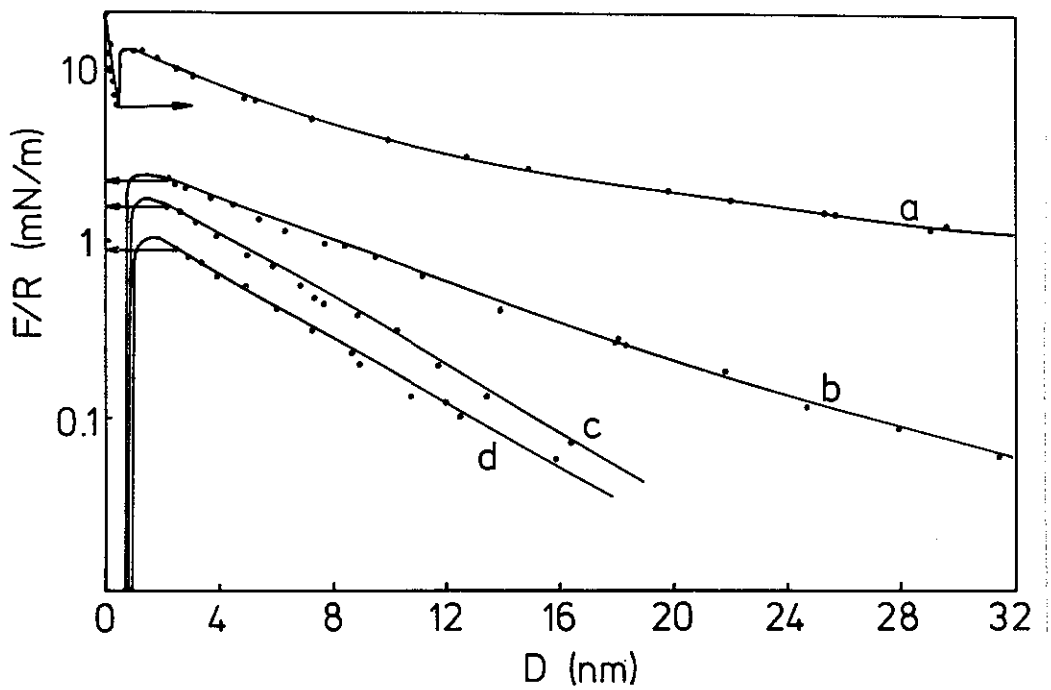

Fig. 35: Measured forces between DOA bilayers in various electrolyte solutions at 22 °C: (a) pure water; (b) 1 mM NaCl + 0.1 mM Na_2SO_4; (c) 1 mM NaF + 1 mM NaOH + 0.89 mM Na_2CO_3; (d) 1 mM NaCl + 1.2 mM Na_2SO_4. The inward and outward jumps are indicated by inward and outward arrows. The solid curves are the theoretical curves with charge regulation in which a Hamaker constant of 6×10^{-21} J has been used.

F^- ions do not appear to bind to the DOA headgroups but Cl^- ions do. That there is a difference between the binding affinity of F^- and Cl^- ions is already clear from the observation in Fig. 34 that the forces between DOA bilayers in a 1 mM NaF solution are more repulsive than in a 1 mM NaCl solution. Addition of 1 mM NaOH results in an interbilayer force that is much weaker. However, it must be remembered that at pH = 11, all the dissolved CO_2 is present in the divalent carboxylate ion CO_3^{2-} form. From the measured pH = 5.4 in pure water and the values for the dissociation constants of H_2CO_3 and HCO_3^-, it is readily calculated that the equilibrium CO_3^{2-} concentration must be about 2×10^{-5} M. Assuming that only the CO_3^{2-} ions bind to the surfactants, a binding constant $K_{CO_3} = 20\ M^{-1}$ was inferred. In a medium containing 1 mM NaOH, 1 mM NaF and 0.89 mM Na_2CO_3, the same value for K_{CO_3} emerged assuming again no OH^- binding. The agreement indicates that the binding affinity of OH^- is probably very small and unimportant in solutions containing Na_2CO_3.

Table VIII: *DOUBLE LAYER AND ADHESION RESULTS FOR DOA BILAYERS AT 22 °C.

Electrolyte monovalent	Concentration divalent	Surface Potential ψ_0^∞ (mV)	Surface Charge σ_0^∞ (C/m^2)	Surface Charge σ_0^∞ (Å)^2/charge	Binding Constants K monovalent (M^{-1})	Binding Constants K divalent (M^{-1})	Adhesion Energy E_0 (dyne/cm)	Equilibrium Separation D_0 (Å)
1 mM NaF	-	178	-0.0603	265	0	-	-	-
1 mM NaCl	-	154	-0.0367	436	12	-	-	-
1 mM NaOH	2×10^{-5} M Na_2CO_3	97	-0.0172	930	0	20	0.32	3.6
	1 mM Na_2SO_3	35	-0.0063	2540	-	60	3.18	2.2
3×10^{-5} M (pure water)	-	213	-0.0214	748	75	-	-	-
1 mM NaCl	0.1 mM Na_2SO_3	72	-0.0122	1308	12	30	0.96	3.2
1 mM NaF + 1 mM NaOH	0.89 mM Na_2CO_3	49	-0.0132	1209	-	20	0.64	4.1
1 mM NaCl	1.2 mM Na_2SO_3	40	-0.0100	1595	12	30	1.43	3.0

* The presence of a backgrounds electrolyte concentration of 3×10^{-5} M with a binding constant K = 75 M^{-1} is always taken into account separately.

Addition of Na_2SO_4, or mixtures of Na_2SO_4 and NaCl, leads to interbilayer forces which also indicate considerable binding of the sulphate counterions.

The adhesion energy E_0 was calculated from the force F_0 needed to separate two bilayers in adhesive contact according to Eq. (40). Values for E_0 are given in Table VIII. Assuming that the origin of the adhesion force stems completely from the sum of the van der Waals force and the double-layer force, we have at the distance $D = D_0$ for the adhesion free energy

$$E_0 = -\frac{A}{12\pi D_0^2} + \frac{F_{DL}(D_0)}{2\pi R}. \tag{45}$$

The first term on the right of Eq. (45) is the expected form for the (non-retarted) van der Waals attraction with the Hamaker constant $A = 6\times 10^{-21}$ J, as expected theoretically for hydrocarbon interacting across water. For bilayer separations much less than the bilayer thickness (about 50 Å) the van der Waals contribution from the mica surfaces can safely be ignored (see Chapter 3). Using the extrapolated magnitude of the double-layer force F_{DL} near bilayer contact, the values for D_0 can be obtained from the measured E_0 with the help of Eq. (45). Although this procedure must be approached with caution because a macroscopic theory is extrapolated into the molecular regime, the results in Table VIII for D_0 show that already a small difference in D_0 can lead to a large change in E_0. The differences between D_0 in various electrolyte solutions are probably roughly related to the difference in the size of the counterions trapped between two bilayers in adhesive contact. D_0 is larger for CO_3^{2-} than for SO_2^{2-} anions, showing that the former has a larger radius than the latter. It is expected that the lesser the hydration of the ions is, the greater their binding affinity will be. Indeed, the binding constant K_{SO_4} was found to be larger than K_{CO_3}. The same is true for the lesser hydrated Cl^- ion as compared to the strongly hydrated F^- and OH^- ions.

The force curves in Figs. 34 and 35 are fitted with the Hamaker constant $A = 6\times 10^{-21}$ J. Like what was found for PG bilayers (and probably because of the same possible reasons), the surface separations where experimentally an inward jump

occurred, were always a little farther out than predicted theoretically, and the theoretically predicted forces below D = 25 Å were always somewhat too repulsive (i.e. experimentally too attractive).

It is evident from the observations in Figs. 33-35 that the various monovalent and divalent ions induce different surface interactions. It is interesting to investigate how much of the observed differences between the various monolayer compression isotherms in Fig. 32 can be explained through the differences in the diffuse double-layer free energy of the monolayers (see Section 1.3 for the equations). Using the values ψ_0^∞ in Table VIII for pure water, 1 mM NaCl, and 1 mM NaF, the calculated values for Π^{el} are 1.0, 1.7 and 2.9 dyne/cm, respectively, at headgroup areas of about 60-70 $Å^2$. The occurrence of phase transitions in the monolayer compression isotherms makes an exact analysis impossible, but it can be seen in Fig. 33 that the monolayer isotherm on water is indeed shifted upward by about 2 dyne/cm when a 1 mM NaF subphase is used. On the other hand, the monolayer isotherm on a 1 mM NaCl subphase is well below the one on pure water, whereas theory predicts that Π^{el} on a 1 mM NaCl subphase should be larger than on pure water.

It also can be shown that when Eq. (30) is used for the monolayer isotherms on 1 mM Na_2SO_4 and 1 mM Na_2CO_3 subphases, a value $\Pi^{el} < 1$ dyne/cm results, i.e. lower than the values for Π^{el} on the monovalent electrolyte containing subphases. Nevertheless, the isotherms are seen to be quite expanded. Apparently, the lateral interactions between DOA salt surfactants can not be explained from the diffuse double-layer theory alone and another explanation involving Stern layer effects related to the specific nature of the counterions must be sought.

6.3 DISCUSSION

It has emerged that both interbilayer and intrabilayer interactions exhibit a pronounced ion specificity. Large hydrated counterions like F^-, OH^- and AcO^- give expanded monolayer compression isotherms. Pashley et al. (1986) and Brady et al. (1985) report that like what has been found here for fluoride and hydroxide, also acetate counterions do not bind to DOA headgroups. Following the lyotropic series $F^- > Cl^- >$

Br^-, the smaller the (hydrated) anion, the more contracted the monolayer isotherm becomes and the stronger the counterions behind to the DOA bilayer. Pashley et al. (1986) found that the intrinsic binding constant K_{Br} is about six times larger than the K_{Cl} found in the present study, in agreement with this expectation. Also, the somewhat more hydrated CO_3^{2-} ions show a lesser degree of binding than SO_4^{2-} ions.

However, the monolayer contraction in Fig. 33 can not be explained only from the decrease in the double-layer free energy. Especially, when divalent counterions are added, the double-layer free energy is quite small and can not account for the fairly expanded nature of the monolayer isoltherms. The latter indicates a significant lateral interaction between the surfactant headgroups.

It should be remembered that the surface potentials given in Table VIII are potentials at the OHP. The actual potential at the surfactant headgroups is quite different when a finite gap or a Stern layer exists between the OHP and the headgroups. The idea of a Stern layer has also been used by Ninham et al. (1983) to explain the unusual properties of didodecyldimethylammonium hydroxide vesicles. The drop in the potential across the Stern layer is proportional to its thickness. Here the nature of the counterions plays a role, since the width of the Stern layer should be related to the counterion size. With this, it can be explained why monolayers on a Na_2CO_3 subphase are quite expanded, while the double-layer potential at the OHP is small. The introduction of small counterions like Cl^- leads to much higher double-layer potentials but gives contracted monolayer compression isotherms. To quantify this matter further is only possible when the dielectric constant in the region between the headgroups and the OHP is known. Force measurements cannot resolve this issue and only from the analysis of the monolayer compression isotherm can we obtain an idea about the actual headgroup size and headgroup interactions in a surfactant aggregate.

The binding constants are evaluated using the existing potentials at the OHP. Because the plane in which the counterions bind is probably somewhat further in, it is clear that the procedure followed here to obtain the magnitude of the binding constants is only an approximation and this might explain why the K_{SO_4} is apparently lower in a mixture of NaCl and Na_2SO_4 than in a solution of Na_2SO_4 only.

In solutions of quaternary ammonium hydroxide surfactants, small vesicles are formed spontaneously which become larger when, for example, bromide counterions are added. The increase in the value of the geometric factor v/al, which is responsible for the vesicle growth, is as we now understand only partly due to the decrease of the double-layer free energy and probably mostly due to the decrease of the potential drop across the Stern layer. From the monolayer compression isotherms it can now be predicted that upon titration of hydroxide vesicles with Na_2CO_3, the size of the vesicles should remain fairly constant. The stability of the vesicles against aggregation however should decrease due to the decrease in the double-layer repulsion.

CHAPTER 7

SUMMARY OF THE RESULTS AND POTENTIAL FOR FUTURE STUDIES

7.1 SUMMARY AND CONCLUSIONS

The controlled deposition of a range of amphiphiles on molecularly smooth mica surfaces now makes it possible to quantitatively study the forces between bilayers in aqueous electrolyte solutions. Simultaneous measurements of the monolayer compression isotherms give an idea of the equilibrium headgroup areas and the lateral interactions between amphiphiles in aggregates.

We have seen that the intermembrane interactions are determined mainly by the van der Waals force, the electrostatic double-layer force and the short-range steric-hydration force. The van der Waals force is always present and can (at least below D = 40 Å) be characterized by a value for the non-retarded Hamaker constant close to the theoretically expected value of 5-7 $\times$ 10^{-21} J (Parsegian and Ninham, 1970). The van der Waals force is screened in concentrated electrolyte solutions to about half its "full" strength, as was verified by measurements on uncharged galactolipid bilayers. Only for the phospholipids PE and PC in pure water is the van der Waals Hamaker constant very small, viz. A = 1.3 $\times$ 10^{-21} J, possibly the consequence of the presence of high concentrations of ionic groups on the bilayer surface which screen the van der Waals force at distances beyond the equilibrium bilayer separation. In these systems, the magnitude of the adhesion force is again consistent with an "ordinary" hydrocarbon-water Hamaker constant, indicating that the screening of the van der Waals force depends on the surface separation. This is also expected theoretically (Mahanty and Ninham, 1976).

Double-layer forces exist whenever the amphiphiles are charged or have acquired a

charge through ion binding. Monovalent cations only show a small binding affinity to the phosphate groups in contrast to divalent cations like Ca^{2+} and Mg^{2+}. There is clear evidence that the binding affinity of ions is correlated with the effective size of the hydrated ions in the way that the least hydrated ions bind strongest. For the phospholipids this becomes clear when Ca^{2+} is compared with Mg^{2+}. In the case of the cationic quaternary ammonium surfactants, the same trend is found for monovalent anions.

The double-layer force between two charged bilayers can be described satisfactorily by taking into account both the binding to the bilayers of and the screening of the surface charge through the electrolyte species present in the aqueous phase, and allowing the surface charge to regulate when the diffuse double-layers of both surfaces begin to overlap. As a rule, the experimental double-layer force law is very close to the case in which the surfaces are supposed to interact at constant potential. A simple adsorption theory based on a mass-action model is adequate for explaining the ion binding as a function of the electrolyte concentration and the surface separation.

The intrinsic binding constants found for the binding of Ca^{2+} ions to the charged phosphate groups of PE, PC and PG could differ from each other by an order of magnitude. This indicates that the chemical micro-environment of the phosphate groups plays an important role with regard to the binding affinity of the cations. Of course, a clear change of micro-environment occurs when the phosphate groups on a PE surface are transferred to a PC or PG surface, but also a change in the phase state of PC and PG bilayers shows up in the magnitude of the binding constants.

For both the van der Waals and the double-layer force, there is no indication of a breakdown of continuum theory at separations greater than about 25 Å. Also at shorter separations, where we enter the molecular regime, there is no evidence of gross deviations (at least in the present systems). The good agreement with theory is unexpected when we remember that the surface charge is considered to be smeared out homogeneously, and in many cases the surface charge density is very small. Discrete charge effects, when the surface separation is less than the average distance between the

surface charges, would be likely to occur. True, small discrepancies between theory and experiment do occur below D $\simeq$ 25 Å which might be related to discrete charge effects, but here it is also possible that ion-ion correlation effects play a role. The deconvolution of these two is not yet clear. Furthermore, there is no need to account for lateral interactions between the adsorbed ions, even not for PG bilayers in $CaCl_2$ solutions, where almost 50% of the lipids carries an adsorbed Ca^{2+} ion. Pashley (1981) and Pashley and Israelachvili (1984) reported that it was necessary to account for lateral interactions between adsorbed monovalent or divalent cations on mica surfaces. This was done by assigning an effective size to each adsorbed cation on the mica surface. Simultaneously, when ion adsorption occurred, a hydration force was observed between the two mica surfaces. Both the distance-range of the hydration force and the occupied surface area of each adsorbed cation showed a correlation with the size of the hydrated ions. In the case of PG bilayers or DOA bilayers, no hydration force is measured, not even in concentrated electrolyte solutions.

The explanation for the absence of hydration forces between PG and DOA bilayers is not immediately clear. A possibility is that the adsorbed ions sit between the headgroups, probably bridge-bind between two adjacent headgroups, lose most of their hydration water and together with the charged headgroups create no or only a very small dipole moment. This is reinforced by the observation that the equilibrium bilayer separation between PG bilayers and DOA bilayers is only a few Å, i.e. too small to account for the presence of a layer of hydrated ions between the bilayers. On mica surfaces, the ions can not bridge bind and necessarily must create an outward dipole moment with the surface charges. It is the presence of a net dipole moment which, according to a simulation study by Kjellander and Marcelja (1985b), causes a strong polarization of water molecules in the dipole fields near the surface, leading to a hydration force when the polarization becomes disturbed. No doubt, the presence of dipoles on zwitterionic surfaces must also be the prime reason for the measured hydration force between PE or PC bilayers.

Theories of the hydration force developed so far are very model dependent and

have not yet provided an unambiguous insight into the exact relation between the hydration force and the molecular nature of the surface. The difference between the measured distance ranges of the hydration force between PC and PE bilayers has yet to be explained.

From the observation that the effective van der Waals plane of origin of PE and PC bilayers does not coincide with the anhydrous bilayer/water interface but is located about 5 Å farther out per surface, we have concluded that the zwitterionic headgroups must have the ability to protrude into the water phase (this also follows from spectroscopic data). The headgroup protrusion will give rise to an extra steric repulsion via excluded volume effects and contributes to the magnitude and distance range of the short-range repulsion. The comparison of the distance range of the hydration force between bilayers deposited on mica and bilayers free in solution reveal that also thickness fluctuations and/or thermal undulations of bilayers as a whole increase the distance range of the hydration force between free bilayers and hence the equilibrium bilayer separation (especially for fluid bilayers).

Measurements of the monolayer compression isotherms indicate that in general short-range interactions dominate the lateral interactions. The degree of headgroup hydration can be found again when the monolayer compression isotherms of DPPE and DPPC (both in the gel phase) are compared and also when MGDG is compared with DGDG. The hydration differences become directly evident in the measurements of the short-range interbilayer forces. However, as we have seen with the charged monolayers, specifically bound and free counterions can greatly change the lateral interactions between amphiphiles through (probably) bridge-binding and/or Stern layer effects. They also induce changes in the interbilayer interactions, but whereas continuum theory adequately describes the latter, it is unable to account quantitatively for the observed changes in the lateral interactions that accompany the ion binding. Evidently, the molecular nature of the headgroup region with the adsorbed counterions must be considered if one is to understand the complex interactions at the bilayer water interface. From the theory of the self-assembly of amphiphiles (Israelachvili et al., 1980,

1985c), we know that such interactions influence the shape, size, polydispersity and phase state of the aggregates.

No serious attempts appear to have been made to generally correlate intramolecular with intermolecular interactions because it is not readily apparent how the forces between discrete molecular groups on the surface relate to the forces between two apposing surfaces (Israelachvili and Sornette, 1985). Simple equations for the lateral electrostatic pressure within the interfacial region, as derived by Payens (Eq. (32)) in which the surface charge is assumed to be uniform without accounting for Stern layer effects and specific chemical effects, can only be expected to have a limited applicability. The incomplete understanding of steric and hydrophobic interactions in the interfacial region complicates matters even further.

In spite of these difficulties, some qualitative correlations between inter- and intra-aggregate interactions can be made. We have seen that for uncharged amphiphiles (like zwitterionic lipids and galactolipids), a correlation exists between the equilibrium headgroup area in a bilayer, and the repulsive pressure and adhesion force between two apposing bilayers. For ion binding to charged amphiphiles similar correlations can be drawn. Within one lyotropic series, the least hydrated ion binds strongest, increases the force of adhesion, decreases the double-layer repulsion and the equilibrium headgroup area and hence leads to the formation of larger aggregates. This has been found in many studies: monovalent anions ($F^- \rightarrow Cl^- \rightarrow Br^-$) with DOA surfactants (Chapter 6), divalent ions ($CO_3^{2-} \rightarrow SO_4^{2-}$) with DOA surfactants (Chapter 6), monovalent cations ($Li^+ \rightarrow Na^+ \rightarrow Cs^+$) with anionic alkyl sulphate surfactants as shown by Missel et al. (1982), and divalent cations ($Mg^{2+} \rightarrow Ca^{2+}$) with PG lipids according to a monolayer study by Tocanne et al. (1974). However, for charged amphiphiles, a correlation between the effects on the interaggregate forces caused by monovalent counterions as compared to the effects caused by divalent counterions remains difficult to make, since it depends on the system (e.g. PG versus DOA amphiphiles).

7.2 POTENTIAL FOR FUTURE STUDIES

The Langmuir-Blodgett technique for deposition of amphiphiles on mica offers a

broad range of possibilities for future studies. In the biological area, phosphatidylserine (the most abundant charged lipid in animal cell membranes), which contains an ionized phosphate group and an ionized carboxyl group in its headgroup, deserves investigation, as well as the gangliosides, which have a branched chain of up to seven sugar units including sialic acid in their headgroup. The sugar residues are known to contribute to the specific nature of cell surfaces; for instance, they are associated with blood-group specificities (Fukuda and Hakomori, 1982).

In the area of surfactants, one can now study an extensive series of anionic, cationic and uncharged surfactants. The elucidation of their counterion specificity, which follows partly from the force measurements and partly from monolayer compression isotherms, is crucial to understand the phase behaviour of these surfactants in electrolyte solutions, and the design and stability of micelles, vesicles, microemulsions, etc.

Soluble surfactants can easily be adsorbed from solution on mica surfaces. Pashley and Israelachvili (1981) have done this for the cationic cetyltrimethylammonium bromide (CTAB) surfactants. Above the CMC a bilayer of CTAB molecules is formed on mica. Because the mica is negatively charged, the direct adsorption of anionic surfactants from solution is difficult if not impossible. However, using the Langmuir-Blodgett technique, we can first deposit a hydrophobic monolayer of DPPE and then allow anionic surfactants to adsorb from solution as a second layer on this uncharged hydrophobic surface.

With the Langmuir-Blodgett technique, it is also possible to deposit different surfactants on each mica surface, for example a cationic and an anionic surfactant. The study of the attractive electrostatic interaction between the two oppositely charged surfaces is of relevance to heterocoagulation.

Discreteness of charge effects can be investigated quantitatively by increasing the surface charge systematically from zero to full charge and then measuring the surface forces. One reliable way to achieve this, is to mix DMPG with DMPC in various ratios and letting the deposited bilayers interact at pH $\simeq$ 7 and T > 24 °C. Under those

conditions, the DMPG is fully charged and it is known that, unless divalent cations are present, the lipids do not phase separate and remain randomly mixed (Findley and Barton, 1978). Because monovalent ions like Na^+, perhaps even more Li^+, and certainly $(CH_3)_4N^+$ only have a very low binding affinity (or none at all) to the lipid headgroups, the surface charge in monovalent electrolye solutions is known a priori from the mixing ratio of the lipids. The theoretically expected double-layer force, assuming a uniform surface charge density, should then be compared with the experimentally measured forces in electrolyte solutions. The study of discrete charge effects in systems containing divalent counterions is more difficult because virtually all divalent ions show a relatively high degree of binding to charged bilayers, and the surface charge density is not known independently any more. A promising divalent cation that might be used is probably the bulky dimethonium ion $(CH_3)_3N(CH_2)_2N(CH_3)_3^{2+}$, which according to McLaughlin et al. (1983) only screens and does not bind. A knowledge of discrete charge effects on the interbilayer interaction is important to quantitatively estimate binding constants in systems where ions do bind to the surfaces (as we have seen, the surface charge density is usually quite small in those systems) and to recognize ion-ion correlation effects. Remember that in the present study, the force-laws were always analysed with continuum double-layer theory. Except at bilayer separations less than 25 Å, the theoretical fits were always very good and it is not obvious that any substantial discrete charge and/or ion-ion correlation effects exist. According to the theory of Kjellander and Marcelja (1985a)), ion-ion correlation effects exist only when the bound counterions are laterally mobile on the surfaces; any restriction on the mobility would diminish the attractive ion-ion correlation interaction.

It is clear, that the Langmuir-Blodgett technique offers a unique possibility to change the chemical nature of molecularly smooth surfaces completely. By depositing a DPPE monolayer, the mica surface is replaced by a hydrocarbon surface. Hydrocarbon surfaces have already been used successfully to measure the long-range hydrophobic interaction in water (Claesson et al., unpublished work) and to study the oscillatory solvation forces between hydrocarbon surfaces in organic liquids (Christenson,

unpublished work). Instead of a hydrocarbon surface, one can obtain a fluorocarbon surface by deposition of a layer of fluorocarbon surfactants on mica.

The ability to change the nature of the surfaces is particularly interesting when one is interested in the interactions between adsorbed polymers on various surfaces in aqueous or organic solvents. The amount of adsorbed polymer and the polymer conformation on the surface in terms of the so-called trains, loops, and tails, depends on the interaction of the polymer segments with the surface. The surface can be changed from completely hydrophobic (DPPE monolayer) to hydrophilic (deposition of a DPPC bilayer or DGDG bilayer). When one is dealing with the adsorption of polyelectrolytes, the adsorption energy of a polyelectrolyte segment is regulated by a suitable choice of the sign and magnitude of the charge density on the bilayer surface. It is known (Scheutjens, 1985) that the conformation of the adsorbed polymers influences the range and magnitude of the forces between two polymer coated surfaces. The modulation of these forces is most relevant to the understanding of phenomena like steric stabilisation, polymer bridging, and/or flocculation of polymer coated colloidal particles.

Thus, the present work and techniques are seen to contain a broad spectrum of future possibilities that are potentially of great value in aqueous media and non-aqueous media. Hopefully, the next few years will see the completion of further systematic studies which, no doubt, have the potential to yield a large number of new and interesting results.

BIBLIOGRAPHY

Ahkong, Q.F., Fisher, D., Tampion, W., and Lucy, J.A. (1975) *Nature* **253**, 194.

Akatsu, H., and Seelig, J. (1981) *Biochemistry* **20**, 7366.

Albrecht, O., Gruler, H., and Sackmann, E. (1978) *Journal de Physique* **39**, 301.

Altenbach, C., and Seelig, J. (1984) *Biochemistry* **23**, 3913.

Baker, P.F., Knight, D.E., and Whitaker, M.J. (1980) in *Calcium-binding Proteins: Structure and Function* (F.L. Siegel, W. Carafoli, R.H. Kretsinger, D.H. MacLennan, and R.H. Wasserman, eds.) (Elsevier, Amsterdam).

Beunen, J., and Ruckenstein, E. (1983), *J. Colloid Interf. Sci.* **96**, 469.

Brady, J.E., Evans, D.F., Kachar, B., and Ninham, B.W. (1984) *J. Am. Chem. Soc.* **106**, 4279.

Brady, J.E., Evans, D.F., Warr, G., Grieser, F., and Ninham, B.W. (1985) *J. Am. Chem. Soc.* (in press).

Buldt, G., Gally, H.U., Seelig, A., Seelig, J., and Zaccai, G. (1978) *Nature* **271**, 182.

Carnie, S., Israelachvili, J.N., and Pailthorpe, B.A. (1979) *BBA* **554**, 340.

Chan, D.Y.C., Pashley, R.M., and White, L.R. (1980) *J. Colloid Interf. Sci.* **77**, 283.

Cherry, R.J., and Chapman, D. (1969) *J. Mol. Biol.* **40**, 19.

Chow, W.S., Telfer, A., Chapman, D.J., and Barber, J. (1981) *BBA* **638**, 60.

Clunie, J.S., Goodman, J.F., and Symons, P.C. (1967) *Nature* **216**, 1203.

Cohen, F.S., Zimmerberg, J., and Finkelstein, A. (1980) *J. Gen. Physiol.* **75**, 251.

Cohen, F.S., Akabar, M.H., and Finkelstein, A. (1982) *Science* **217**, 458.

Cowley, A.C., Fuller, N.L., Rand, R.P., and Parsegian, V.A. (1978) *Biochemistry* **17**, 3163.

Davies, B., and Ninham, B.W. (1972) *J. Chem. Phys.* **56**, 5797.

Derjaguin, B.V. (1934) *Kolloid. Z.* **69**, 155.

Dolan, A.K., and Edwards, S.F. (1974) *Proc. R. Soc. London* A **337**, 509.

Dolan, A.K., and Edwards, S.F. (1975) *Proc. R. Soc. London* A **343**, 427.

Evans, D.F., Mitchell, D.J., and Ninham, B.W. (1985) *J. Phys. Chem.* (in press).

Evans, D.F., and Ninham, B.W. (1986) *J. Am. Chem. Soc.* (submitted).

Fendler, J. (1983) *Membrane Mimetic Chemistry* (Wiley, New York), and references listed therein.

Findly, E.J., and Barton, P.G. (1978) *Biochemistry* **17**, 2400.

Finer, E.G., and Darke, A. (1974) *Chem. and Physics of Lipids* **12**, 1.

Franks, F. (1973) *Water: A Comprehensive Treatise*, vol. 4, Chapter 1 (F. Franks, ed.) (Plenum, New York).

Franks, N.P. (1976) *J. Mol. Biol.* **100**, 345.

Fukuda, M.N., and Hakomori, S. (1982) *J. Biol. Chem.* **257**, 446.

Gottlieb, M.H., and Eanes, E.D. (1972) *Biophys. J.* **12**, 1533.

Grasdalen, H., Eriksson, L.E.G., Westman, J., and Ehrenberg, A. (1977) *BBA* **469**, 151.

Gray, E.G. (1973) *The Synapse* (Oxford Univ. Press, London).

Gruen, D.W.R. (1980) *BBA* **595**, 161.

Gruen, D.W.R., and Marcelja, S. (1983) *J. Chem. Soc. Faraday Trans. 2* **79**, 225.

Guldbrand, L., Jonsson, B., Wennerstrom, H., and Linse, P. (1984) *J. Chem. Phys.* **80**, 2221.

Hashimoto, S., Thomas, J.K., Evans, D.F., Mukerjee, S., and Ninham, B.W. (1983) *J. Colloid Interf. Sci.* **95**, 594.

Hauser, H., Pascher, I., and Sundell, S. (1981) *BBA* **650**, 21.

Helfrich, W. (1978) *Z. Naturforsch. A: Phys., Phys. Chem., Kosmophys.* **33A**, 305.

Hong, K., Duzgunes, N., and Papahadjopoulos, D. (1982) *Biophys. J.* **37**, 297.

Horn, R.G. (1984) *BBA* **778**, 224.

Huh, C. (1979) *J. Colloid Interf. Sci.* **71**, 408.

Hui, S.W., Steward, T.P., Boni, L.T., and Yeagle, P.L. (1981) *Science* **212**, 921.

Hunter, R. (1981) *Zeta Potential in Colloid Science* (Academic Press, London).

Israelachvili, J.N. (1973) *J. Colloid Interf. Sci.* **44**, 259.

Israelachvili, J.N. (1985a) *Intermolecular and Surface Forces* (Academic Press, New York).

Israelachvili, J.N. (1985b) *Chemica Scripta* (in press).

Israelachvili, J.N. (1985c) in *Physics of Amphiphiles, Vesicles and Microemulsions* (Degiorgio, V., and Corti, M., eds.) (North-Holland, Amsterdam).

Israelachvili, J.N., Mitchell, D.J., and Ninham, B.W. (1976) *J. Chem. Soc. Faraday Trans. 2* **72**, 1525.

Israelachvili, J.N., Mitchell, D.J., and Ninham, B.W. (1977) *BBA* **470**, 185.

Israelachvili, J.N., and Adams, G.E. (1978) *J. Chem. Soc. Faraday Trans. 1* **74**, 975.

Israelachvili, J.N., Marcelja, S., and Horn, R.G. (1980) *Quart. Rev. Biophys.* **13**, 121.

Israelachvili, J.N., and Pashley, R.M. (1982) *Nature*, **300**, 341.

Israelachvili, J.N., and Pashley, R.M. (1984) *J. Colloid Interf. Sci.* **98**, 500.

Israelachvili, J.N., and Sornette, D. (1985) *Journal de Physique* (Paris) **46**, 127.

Jonsson, B., and Wennerstrom, H. (1983) *J. Chem. Soc. Faraday Trans. 2* **79**, 19.

Kauzmann, W. (1959) *Adv. Protein Chem.***14**, 1.

Kjellander, R., and Marcelja, S. (1985a) *Chemica Scripta* **25**, 112.

Kjellander, R., and Marcelja, S. (1985b) in *Hydration Forces and Molecular Aspects of Solvation* (Wennerstrom, H., and Jonsson, B., eds.) (Cambridge Univ. Press, London) (in press).

Klein, J., and Luckham, P.F. (1984) *Macromolecules* **17**, 1041.

Lau, A.L.Y., McLaughlin, A.C., MacDonald, R.C., and McLaughlin, S.G.A. (1980) in *Bioelectrochmistry: Ions, Surfaces, Membranes* (Blank, M., ed.) **49**, Am. Chem. Soc., Washington.

Lau, A.L.Y., McLaughlin, A.C., and McLaughlin, S.G.A. (1981) *BBA* **645**, 279.

Lehninger, A.L. (1975) *Biochemistry* (Worth Publishers, New York).

Le Neveu, D.M., Rand, R.P., and Parsegian, V.A. (1976) *Nature* **259**, 601.

Le Neveu, D.M., Rand, R.P., Parsegian, V.A., and Gingell, D. (1977) *Biophys. J.* **18**, 209.

Lewis, B.A., and Engelman, D.M. (1983) *J. Mol. Biol.* **166**, 211.

Liao, M., and Prestegard, J.H. (1979) *Biochem. Biophys. Res. Comm.* **90**, 1274.

Lis, L.J., Parsegian, V.A., and Rand, R.P. (1981) *Biochemistry* **20**, 1761.

Lis, L.J., McAlister, M., Fuller, N., Rand, R.P., and Parsegian, V.A. (1982a) *Biophys. J.* **37**, 657.

Lis, L.J., McAlister, M., Fuller, N., Rand, R.P., and Parsegian, V.A. (1982b) *Biophys. J.* **37**, 667.

Lyklema, J., and Mysels, K.J. (1965) *J. Am. Chem. Soc.* **87**, 2539.

Mahanty, J., and Ninham, B.W. (1976) *Dispersion Forces* (Academic Press, New York).

Marcelja, S. (1974) *BBA* **367**, 165.

Marcelja, S., and Radic, N. (1976) *Chem. Phys. Lett.* **42**, 129.

McLaughlin, A., Grathwohl, C., and McLaughlin, S. (1978) *BBA* **513**, 338.

McLaughlin, A., Eng, W., Vaio, G., Wilson, T, and McLaughlin, S. (1983) *J. Membr. Biol.* **76**, 183.

Missel, P.J., Mazer, N.A., Carey, M.C., and Benedek, G.B. (1982) in *Solution Behaviour of Surfactants*, Vol. 1, 373 (K.L. Mittall and E.J. Fendler, eds.) (Plenum Press, New York).

Mitchell, D.J. and Richmond, P. (1973) *Chem. Phys. Lett.* **21**, 113.

Mitchell, D.J., and Ninham, B.W. (1981) *J. Chem. Soc. Faraday Trans. 2* **77**, 601.

Murphy, D.J. (1982) *FEBS Lett.* **150**, 19.

Ninham, B.W., and Parsegian, V.A. (1970) *J. Chem. Phys.* **52**, 4578.

Ninham, B.W., Evans, D.F., and Wei, G.J. (1983) *J. Phys. Chem.* **87**, 5020.

Ohki, S. (1982) *BBA* **689**, 1.

Ohshima, H., Inoko, Y., and Mitsui, T. (1982) *J. Colloid Interf. Sci.* **86**, 57.

Ohshima, H., and Ohki, S. (1985) *J. Colloid Interf. Sci.* **103**, 85.

Padday, J.F., Pitt, A.R., and Pashley, R.M. (1975) *J. Chem. Soc. Faraday Trans. 1* **71**, 1919.

Papahadjopoulos, D. (1978) in *Membrane Fusion* (G. Poste and G.L. Nicholson, eds.) (North-Holland, Amsterdam).

Parsegian, V.A. (1973) *Ann. Rev. of Biophys. and Bioeng.* **2**, 221.

Parsegian, V.A., and Ninham, B.W. (1970) *Biophys. J.* **10**, 664.

Parsegian, V.A., Fuller, N., and Rand, R.P. (1979) *Proc. Natl. Acad. Sci. USA* **76**, 2750.

Pashley, R.M. (1981) *J. Colloid Interf. Sci.* **83**, 531.

Pashley, R.M., and Israelachvili, J.N. (1981) *Colloids and Surfaces* **2**, 169.

Pashley, R.M., and Israelachvili, J.N. (1984) *J. Colloid Interf. Sci.* **101**, 511.

Pashley, R.M., McGuiggan, P.M., Ninham, B.W., Brady, J., and Evans, D.F. (1986) *J. Phys. Chem.* (submitted).

Payens, Th.A.G. (1955) *Philips Res. Repr.***10**, 245.

Phillips, M.C., and Chapman, D. (1968) *BBA* **163**, 301.

Porte, G., and Appell, J. (1982) in *Surfactants in Solution*, Vol. 2, 805 (K.L. Mittall and B. Lindman, eds.) (Plenum Press, New York).

Punnett, T. (1970) *Science* **171**, 284.

Sacre, M.M., and Tocanne, J.F. (1977) *Chem. and Phys. of Lipids* **18**, 334.

Scheutjens, J.M.H.M. (1985) Thesis *Macromolecules at Interfaces* (Agricultural Univ., The Netherlands).

Schindler, H., and Seelig, J. (1975) *Biochemistry* **14**, 2283.

Sculley, M.J., Duniec, J.T., Thorne, S.W., Chow, W.S., and Boardman, N.K. (1980) *Arch. Biochem. Biophys.* **201**, 339.

Seddon, J.M., Cevc, G., Kaye, R.D., and Marsh, D. (1984) *Biochemistry* **23**, 2634.

Seelig, J., and Seelig, A. (1974) *Biochemistry* **13**, 4839.

Small, D.M. (1967) *J. Lipid Res.* **8**, 551.

Sornette, D., and Ostrowsky, N. (1984) *Journal de Physique* **45**, 265.

Stigter, D. (1975) *J. Phys. Chem.* **79**, 1015.

Sundler, R., Duzgunes, N., and Papahadjopoulos, D. (1981) *BBA* **649**, 751.

Talmon, Y., Evans, D.F., and Ninham, B.W. (1983) *Science* **221**, 1047.

Tanford, C. (1972) *J. Phys. Chem.* **76**, 3020.

Tocanne, J.F., Vervegaert, P.H.J.T., Verkley, A.J., and Van Deenen, L.L.M. (1974) *Chem. and Phys. of Lipids* **12**, 201.

Trauble, H., Teubner, M., Woolley, P., and Eibl, H. (1976) *Biophys. Chem.* **4**, 319.

Van Dyck, P.W.M., Vervegaert, P.H.J.T., Verkley, A.J., Van Deenen, L.L.M., and De Gier, J. (1975) *BBA* **406**, 465.

Van Dyck, P.W.M., de Kruyff, B., Verkley, A.J., Van Deenen, L.L.M., and de Gier, J. (1978) *BBA* **512**, 84.

Van Olphen, H. (1977) *Clay Colloid Chemistry*, Chapter 10 (Wiley, New York).

Verkley, A.J., de Kruyff, B., Vervegaert, P.H.J.T., Tocanne, J.F., and Van Deenen, L.L.M. (1974) *BBA* **339**, 432.

Verwey, E.J.W., and Overbeek, J.Th.G. (1948) *Theory of the Stability of Lyophobic Colloids* (Elsevier, Amsterdam).

Worcester, D.L. (1976) in *Biological Membranes* (D. Chapman and D.F.H. Wallach, eds.), Vol. 3, pp.1-46 (Academic Press, London).

Worcester, D.L. and Franks, N.P. (1976) *J. Mol. Biol.* **100**, 359.

Zaccai, G., Buldt, G., Seelig, A., and Seelig, J. (1979) *J. Mol. Biol.* **134**, 693.